1982

Effects of media design on anaerobic filter performance

Mohamed Fituri Dahab
Iowa State University

Dahab, Mohamed Fituri

EFFECTS OF MEDIA DESIGN ON ANAEROBIC FILTER PERFORMANCE

Iowa State University PH.D. 1982

PLEASE NOTE:

In all cases this material has been filmed in the best possible way from the available copy. Problems encountered with this document have been identified here with a check mark __✓__.

1. Glossy photographs or pages _____
2. Colored illustrations, paper or print _____
3. Photographs with dark background _____
4. Illustrations are poor copy _____
5. Pages with black marks, not original copy _____
6. Print shows through as there is text on both sides of page _____
7. Indistinct, broken or small print on several pages ✓
8. Print exceeds margin requirements _____
9. Tightly bound copy with print lost in spine _____
10. Computer printout pages with indistinct print ✓
11. Page(s) _____ lacking when material received, and not available from school or author.
12. Page(s) _____ seem to be missing in numbering only as text follows.
13. Two pages numbered _____. Text follows.
14. Curling and wrinkled pages _____
15. Other _____

Effects of media design on anaerobic filter performance

by

Mohamed Fituri Dahab

A Dissertation Submitted to the

Graduate Faculty in Partial Fulfillment of the

Requirements for the Degree of

DOCTOR OF PHILOSOPHY

Department: Civil Engineering
Major: Sanitary Engineering

Approved:

Signature was redacted for privacy.

In Charge of Major Work

Signature was redacted for privacy.

For the Major Department

Signature was redacted for privacy.

For the Graduate College

Iowa State University
Ames, Iowa

1982

TABLE OF CONTENTS

LIST OF TABLES

LIST OF FIGURES

LIST OF ABBREVIATIONS

BOD_5	five-day biochemical oxygen demand
$CaCO_3$	calcium carbonate
C_i	influent waste concentration
CH_4	methane gas
cm	centimeter
COD	chemical oxygen demand
CO_2	carbon dioxide
^oC	degrees Celsius
^oF	degrees Fahrenheit
ft	feet
gal	gallon
gm	gram
hp	horsepower
hr	hour
HRT	hydraulic retention time
in	inch
kg	kilogram
L	liter, length units
lb	pound
m	meter
M	mass units
MCF	one thousand cubic feet
mg	milligram
MGD	million gallons daily

mg/L	milligrams per liter
ml	milliliter
mm	millimeter
PBR	packed-bed reactor
pH	logarithm of the reciprocal of the hydrogen ion concentration
PSF	packing shape factor
PVC	polyvinyl chloride
SS	suspended solids
T	time
TKN	total Kjeldahl nitrogen
VFA	volatile fatty acids
VSS	volatile suspended solids

INTRODUCTION

Anaerobic filter treatment is relatively new to the diversified family of wastewater treatment processes. This process is basically a modification of the more familiar anaerobic digestion process. An anaerobic filter, or an anaerobic packed-bed reactor (PBR) as it is often labeled, is a column packed with highly porous material through which wastewater is passed, normally in an upwards manner. The reactor medium, or column packing, serves as a support for microorganisms which become attached to or otherwise retained within its interstitial pore spaces. As wastewater is passed through this medium, the attached and flocculated microorganisms decompose the organic materials in the wastewater and utilize them for growth and multiplication. The major by-products of this anaerobic reaction are methane and carbon dioxide gases. The anaerobic filter is considered to be an extremely stable process for treating high strength wastewaters and for producing a valuable energy by-product that could be instrumental in augmenting the continually dwindling world fossil fuel supplies.

Whereas many aspects of the anaerobic filter process have been investigated thoroughly, including its ability to handle a variety of high strength wastewaters, the effects of packing design and configuration on the degree of wastewater treatment have not been explored in much detail. The amount of treatment attributed to attached bacterial growth as compared to that attributed to interstitially-suspended growth is not well-known. Some researchers have treated the anaerobic filter as a series of individual suspended growth completely mixed subreactors the total of which comprise an entire packed-bed reactor. Other researchers have tended to

treat this process as a series of completely attached growth subunits the total of which make up an entire anaerobic reactor. Current thinking is that anaerobic filter performance depends on both attached and suspended growths that are intrinsically and mutually responsible for the filter's total function.

The extent of bacterial attachment, or lack of it, brings out questions concerning the medium's role in the treatment process, its total surface area, and its ability to enhance suspended solids growth, settling, and retention. These factors as well as others dealing with the overall effects of media design and configuration in enhancing effective treatment need to be explored so that a better understanding of the anaerobic filter process is attained. Consequently, a study was designed with the broad objectives of attempting to arrive at a better delineation of these media effects on anaerobic wastewater treatment so that, at the end, better design and operating criteria could be established in an area of ever increasing importance to both waste treatment as well as energy recovery.

OBJECTIVES AND SCOPE OF STUDY

A general review of literature available on anaerobic filter treatment indicated that most research in this area of waste treatment has been conducted using laboratory or bench-scale columns typically ranging in inner diameter from 4 to 6 in. (100 to 500 mm) and a few feet in height. The media used in such small units frequently were limited to small quartzite stones or small-sized plastic or ceramic loose-fill type materials. The sizes of these materials generally ranged from about 1.0 to 1.5 in. (25 to 40 mm). The effective porosities of such media generally ranged from about 40 to 90 percent.

Although anaerobic filters have been designed and built at a few localities around the United States for the treatment of industrial wastes, such designs were often based on limited data and their long-term performance occasionally fell short of expectation. Many design parameters need to be more adequately established before widespread use of the anaerobic filter process can be realized. Some of these design factors undoubtedly include the effects of media shape and size on the expected performance.

A mathematical model of the anaerobic filter process developed by Young (65, 69) suggested that critical factors such as biomass transport, entrapment, the surface area of attached growth, and the concentration of flocculated suspended solids within the anaerobic filter matrix all are related to media design and size. The anaerobic process in general is a low solids production system and therefore the anaerobic filter's ability to store such solids for long periods of time is one of the attractive features of this process. However, solids must be wasted occasionally from

the anaerobic filter reactor so that solids breakthrough from the reactor does not contribute to deterioration of the effluent quality. The need to waste solids from anaerobic filters is expected to be related inversely to reactor porosity, or the extent of free space available within its packing. It is obvious that optimization of reactor medium should lead to optimization of solids wasting frequency.

Some of the problems encountered in full-scale operation of anaerobic filters can be traced to improper, or inadequate, development of scale-up factors. Scale-up factors developed from small anaerobic reactor experiments using small-sized packing materials applied to the design of full-scale units using much larger or entirely different media could, therefore, introduce considerable design error and a great deal of wasted time and capital expenditure.

With the above considerations in mind, the specific objectives of this study were:

1. To investigate the effects of differing media designs and shapes on the performance of anaerobic filters operated under similar organic loading conditions and similar environmental conditions. The explicit goal was to optimize gas production, organic removal, and solids wasting frequency through proper selection of filter media.
2. To define more clearly the relationships between variable organic loading rates, overall filter performance, and media characteristics. The goal was to identify design parameters and criteria to be used for process scale-up.
3. To refine a mathematical model to arrive at a better

fundamental understanding of the operation of the anaerobic filter process. The principal goal here was to identify parameters of greatest sensitivity to the design and operation of anaerobic filters particularly those that relate directly to media characteristics.

LITERATURE REVIEW

Anaerobic Treatment

Anaerobic treatment is a process whereby organic materials are degraded biologically to form carbon dioxide (CO_2) and methane (CH_4) gases in the absence of molecular oxygen. The process has been employed at wastewater treatment facilities for a good number of years to stabilize wastewater solids by a process known as anaerobic digestion. Dague (9) has presented an excellent historical overview of the process indicating that the discovery of anaerobic life was first made in 1861 by Pasteur while studying fermentive reactions. The process was not utilized for waste treatment in the United States until late in the nineteenth and early in the twentieth centuries (9).

Anaerobic digestion is carried out by two groups of microorganisms. The first group is a collection of facultative microorganisms that convert organics into simple volatile fatty acids, henceforth named "acid formers." The second group of microorganisms utilizes the by-products of the first group and converts volatile acids into methane gas and therefore are named "methane formers" (Figure 1). Although the process is commonly described in these two distinct phases, some researchers prefer to include a separate first-stage reaction involving the hydrolysis of complex organic materials to form somewhat simpler organic molecules. These simpler organic molecules are then acted upon by the "acid formers" to produce simple volatile fatty acids such as acetic, propionic, and butyric acids. In this context, anaerobic digestion represents a symbiotic process where each group of microorganisms constitutes an important link in a complicated chain of bacterial interdependence.

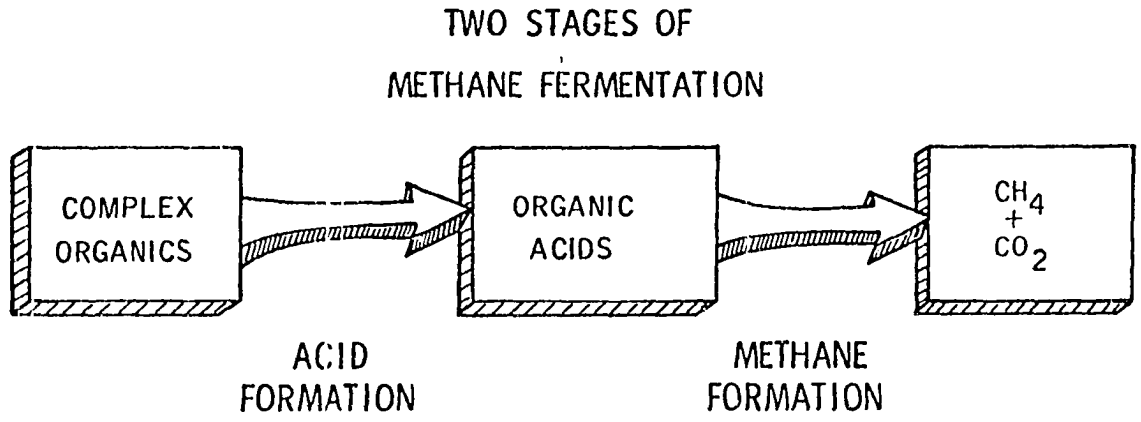

Figure 1. Two stages of methane fermentation of complex organics (65)

Figure 2 shows a simplified illustration of the anaerobic process (38). The numerical values shown represent the relative energy flow through the various pathways in the conversion of complex organics to methane gas. The fraction converted to bacterial biomass is not shown. However, this value should correspond to about 5 to 10 percent of the amounts shown (65, 8).

The stability of anaerobic fermentation is dependent upon the balance that can be maintained between the basic groups of microorganisms. For instance if the activity of methane formers lags behind acid formers, an excess of volatile acids can develop rapidly leading to a decrease in pH and possible upsetting of the fermentation process. Such upsets are often caused by shock loadings of organic solids to the system. The same can happen if the system buffering capacity is suddenly decreased or toxic materials are added to the system (39, 65).

Such upsets usually occur as a result of the difference in growth rates between acidogenic and methanogenic bacteria. The growth rate of methane formers is extremely low compared to that of acid formers; a fact that often makes it difficult to achieve a balanced anaerobic process. The difference in growth rates between these two species has led to the conclusion that the entire process is dependent on the vitality of methane formers; that is to say that the metabolism of the latter group is rate limiting (9, 38, 65, 66, 67).

The smaller amounts of biomass produced during anaerobic treatment as compared to that produced during aerobic treatment gives the process an economic advantage by minimizing the need for excessive solids wastage, handling, and ultimate disposal. This important feature allows anaerobic reactor columns to be operated for long periods of time without having to

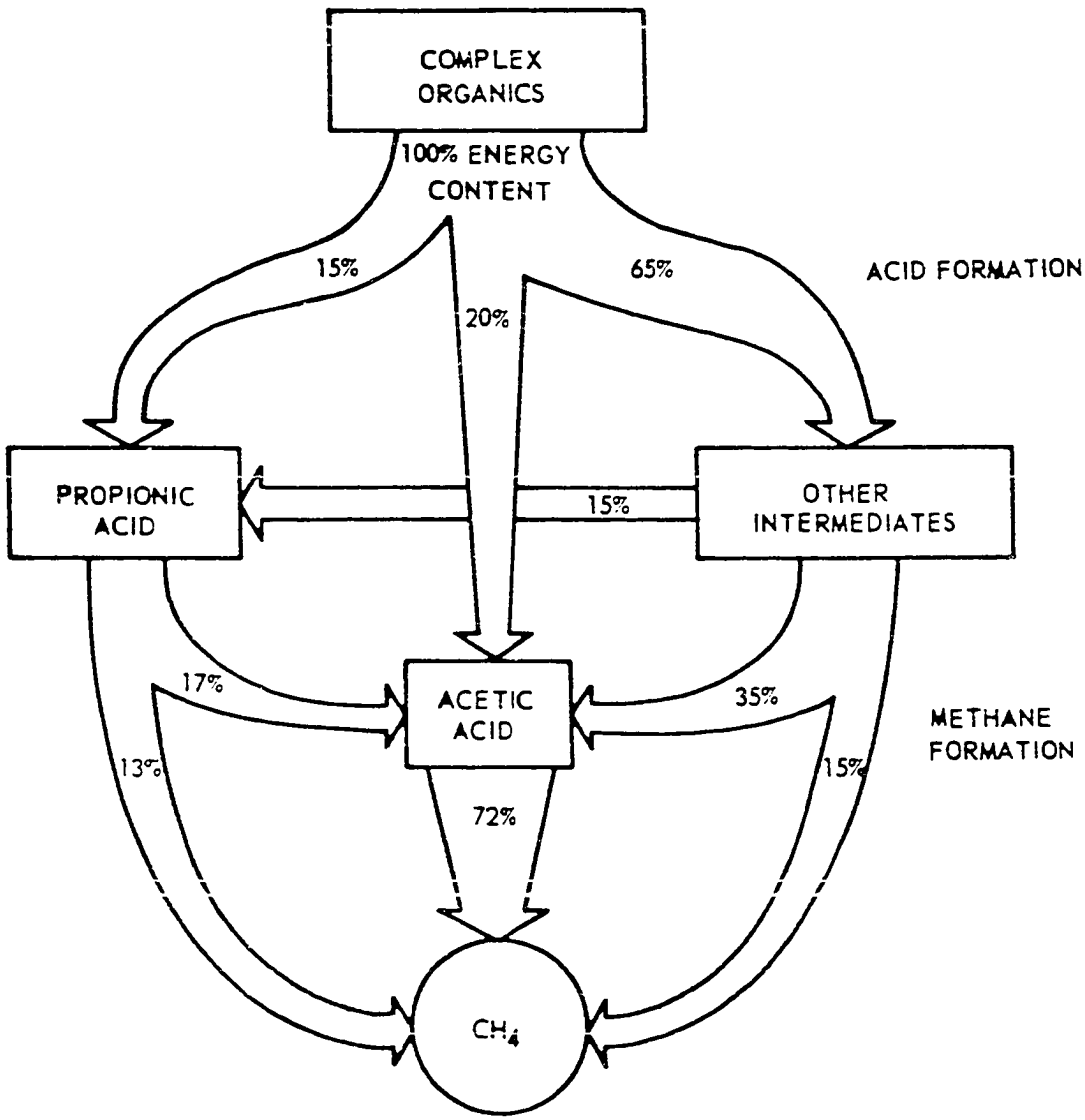

Figure 2. Methane fermentation of complex organic waste (38)

waste solids from the system, thus adding an important cost saving advantage over conventional aerobic treatment (9, 66-69).

Environmental Requirements of Anaerobic Treatment

The sensitivity of anaerobic waste treatment is such that a variety of environmental controls must be maintained in order for the process to proceed without any failures or upsets. Such environmental controls include a maintenance of proper system pH, proper temperature, and an absence of materials that could be toxic to the system (8, 39, 40, 65, 67, 32).

Hydrogen ion concentration

Anaerobic waste treatment proceeds most favorably at a system pH of near neutrality, but a pH range of about 6.5 - 8.0 usually provides a satisfactory working range (39, 65, 67). The process efficiency (i.e. organics removal) decreases considerably at pHs lower than about 6.5. Low pH conditions are known to occur when the capacity of methane formers is overtaxed due to increases in available volatile acids concentrations. This condition usually occurs when the system is either organically overloaded (i.e. shock loaded) or hydraulically stressed by washing out excessive amounts of the usually fewer methane formers (67).

Maintenance of the proper pH range is most critical during start up. A decrease of pH to 6.5 or lower can have pronounced effects by increasing the length of start-up periods considerably (65, 67). During steady-state conditions, pH tolerance becomes somewhat better and anaerobic systems can recover rapidly from short-term pH departures from near neutrality (7, 65).

Preventing pH imbalances in anaerobic treatment may require the

addition of a good buffering system, such as bicarbonate alkalinity or the addition of lime or caustic soda to maintain pH levels near neutrality (5, 8, 9, 67). Desirable levels of alkalinity are often around 2,500 to 5,000 mg/L (as $CaCO_3$) depending on organic loading conditions. Because of its lower cost, lime is most often added to anaerobic systems to either raise the pH or keep it near neutrality. Lime addition, however, must be practiced with caution to prevent calcium ion toxicity (39).

Temperature

Anaerobic systems perform better at somewhat elevated temperatures; i.e. thermophilic temperatures in the range of 120-150°F (49-65°C). At such temperatures the reaction rate is higher thus reducing solids residence times. However, the costs associated with maintaining such high temperatures often offset the benefits of faster reactor rates and thus the mesophilic treatment range of 68-110°F (20-45°C) is the usual preferred range (9).

Anaerobic treatment can be carried out at lower temperatures (i.e. 68°F (20°C). However, this psychrophilic range is disadvantageous due to the extremely reduced reaction rates and the associated longer solids residence times (SRT) required for adequate organics stabilization. In addition, at low temperatures hydrolysis rates of complex wastes become limiting. Kotze et al. (31) indicated that temperature selection in anaerobic treatment should be made on the basis of the waste characteristics to be treated.

Toxic materials

In order for an anaerobic treatment system to proceed satisfactorily, the system must be maintained free of toxic or otherwise inhibitory

substances. Inhibition in biological treatment is generally viewed as a relative phenomenon since the degree of inhibition is generally in direct proportion to the concentration of an inhibiting substance. McCarty (40) has shown that the metallic salts and other inhibiting materials at low concentrations can have a stimulating effect on the rate of anaerobic reactions. Examples of such materials include alkali and alkaline-earth cations (40). Heavy metals generally have little effect on anaerobic treatment at low concentrations, but at high concentrations these metals can be extremely toxic and should, therefore, be closely monitored.

Organic chemical pollutants can be extremely toxic to the anaerobic treatment process. Johnson and Young (30) studied the effects of some organic priority pollutants on the anaerobic digestion process and found that some of these chemicals can have irreversible toxic effects at concentrations of 100 mg/L or less.

Anaerobic Treatment Processes

Although there is a large variety of anaerobic treatment systems currently being utilized, most of these systems can be classified in four basic processes:

1. Conventional anaerobic processes
2. Anaerobic contact processes
3. Expanded-bed submerged-media reactors
4. The anaerobic filter process

The first two types of processes represent mixed-tank digesters and will not be discussed in detail in this report. The third type of process represents a modification of the basic anaerobic filter process and will not

be discussed in great detail either since it falls basically outside the scope of this study.

Conventional anaerobic processes

Conventional anaerobic digestion consists basically of one-tank or two-tank (i.e. two-stage) systems as shown in Figure 3-A. Waste which is generally high in solids content (more than 1 to 2% solids) is introduced into the digestion tank (normally the first tank in two-stage systems) and mixed with its contents where the microbial reaction takes place. The effluent of this tank which includes active biomass is pumped to the second tank in two-stage systems or simply removed for further processing or more commonly for final disposal. In two-stage systems the second tank is used for digested sludge storage and/or solids separation.

The digestion tank contents typically are mixed using either turbine or gas recirculation mixers (8, 9, 65). In addition to providing heat to keep the tank contents at a constant operational temperature, such tanks are often earth-sheltered to minimize heat loss.

Anaerobic contact processes

Anaerobic contact or "anaerobic activated sludge" (Figure 3-B) processes were designed to alleviate some of the problems associated with single-tank conventional processes such as long detention times and the washout of active microbial mass (8, 54, 65). The anaerobic activated sludge system is similar to the conventional process except that the second tank is used to separate the suspended solids from the effluent of the first reaction tank so that they can be recirculated back to the digestion unit. This concept, at least in theory, makes the process more amenable to the

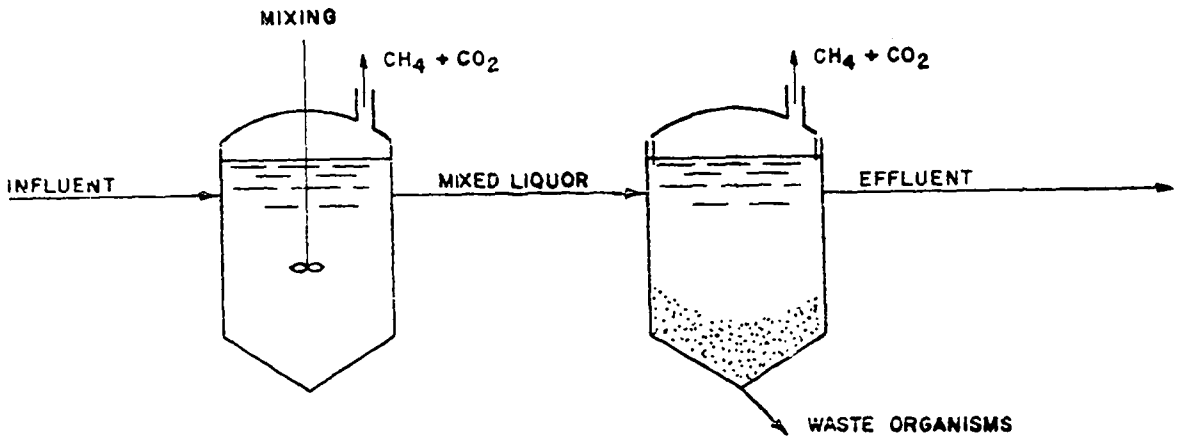

(A)

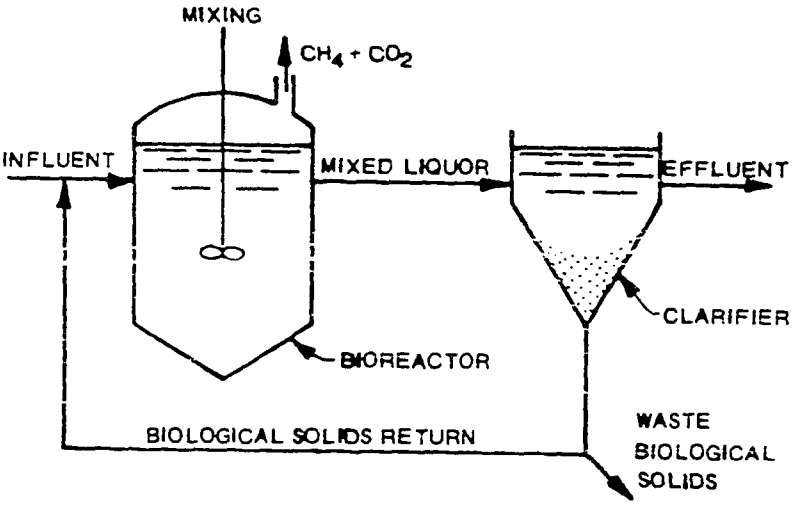

(B)

Figure 3. Schematic diagram of (A) conventional anaerobic digestion and (B) the anaerobic activated sludge process

treatment of dilute wastes. The recycling of active microbial mass to the reaction tank allows for increased efficiency and system reliability (8, 9, 65). The basic problem with this process is that anaerobic solids are not easily settled and, therefore, a variety of mechanical solids separation schemes are often added to mitigate this difficulty.

Another variation on the theme of anaerobic contact processes is Lettinga's "Upflow anaerobic sludge blanket" (UASB) process (8, 34, 35) (See Figure 4). This process attempts to combine the anaerobic reaction vessel and the settling vessel in one chamber by equipping the upper portion of the chamber with a settler/gas separator device (8, 34). This system has been shown to be quite effective for treatment of dilute soluble and insoluble wastes (8, 15, 35).

Expanded-bed submerged-media reactors

Expanded-bed reactors like anaerobic filters represent perhaps the latest concept in anaerobic treatment. These processes were developed to overcome many of the difficulties and problems associated with conventional as well as anaerobic contact processes such as the inability to treat dilute wastes at relatively short hydraulic retention times and long cell residence times.

An expanded-bed submerged-media reactor consists of a column (i.e. reactor vessel) containing small-diameter granular packing material that serves as a matrix for cellular solids retention (Figure 5). As the name indicates, the reactor packing medium is normally expanded (or fluidized) during operation and therefore the active bacterial mass in the system is limited to the solids attached to the surface of the medium.

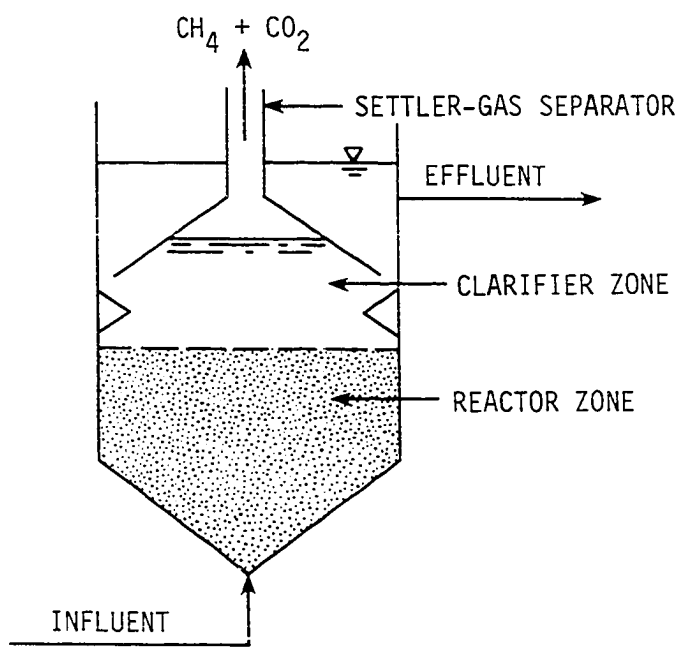

Figure 4. Schematic diagram of the "upflow anaerobic sludge blanket" process (34)

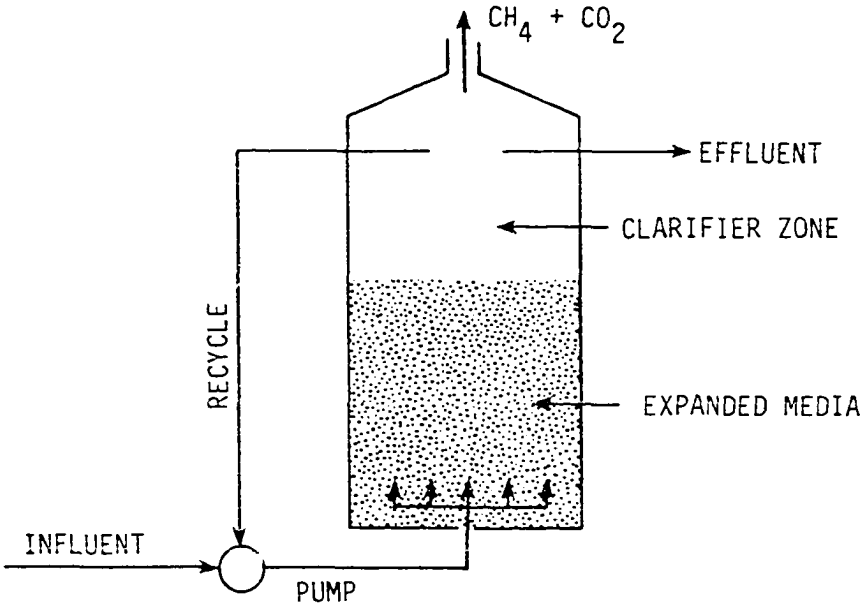

Figure 5. Schematic diagram of the expanded-bed anaerobic reactor (8)

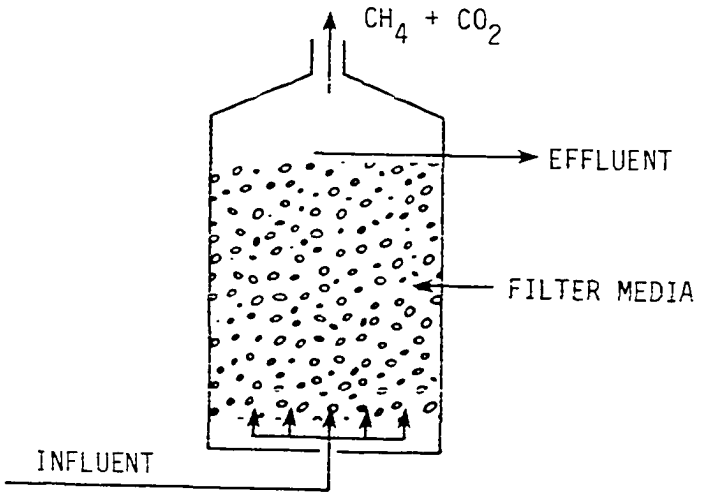

Figure 6. Schematic diagram of the anaerobic filter process

The need to expand the reactor contents in this process represents a potential disadvantage that must be seriously considered in comparison to other submerged-media anaerobic systems where there is no need to expand the reactor medium. Often, the need to expand the reactor medium requires recirculation of the reactor effluent, sometimes at ratios approaching few hundred times the original waste stream (8, 56).

Aside from the differences of media and regime of operation, expanded-bed reactors are otherwise similar to anaerobic filters and represent an extension of the basic anaerobic filter concept. Much of the substantive research in this area of waste treatment was conducted by Switzenbaum and Jewell (8, 56) in the late 1970s. The studies conducted by these investigators suggest that the expanded-bed anaerobic reactors are perhaps more suitable for dilute wastes than are conventional anaerobic processes.

The expanded bed process is said to withstand temperature as well as organic loading shocks in addition to being amenable to operation at ambient temperatures (8, 56). In these respects it is very similar to the capabilities of the anaerobic filter process. It is not known, however, if this process is able to support conditions of intermittent operation as might happen during extended power or equipment failures or intermittent flows of influent wastewaters. Although the expanded-bed process will not be discussed in more detail, cases where comparison between it and the anaerobic filter process are beneficial will be pointed out or emphasized.

The anaerobic filter process

The anaerobic filter process represents a significant development in anaerobic waste treatment. This process (Figure 6) was developed and laboratory-tested by Young and McCarty during the late 1960s (65-70).

Since then, research on anaerobic filter treatment has multiplied several times over and the process has been used to treat a variety of waste streams such as animal wastes (53), food processing wastes (2, 47), brewery wastes (36), pharmaceutical wastes (26, 27), petrochemical wastes (24), in addition to other industrial wastes (6, 13, 14, 16, 22, 23, 25, 29, 57, 64). Some of these applications will be briefly discussed below.

The original work by Young and McCarty (65, 68, 69) and subsequent studies by numerous researchers have led to extensive documentation of the advantages offered by the anaerobic filter process which include:

1. The process has a tremendous capacity to handle high organic loading rates. This process could in fact be loaded at rates several times as high as those experienced in conventional anaerobic and aerobic treatment processes.
2. The anaerobic filter process is relatively insensitive to variable organic loading rates and shock loads and it is capable of sustaining an active microbial culture even after a period of relative starvation.
3. Once an active microbial culture is established, the anaerobic filter demonstrates a remarkable resilience to moderate environmental changes such as pH and temperature. This resilience affords the anaerobic filter a degree of stability often unattainable with other biological treatment processes.
4. Anaerobic filter treatment provides all of the advantages offered by anaerobic treatment such as energy recovery, low sludge production rates, relatively low nutrient requirements, and remarkable energy efficiency since high-cost oxygen is not needed.

5. The anaerobic filter process can be mechanically simpler than other treatment processes. There is no need for mixing and there may be no need for effluent recirculation. Therefore, no blowers or excessive pumping equipment are needed.

Applications of Anaerobic Filter Treatment

The original anaerobic filters tested by Young and McCarty (68, 69) were constructed of plexiglass columns, 5.5 in. (140 mm) in diameter and 6.0 ft. (1.83 m) in height, each having a total volume of 1 ft^3 (28.3L). The filter medium consisted of smooth quartzite stones 1 - 1.5 in. (25 - 38 mm) in diameter and having a porosity of about 42 percent. Two different types of synthetic wastes were used in these studies; a protein-carbohydrate waste and a volatile acids waste (65, 68, 69). These units were operated at organic loading rates ranging from 26.5 lb COD/MCF-day (0.43 gm COD/L-day) to 212 lb COD/MCF-day (3.4 gm COD/L-day). Influent COD concentrations ranged from 375 mg/L to 12,000 mg/L. All filters were operated at a constant temperature of 25°C (77°F). These basic experiments led to the conclusion that anaerobic filter treatment added to anaerobic processes a dimension of stability and reliability that was often absent in conventional anaerobic digestion. Since Young and McCarty completed their basic experiments with anaerobic filters, the newly developed process has been utilized by numerous researchers for the treatment of a variety of waste waters.

Plummer et al. (47) operated four pilot anaerobic filters measuring 6 in. (152 mm) diameter and 0.9 ft. to 1.3 ft. (27.4 cm to 39.6 cm) tall using food processing carbohydrate waste. These filters were packed with a combination of Raschig rings and Berl saddles having an approximate

porosity of 65 to 70 percent. These columns were operated at organic (COD) loading rates ranging from 101 to 638 lb COD/MCF-day (1.6 to 10.2 gm COD/L-day) and a constant temperature of 35°F. An overall COD removal efficiency ranging from 30 to 86% was achieved depending on the organic loading rates and the hydraulic detention time (47).

Arora et al. (2) used laboratory-scale anaerobic filters to treat vegetable tanning waste waters. These filters consisted of plexiglass columns, 4 in. (15 cm) in diameter and 6.1 ft. (1.85 m) high, and were filled with 70 in. (1.7 m) of 1.6 in. (40 mm) quartzite stones as the filter medium. These anaerobic filters were progressively loaded at COD loading rates ranging from 0.19 gm/L-day (12 lb COD/MCF-day) to 3.26 gm/L-day (200 lb COD/MCF-day) with influent concentrations ranging from 330 mg/L to 5610 mg/L. COD removal efficiencies ranging from about 25% at the highest loading rate to 90% at the lowest loading rate were reported (2).

El-Shafie and Bloodgood (17) investigated the performance of a multistage anaerobic filter system using "Metrecal" (vanilla flavored) as the food substitute. This multistage system consisted of six bench-scale units arranged in series. Each reactor was a plexiglass column of 5.5 in. (142 mm) in diameter and 18 in. (0.46 m) tall. The filter packing was 1.0 to 1.5 in. (25-38 mm) diameter gravel having a porosity of about 45%. The feed substrate was fed at an organic loading rate of 2560 lb/MCF-day (41 gm/L-day) and an influent concentration of 10,000 mg/L to the first filter unit in the series. The temperature of operation was 30°C (86°F). El-Shafie and Bloodgood's main conclusions were that at a given loading rate removal efficiency was constant regardless of influent COD concentrations and that biological activity seemed to increase dramatically with

increased hydraulic detention time (17). These results agreed favorably with those reported by Young (65).

Lovan and Foree (36) used laboratory scale anaerobic filters measuring 6 in. (152 mm) in diameter and 6 ft. (1.83 m) in height to treat brewery press liquor waste. The filter medium was crushed limestone 1-1.5 in. (25-38 mm) having a porosity of about 46 percent. These columns were loaded at 50 and 100 lb COD/MCF-day (0.8 and 1.6 gm COD/L-day) with influent concentrations ranging from 6,000 to 24,400 mg/L. These authors found the process to be particularly efficient at those loadings with COD removals exceeding 90 percent (36).

Haug et al. (22) reported the use of a laboratory-scale anaerobic filter, 5.5 in. (140 mm) in diameter and 6.5 ft. (1.98 m) high, for the treatment of waste activated sludge heat treatment liquor with remarkable success rates. The filter used by these researchers contained smooth quartzite stones, 1.0 to 1.5 in. (25 to 38 mm) in diameter as the packing medium (porosity = 43%).

Dague et al. (11) also conducted experiments with an anaerobic filter to treat the decant from waste activated sludge thermal conditioning operations from the city of Dubuque, Iowa. These researchers used an anaerobic filter column with an inside diameter to 5.5 in. (150 mm) and a packed depth of 4 ft. (1.22 m) of ring type plastic media having a porosity of 90 percent. The units were operated at a BOD_{20}[1] loading rate of 200 and 400 lb BOD_{20}/MCF-day (3.2 and 6.45 gm/L-day). Treatment efficiencies exceeding 60% were reported (as BOD_L removed) at both of

---

[1]The 20-day biochemical oxygen demand (BOD_{20}) is essentially equivalent to the wastes' ultimate oxygen demand (BOD_L) (11).

these loading rates with COD removal efficiency being slightly lower. Overall removal efficiency (as BOD_{20}) was considerably higher when two columns were operated in series, thus comprising a total active bed of about 8.0 ft. (2.74 m) (11).

Anaerobic filters also have been used successfully, and more importantly on a full-scale basis, for the treatment of wheat starch-gluten plant wastes. Taylor and Brum (57) reported the use of three anaerobic filters (operated in parallel) which were 30 ft. (9.1 m) in diameter and 20 ft. (6.1 m) high and filled with 2 to 3 in. (51 to 76 mm) diameter rocks in the bottom half of each tank and 1 to 2 in. (25 to 51 mm) in the top half. An estimated overall bed porosity of about 50 percent was obtained. These filters were loaded at the rate of about 237 lb COD/MCF-day (3.8 gm/L-day) and were operated at a temperature of 32°C (90°F). An average COD removal efficiency of 65 percent was reported with good start-up and restart (after a period of dormancy of about 30 days) characteristics.

Jennet and Dennis (26) applied the anaerobic filter process to the treatment of pharmaceutical wastes using four plexiglass columns each 5.5 in. (142 mm) in inner diameter and 3 ft. (0.92 m) high. The medium used in these columns was quartzite stone 1 to 1.5 in. (25 to 38 mm) having a porosity of 47 percent. The waste was fed at organic loading rates ranging from 13.8 lb COD/MCF-day (0.22 gm/L-day) to 220 lb COD/MCF-day (3.5 gm/L-day) and influent COD concentrations ranging from 1250 to 16,000 mg/L. Chemical oxygen demand removal efficiencies of 94 to 98 percent were reported (26).

In a later study Jennet and Rand (27) compared the performance of anaerobic filters versus aerobic treatment of pharmaceutical waste. Six anaerobic filters 5.5 in. (142 mm) in diameter, 48 in. (1.22 m) high, and

filled with 1.5 in. (38 mm) stones and an "exemplary" aerobic treatment system were used in this study. Chemical oxygen demand (COD) removal of 70 to 80 percent and BOD_5 removal efficiency of about 94% when treating pharmaceutical waste at an influent COD concentration of 2000 mg/L and a hydraulic retention time of 36 hours were reported (27).

Anaerobic filters also have been used in the treatment of unusual types of wastewaters. Chian and DeWalle (6) reported the use of anaerobic columns, 7.36 in. (187 mm) in diameter and 8.1 ft. (246 cm) tall for treatment of acidic leachate from solid waste lysimeters to which simulated rainwater was added. The medium used by these investigators was plastic "Surpac" slabs with a specific surface area of 63 ft^2/ft^3 (206 m^2/m^3) and a porosity of 94%. In order to avoid low pH problems and the need to add excessive amounts of buffer, the anaerobic filters were operated at recirculation ratios ranging from 1:4.4 to 1:20. These investigators showed that organics removals were a strong function of the hydraulic retention time (HRT) and that at HRT values exceeding 7 days, removal efficiency was almost consistently above 90 percent (6).

Using the same anaerobic filter apparatus described above, DeWalle et al. (14) studied heavy metal removal in the anaerobic filter process. The waste used in this study was the leachate collected from sampling wells located at the toe of a municipal solid waste sanitary landfill. DeWalle et al. (14) indicated that heavy metals were precipitated as sulfides, carbonates, and hydroxides and were removed from the anaerobic filter as slurry. Overall heavy metal removal efficiencies ranging from about 52 percent for cadmium to about 97 percent for iron and 91 percent for chromium were reported.

Dague (10) reported the results of anaerobic treatability studies of process wastewaters generated at municipal refuse pyrolysis operations using both anaerobic suspended growth and attached growth systems. The attached growth system consisted of two sets of two anaerobic filter columns operated in series. Each column was 4 ft. (1.22 m) tall and 5.5 in. (140 mm) in diameter and contained 5/8 in. (16 mm) plastic Pall rings. These columns were operated at 35°C (95°F) using variable mixtures of soluble substrate and pyrolysis wastes. Dague (10) reported that the maximum feed rate of pyrolysis waste was 30 percent of the total influent COD without inhibition. Total removal of influent pyrolysis COD was reported at 70 percent which was the same removal as obtained with the suspended growth system. Dague indicated that anaerobic filters are preferred in the treatment of pyrolysis wastewater since they are more adaptable to treating dilute wastes than are conventional digestion processes (10).

Van den Berg and Lentz (59) studied the performance of anaerobic filters under varying conditions of flow (upflow and downflow), film area to reactor volume ratios, loading criteria, and column packing. The waste used in their studies was composed of bean blanching waste (about 1% total solids). Some of the factors studied were:

1. Film area to volume ratio (50 to 400 m^2/m^3).
2. Reactor inner diameters (0.01 to 0.075 m) and height (0.55 m to 2.2 m).
3. Packing medium, (baked clay, PVC, and glass).
4. Direction of flow-through reactors (up- and down-flow).

The organic loading rates used in this study ranged from 3.9 gm COD/L-day

to 19 gm COD/L-day. COD removal efficiencies ranged from 85 to 95 percent. Van den Berg and Lentz concluded that column packing surface area to volume ratios as well as packing design played an important role in filter performance and that upflow reactors tended to be a combination of a fixed-film and up-flow anaerobic sludge blanket reactors with most of the activity associated with the suspended growth (57).

Donovan (16) compared the performance of a laboratory-scale anaerobic filter unit with that of two larger pilot-scale units. The laboratory unit was 2 in. (51 mm) in diameter and contained a 49 in. (1.25 m) bed of 0.63 in. (16 mm) Pall rings having a porosity of 85%. The pilot columns were 23.6 in. (0.60 m) square and 11.5 ft. (3.5 m) high and contained 73 in. (1.85 m) bed of 3.5 in. (90 mm) plastic Pall rings (porosity of 95%). All filters were operated at 95°F (35°C) using the decant of a sludge heat treatment process at organic loading rates ranging from 155 lb COD/MCF-day (2.5 gm COD/L-day) to 434 lb COD/MCF-day (7 gm COD/L-day). Chemical oxygen demand, COD, removal efficiencies ranged from 55 to 80 percent depending on the loading rate and hydraulic retention time (HRT). Biochemical oxygen demand removals were consistently higher and ranged from 65 to 95 percent (16).

Genung et al. (20) reported the use of a pilot-scale anaerobic filter in the treatment of municipal wastewater. The reactor was 5 ft. (1.5 m) in diameter and 18.3 ft. (5.6 m) high and contained 10 ft. (3.1 m) of packing material consisting of 1.0 in. (25 mm) ceramic Raschig rings. This system was operated for two years mostly at ambient wastewater temperatures ranging from 10 to 25°C (50 to 77°F). Average overall removal efficiencies of 55% for BOD_5 and 75% for total suspended solids were reported (20).

Kinetics of Anaerobic Filter Treatment

As was pointed out earlier, anaerobic waste treatment involves an extremely complex system of microbial cultures that work symbiotically to decompose organic materials. Mathematical analysis and simulation of anaerobic reactions have been attempted by numerous researchers and various models have been proposed to approximate the mechanics and kinetics of anaerobic treatment. One of the pioneering models formulated to account for anaerobic suspended growth systems was proposed by McCarty (42, 43) and later refined by Andrews and Graef (1). Kinetic models describing anaerobic attached growth systems also have been proposed by numerous investigators (65, 44, 62, 49, 50, 28).

Anaerobic waste treatment, like other forms of biological treatment (i.e. aerobic treatment) is usually carried out as continuous or semi-continuous (i.e. batch type) culture growth systems. The growth rate of microorganisms in such systems can be expressed as follows:

$$\frac{dM_n}{dt} = a\left(\frac{dS}{dt}\right) - bM \qquad (1)$$

where

$\frac{dM_n}{dt}$ = Net rate of change of biological solids in the system ($ML^{-3}T^{-1}$)

$\frac{dS}{dt}$ = Rate of change of waste (substrate) concentration ($ML^{-3}T^{-1}$)

M = Concentration of active biomass (biomass effectively available for waste removal) (ML^{-3})

a = Growth yield coefficient, mass of bacteria produced per unit substrate removed.

b = Decay rate of microorganisms, T^{-1}.

The rate of substrate removal, $\frac{dS}{dt}$, is related to the total waste concentration in the system by the following relationship (65):

$$\frac{dS}{dt} = - \frac{kSM}{K_s + S} \tag{2}$$

where

k = Maximum rate of waste utilization (mass/day/mass of active organisms).

K_s = Half velocity coefficient, or waste concentration at which $(dS/dt)/M = 0.5$.

S = Waste concentration (ML^{-3})

Equation 2 is similar to a classical expression that was developed by Monod in the study of pure culture microbial growth (see 65, 9, 32, 43).

Combining Equations 1 and 2, the net growth rate of biomass is expressed as follows (65):

$$\frac{dM_n}{dt} = a\left(\frac{kSM}{K_s + S}\right) - bM \tag{3}$$

Equation 3 is applicable to suspended growth systems. Although similar relationships have been used in simulating anaerobic filter attached growth systems with some success (44), substrate diffusion kinetics into bacterial biofilms should also be considered before a true simulation model is attained. The use of Equation 3 must be limited to cases where the concentration of active biomass is known. Young (65) suggested that upon decay of active biomass an inactive fraction (equal to about 20 percent) remains as a stable fraction which is not subject to further decomposition. It was further assumed that this process of inactive mass production is continuous and therefore:

$$\frac{dMi}{dt} = (1 - e)\, a \frac{kSM}{K_s + S} \tag{4}$$

where,

$\frac{dMi}{dt}$ = rate of inactive mass production ($ML^{-3}T^{-1}$), and

e = fraction of newly synthesized cell mass remaining active for further waste stabilization.

Subtracting Equation 4 from Equation 1 gives the net rate of active biomass production, dM/dt, or

$$\frac{dM}{dt} = ea\left(\frac{kSM}{K_s + S}\right) - bM \tag{5}$$

In the anaerobic filter process microorganisms flocculate and accumulate in the void spaces of the packing medium in addition to being attached in layers on the surface of this packing medium. Because the bacterial biofilm is generally responsible for a considerable amount of waste stabilization, this fraction should also be considered before a complete account of the total biomass activity in the system is reached.

The degree of waste removal by bacterial biofilms is governed by the rate of substrate diffusion into the biofilm (65, 62, 49, 28). Figure 7 shows a conceptual model of the bacterial biofilm (65, 21). The substrate utilization within the biofilm is assumed to follow the Monod relationship (Equation 2). Substrate transport through the biofilm is achieved by molecular diffusion which is the only means of transport available. This substrate diffusion is related to the substrate concentration in the bulk liquid outside the biofilm by Fick's second law of diffusion, or

$$\frac{dS_f}{dt} = D_f \frac{d^2S_f}{dz^2} \tag{6}$$

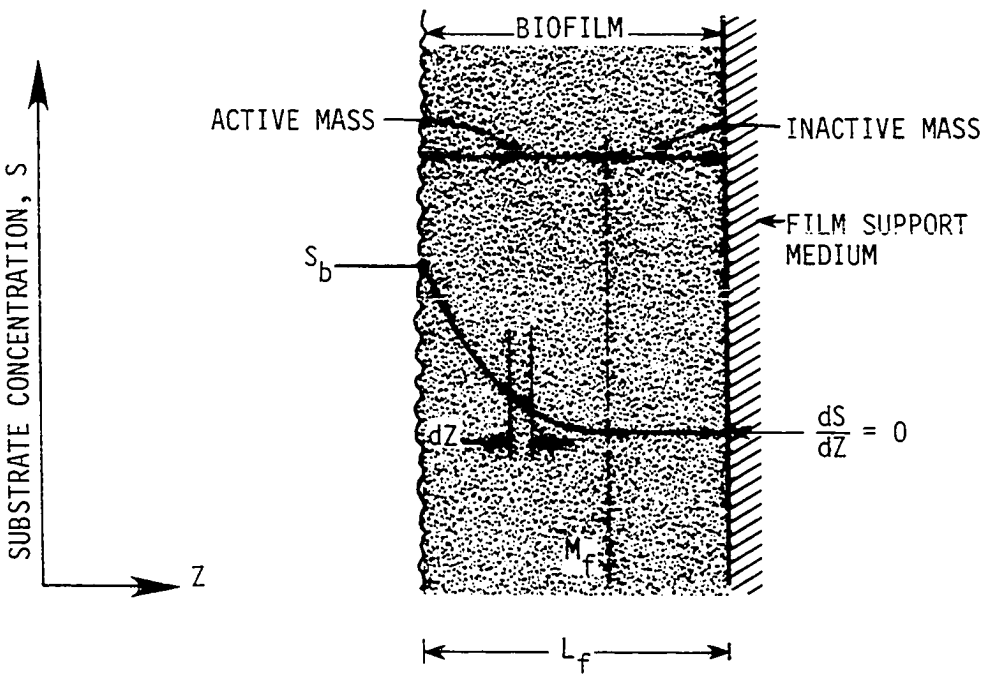

Figure 7. Conceptual illustration of how the concentration of substrate may decrease within an heterogenous biofilm layer (21, 65)

where

D_f = The substrate molecular diffusivity in the biofilm (L^2T^{-1}),

z = direction of diffusion, L, (Figure 7), and

S_f = denotes substrate concentration at any point within the biofilm layer (ML^{-3})

Combining Equations 2 and 6, and assuming steady-state conditions ($dS_f/dt = 0$), an expression for total substrate utilization within the biofilm can be obtained as follows:

$$\frac{d^2S_f}{dz^2} = \frac{1}{D_f}\left(\frac{kS_fM_f}{K_s + S_f}\right) \tag{7}$$

where

M_f = Biomass density within biofilm (ML^{-3})

Equation 7 is based on the assumption that substrate diffusion takes place in a direction normal to the media surface; there is no axial dispersion through the biofilm. Equation 7 is a second order nonlinear differential equation and as such has no simple explicit solution. However, this equation could be solved once a set of specific boundary conditions are established. Such solutions were proposed by Young (65), Haug and McCarty (21), and others (62, 49).

Young (65) and Haug and McCarty (21) presented a solution for Equation 7 for the following conditions:

Case 1 : $S_f >> K_s$, and

Case 2 : $S_f << K_s$.

These solutions are discussed briefly below.

Case 1: Assuming that no substrate flux occurs through the biofilm-biofilm support (media) interface, which is a reasonable assumption for

most impervious (i.e. plastic or ceramic) anaerobic filter packings, then the term dS_f/dz must be equal to zero. In addition, if the substrate concentration at the liquid-biofilm interface, S_i, is assumed to equal the substrate concentration at the bulk liquid phase (21), then

$$S_f = S_i \text{ at } Z = 0$$

and

$$\frac{dS_f}{dz} = 0 = \frac{dS_o}{dz} \text{ at } z = L$$

Therefore, for the case where $S_f >> K_s$ equation 7 reduces to

$$\frac{d^2S_f}{dz^2} = \frac{kM_f}{D_f} \tag{8}$$

Equation 8 can be integrated (65, 21) to yield an expression for the substrate gradient at the film-bulk liquid interface as follows:

$$\left.\frac{dS_f}{dz}\right|_{z=0} = -\frac{kM_f h}{D_f} = \frac{dS_i}{dz} \tag{9}$$

where h = thickness of the active portion of the biofilm (L).

Subsequently, the substrate flux across a unit cross-sectional area of the biofilm interface is

$$\left.\frac{dF}{dt}\right|_{z=0} = kM_f h \tag{10}$$

Equation 10 states that the rate of substrate removal is independent of the substrate concentration in the system, however, it is directly proportional to biofilm thickness. DeWalle and Chian (13) presented an expression for approximating biofilm thickness based on the work of Pirt (46) and Saunders and Bazin (51) as follows:

$$h = \sqrt{\frac{zD_f S_b}{kM_f}} \tag{11}$$

where S_b is the bulk liquid substrate concentration. Equation 11 was based on the assumption that substrate concentration at the biofilm-support interface is equal to zero. This equation is, therefore, an approximation since it violates the basic constraint that $S_f >> K_s$. A similar expression for biofilm thickness was adopted by Rittman and McCarty (49) in the development of their "variable order model" of substrate utilization. This model will be discussed later.

Case 2: By assuming that $S_f << K_s$, Equation 7 reduces to the form:

$$\frac{d^2S_f}{dz^2} = \frac{kSM_f}{D_f K_s} \tag{12}$$

Integration of Equation 12 yields a hyperbolic function for the solution of substrate concentration as a function of the biofilm thickness, h (65, 21). Considering thick biofilm layers an expression for both substrate gradient and substrate flux across the biofilm bulk liquid interface can be obtained as follows:

$$\left.\frac{dS_f}{dz}\right|_{z=0} = -S_i\left\{\frac{kM_f}{D_f K_s}\right\}^{\frac{1}{2}} \tag{13}$$

and

$$\left.\frac{dF}{dt}\right|_{z=0} = S_i\left\{\frac{D_f M_f k}{K_s}\right\}^{\frac{1}{2}} \tag{14}$$

It should be noted that Equations 13 and 14 are valid only for cases where the substrate concentration through the biofilm layer is much less than the half-velocity coefficient, K_s. Haug and McCarty (21) pointed

out that such condition is not applicable to many wastes with heterogenous reactions since S_f may be much greater than K_s at the film-bulk liquid interface although the opposite case may be true somewhere in the depths of the biofilm.

Haug and McCarty (21) also presented a general solution for Equation 7 using a Runge-Kutta numerical finite differences integration technique. The solution technique depended on defining two boundary conditions which were either of the boundary value or the initial value type. This solution is of doubtful practical utility due to the cumbersome nature of the trial and error procedure.

In an earlier study, Young (65) tackled the question of substrate diffusion in biofilm layers using an entirely different approach by assuming that a substrate gradient existed entirely within the biofilm layer as shown on Figure 8. Young (65) also proposed that a "substrate gradient factor", SF, existed such that:

$$\bar{S} = S_m/SF \tag{15}$$

In Equation 15, $\bar{S}$ is defined as the effective substrate concentration that would result in the same rate of removal per unit biomass if the mass in the biofilm was completely mixed with the substrate. This effective concentration would always be less than the measured concentration in the bulk liquid outside the film layer so that the value of SF would always be greater than unity (65). Substituting Equation 15 in Equation 2, a new expression for substrate utilization is obtained as follows:

$$\frac{dS}{dt} = -\frac{k(S_m/SF)M_f}{K_s+(S_m/SF)} \tag{16}$$

Multiplying Equation 16 by SF/SF gives

$$\frac{dS}{dt} = -\frac{kS_m M_f}{K_s(SF)+S_m} \qquad (17)$$

A new "effective half-velocity coefficient", $K_s(SF)$, is therefore obtained. This half-velocity coefficient should be equal to or greater than the K_s value measured in completely mixed systems. It was reported that a value for K_s (for attached growth systems) of 121 mg/L as glucose was measured for an aerobic system while a value of 4 mg/L was measured for suspended growth systems (65).

Young (65) proposed an expression relating the "substrate gradient factor" to the measured substrate concentration in the bulk liquid S_m in anaerobic packed-bed reactors as follows:

$$SF = 1 + (SF_o - 1)\, e^{-k_g S_m} \qquad (18)$$

Where: SF_o = Maximum value for "substrate gradient factor" (see Figure 9), and

k_g = coefficient $(mg/L)^{-1}$ - determined experimentally

It should be emphasized that Equation 18 represents an approximation of the relationship between the "substrate gradient factor" and the waste concentration in an anaerobic filter system. Figure 8 shows an illustration of how the "substrate gradient factor" is expected to vary as a function of the measured substrate concentration, Sm (65).

Young (65) devised a mathematical anaerobic filter model to simulate a plug flow type reactor system. This model was tested using the results from an extensive study of anaerobic filters that utilized volatile acids and protein-carbohydrate synthetic wastes. The substrate gradient factor concept as defined by Young (i.e. Equation 18) was used in this model to

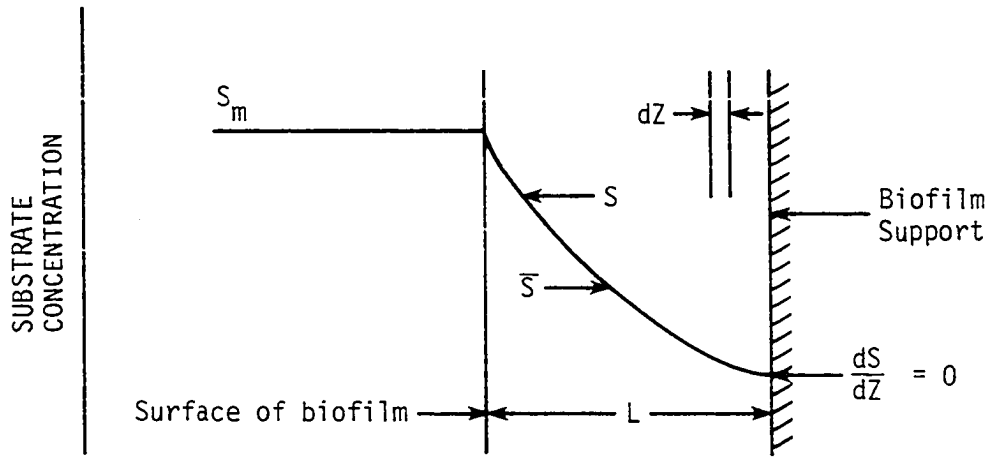

Figure 8. Conceptual illustration of substrate concentration profile within a biofilm (65)

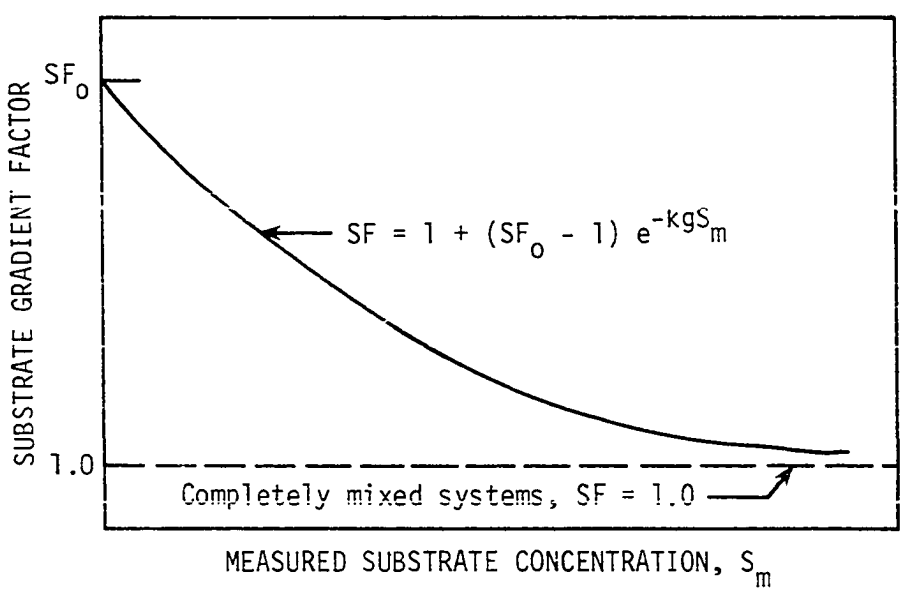

Figure 9. Illustration of how the "substrate gradient factor" is assumed to vary as a function of the measured substrate concentration (65)

approximate diffusion kinetics in anaerobic attached biofilms. It was concluded that a 25 percent change in the coefficients of the substrate gradient factor expression did not significantly alter the calculated performance when testing a 3000 mg/L volatile acids waste. Somewhat similar results were obtained when using wastes with influent COD concentration of 1500 mg/L (65, 66).

While the concept of the substrate gradient factor is based on a sound definition of attached biomass films uptake of substrates, its use has been hampered probably due, at least in part, to the fact that it may be an undefined function. Haug and McCarty (21) postulated that the substrate gradient factor concept represents a complex function which depended on the diffusion coefficient within the bacterial biofilm, the mass of microorganisms, and the kinetic coefficients within the biofilm layer. Unfortunately, there seemed to be no methods available for determining this substrate gradient factor for any particular situation (65, 66).

Williamson and McCarty (62, 63) introduced a set of modifications to the model developed by Young (65) to predict flux and substrate limitations within bacterial biofilms. Because Equation 7 above has no explicit solution, a numerical integration technique similar to that developed by Haug and McCarty (21) was used to obtain approximate graphical solutions. Application of the Williamson and McCarty (62, 63) model requires that a determination of whether the electron donor (i.e. substrate) or the electron acceptor (i.e. dissolved oxygen in aerobic systems) approach a near-zero value; a condition termed flux limitation. In the case of anaerobic treatment a certain substrate (i.e. acetate) is both substrate and flux limiting regardless of concentration since no electron donor or

electron acceptor combinations are required (62). Application of Williamson and McCarty's model also requires that a flux limiting species must also be substrate limiting throughout the biofilm. This latter condition almost limits the use of this model to deep bacterial biofilms where it is reasonable to assume that a certain substrate is both substrate as well as flux-limiting although it was indicated (63) that the model can be modified to predict substrate utilization rates in thin biofilms. This model was shown to accurately predict substrate utilization rates in nitrifying systems although its use is dependent on the accuracy of determining such parameters as the Monod maximum utilization rate and half-verocity coefficient, substrate diffusion coefficients and biofilm density.

Rittman and McCarty (49) proposed a "variable-order model" to solve Equation 7 above. An idealized conceptual illustration of bacterial biofilms in attached growth system as visualized by Rittman and McCarty (49) which is similar to a model proposed by Williamson and McCarty (62) is shown on Figure 10. By assuming a group of dimensionless quantities to substitute for the parameters in Equation 7, this equation was replaced by a similar dimensionless expression in the form of a second-order differential equation which was integrated for the case of "deep" biofilms. For the case of deep biofilms, the (dimensionless) substrate flux into the biofilm $(J/A)^*$ was expressed as a variable order function of the (dimensionless) bulk liquid substrate concentration $(S)^*$. For a plug-flow type reactor with a specific surface, a, (L^{-1}) and a surface loading rate, ν , (LT^{-1}) a steady-state mass balance is written as follows (49):

$$\frac{dS}{dt} = -CaS^q - \nu\frac{dS}{dt} \qquad (19)$$

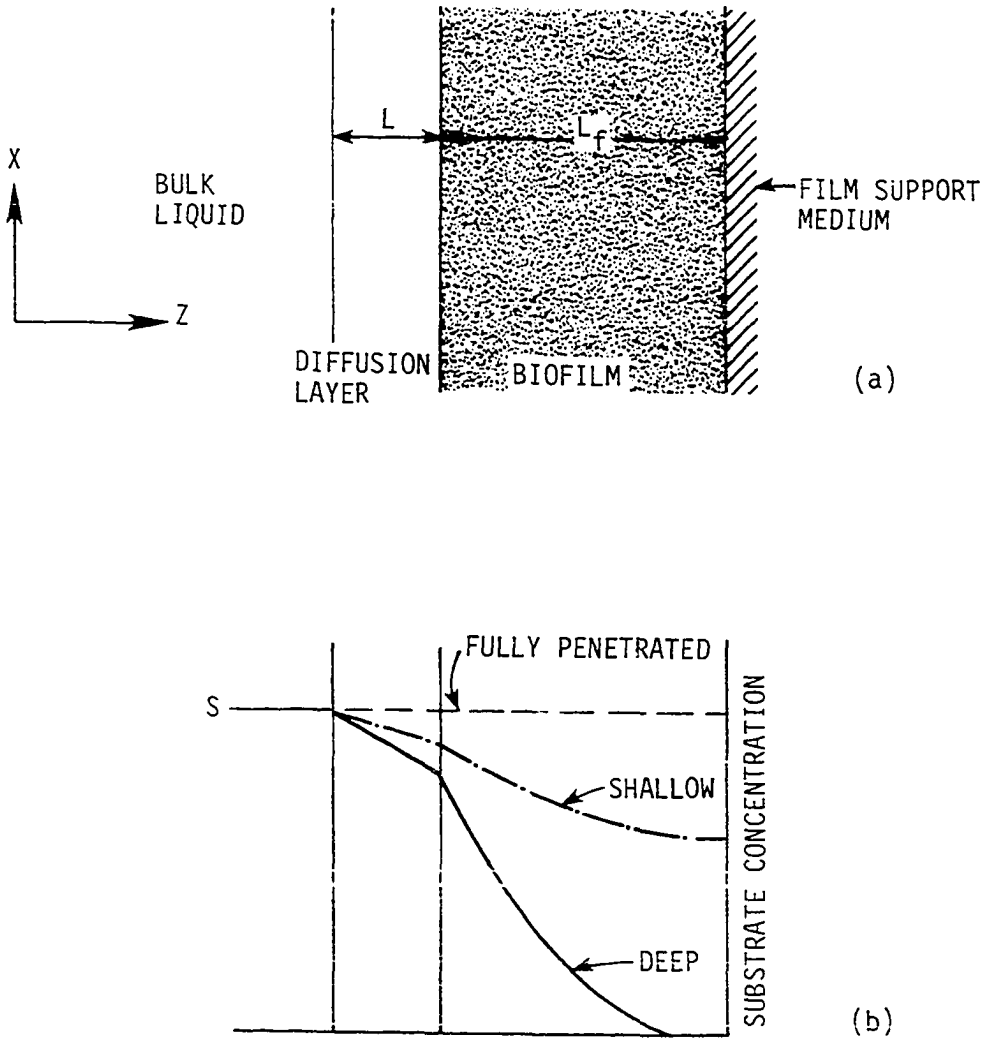

Figure 10. A conceptual model of bacterial biofilms. (a) physical concept and (b) substrate concentration profiles. After Rittman and McCarty (49)

where q = reaction rate constant,

C = variable order reaction coefficient (49),

S = bulk liquid substrate concentration (ML^{-3})

Rittman and McCarty (49) integrated Equation 19 to yield:

1. For $q = 1$

$$S = So \exp\left(1 - \frac{Ca}{\nu} x\right) \tag{20}$$

2. For $q < 1$

$$S = \left\{(So)^{1-q} - \frac{cas\ (1-q)}{\nu}\right\}^{1/1-q} \tag{21}$$

where So is the influent substrate concentration to the reactor and x is the distance along the reactor. Equations 20 and 21 are subject to the constraint that $S \geq 0$.

In order to use the "variable-order model" a number of kinetic parameters must be known or estimated including the biofilm layer thickness, the diffusivity of the substrate in both the bulk liquid stream and the film layer. and the density of active biomass in the film layers. Estimation or measurement of these parameters particularly active mass density and the (idealized) film thickness is undoubtedly subject to a great deal of guess work and subsequently mounting degrees of error. It was found that during examination of modular media blocks used in this study (as will be discussed in detail later) that the film thickness of relatively flat surfaces can easily vary over at least one order of magnitude. It is seen, therefore, that despite the seemingly accurate nature of the "variable-order model" itself, its application to practical situations is severely limited.

The general procedure for using the "variable-order model" is to identify all kinetic parameters and constants and then use these parameters

to calculate the models dimensionless quantities, coefficients, and reaction order. Once this is accomplished, the substrate flux across the biofilm layer or substrate concentration within the biofilm would be easily determined (49).

Anaerobic Filter Simulation

Regardless of the type or shape of the media used in anaerobic filters, the process is basically a plug-flow type reactor system. The nature of this flow regime not only makes the process highly efficient in treating high strength wastewaters but also renders it amenable to mathematical simulation. Hence, the process has been simulated with striking degrees of success (65, 44, 21). In fact, the mode of operation of anaerobic filters is such that a typical reactor functions as a series of plug flow reactors with the highest rate treatment at the lower sections of the filter and polishing and solids separation in the higher sections of the reactor.

Mueller and Mancini (44) developed an anaerobic filter simulation model based on complete-mix anaerobic reactor kinetics. This model treats the anaerobic filter reactor as a series of complete-mix reaction subunits the total performance of which make up an entire reactor column. This model completely neglects solids transport and substrate diffusion into the biofilm and therefore it is not a true representation of what is basically a fixed-film waste treatment system. For this reason the Mueller and Mancini model was deemed inadequate for anaerobic filter simulation despite its reported ability to approximate steady-state data.

As it was pointed out previously, Young (65, 66) developed a rigorous mathematic model for anaerobic filter simulation. This model is hence

termed the "Anaerobic Filter Model" (AFM) and will be discussed in some detail below.

The Anaerobic Filter Model

The basic kinetic equations utilized in the development of the anaerobic filter model have been discussed above including the "substrate gradient factor" concept (i.e. Equations 1 through 7 and 15 through 17). The applicability and adequacy of this model will be tested further using the results from this anaerobic filter study.

Physical characteristics of the anaerobic filter

The following discussion of the physical characteristics of the anaerobic filter is based on prior developments by Young (65, 66). In the development of the anaerobic filter model, the anaerobic reactor is considered basically a plug-flow reactor in which the waste stream is introduced at the bottom of the packed column. This waste stream, therefore, travels in an upflow manner. Mixing in the reactor is limited to that effected by the media configuration and to that produced by the action of the product gas as it travels upwards through the column. The organic compounds in the waste stream are continually contacted and decomposed by the biomass inside the reactor as the waste stream moves through the packing material. The highest microbial reaction rates are expected to be in the lower levels of the anaerobic filter. These rates are expected to decrease as the concentrations of organic substances becomes lower as the waste stream flows through the reactor.

Despite the basic assumption of plug flow in the anaerobic filter reactor, departures from ideal plug flow are also expected to occur due to

media-induced hydraulic mixing and mixing due to the action of gas bubbles as gas travels upward through the reactor. Short-circuiting in the reactor vessel could take place due to the accumulation of excessive biological solids particularly in the bottom of the reactor. Factors contributing to deviations from ideal plug flow are discussed below.

Biomass accumulation: The continual accumulation of biological solids in the reactor void spaces is expected to decrease the total (effective) volume available for waste removal. Young (65) assumed that this decrease in total void volume was proportional to the biomass concentration in the reactor. Accordingly:

$$V_1 = \alpha V_o(1-k_v M_t) \quad (22)$$

where

V_1 = Void volume corrected for accumulated biomass (L^3)

α = Filter porosity,

V_o = Initial volume of filter with filter packing (L^3),

k_v = Fractional change in void volume per gm/L of biomass concentration, and

M_t = Total biomass concentration (ML^{-3}).

Young (65) estimated the value of the fractional change in void volume, k_v, to be about 0.01 to 0.02 L/gm VSS per liter of void volume.

Short-circuiting: Young (65) stated that short-circuiting in an anaerobic filter is a function of filter geometry, hydraulic dispersion, and the movement of gas through the filter matrix. For a filter with uniform geometry short-circuiting is considered to reduce the effective volume of the reactor according to the relationship:

$$V_{actual} = V_{plug} \times (\text{correction factor}) \quad (23)$$

The correction factor in the above relationship is a function of the intensity of fluid mixing, reactor geometry, and reaction rate. This correction factor is obviously a complex function. Young (65) postulated that the major cause of mixing in an anaerobic filter column is the upward movement of gas that could cause channels to form through which the bulk of the waste stream would likely follow due to reduced hydraulic resistance. Following this argument, the effects of short-circuiting could, therefore, be related to total gas production in any given anaerobic reactor system.

The effect of short-circuiting can be viewed as decreasing the effective void volume of the filter as follows:

$$V_e = V_1(1-r_s q) \tag{24}$$

where

V_e = Effective void volume of the filter (L^3),

V_1 = Void volume of the filter corrected for biomass accumulation (equation 22) L^3,

r_s = Fractional change in void volume per unit volume of gas flow per day per unit cross sectional area, and

q = Gas flow rate at given filter height (unit volume per day per unit cross-sectional area).

Combining Equations 22 and 24, an expression for the effective volume, V_e, of the anaerobic filter is obtained:

$$V_e = \alpha\, Vo(1-k_v M_t)\,(1-r_s q) \tag{25}$$

It should be emphasized that Equation 25 is a simplified form of the effects of short-circuiting. This expression is expected to be useful only over a limited range of gas flow rates since it suggests that at a certain high gas flow rate the effective void volume would approach zero which in reality is not true.

Biomass transport: The concentration of biological mass in the anaerobic filter system is limited by the available void volume, bacterial decay and removal in the effluent, and by intentional wastage. Biomass transport from one level of the anaerobic filter to another is generally the result of either hydraulic uplifting or floatation by gas bubbles attached to biomass flocs or both. Since hydraulic detention times in anaerobic filters are generally sufficiently long enough so that the settling velocity of biomass floc is greater than the upward liquid velocity, the most significant factor causing biomass transport would be the floatation action caused by gas movement through the filter matrix. Due to the normally co-current movement of liquid and gas streams in an anaerobic filter, net biomass movement at any given horizontal cross-sectional area, A, at height H tends to be upwards.

Young (65) assumed that the fraction of biomass transported upwards is proportional to the rate of gas flowing through the cross-sectional area A. For an incremental anaerobic filter volume of area A and thickness dx, a mass transport balance is written as follows (assuming no growth or decay):

$$\text{In} - \text{Out} - \text{Rate of change in storage} = 0 \tag{26}$$

And the rate of upwards solids transport is as follows:

$$\text{In} = A(r_m q M) \tag{27}$$

where

r_m = Fraction of biomass transported when q equals one unit volume per day per unit cross-sectional area, $(\text{liters/unit volume})^{-1}$

And:

$$\text{Out} = A\, r_m \left(q + \frac{\partial q}{\partial x}\, dx\right) \left(M + \frac{\partial M}{\partial x}\, dx\right) \tag{28}$$

And:

$$\text{Rate of change in storage} = Adx\left(\frac{\partial M}{\partial t}\right)_f \tag{28a}$$

Substituting Equations 27, 28, and 28a into Equation 26, then the rate of change in biomass concentration, measured as VSS, in an incremental volume Adx is:

$$\left(\frac{\partial M}{\partial t}\right)_f = \frac{r_m}{dx} qM - \frac{r_m}{dx}\left(q + \frac{\partial q}{\partial x} dx\right)\left(M + \frac{\partial M}{\partial x} dx\right) \tag{29}$$

Substrate diffusion: As was discussed previously, the "Substrate Gradient Factor" concept was developed to account for substrate diffusion and utilization by bacterial biofilms in anaerobic filters. This concept was expressed mathematically by Equations 15 through 18.

Development of the Anaerobic Filter Model

Using the basic kinetic equations (Equations 1 through 5), a materials balance for organic substrate and biological solids in the anaerobic filter was made by Young (65) for elemental sections of the basic anaerobic filter. Figure 11 shows a schematic diagram of such elemental sections. This section represents a "finite" anaerobic filter. It has an effective void volume, dV_e, a total void volume, dV, a cross-sectional area, A, an average active biomass concentration, M, a measurable substrate concentration, S, and an effective concentration, $\bar{S}$. The expressions devised to describe the physical characteristics of the anaerobic filter (Equations 22 through 29) are also included in the development of the anaerobic filter model (65).

The solution technique used in the anaerobic filter model was basically that of finite differences analysis. The filter height was divided into

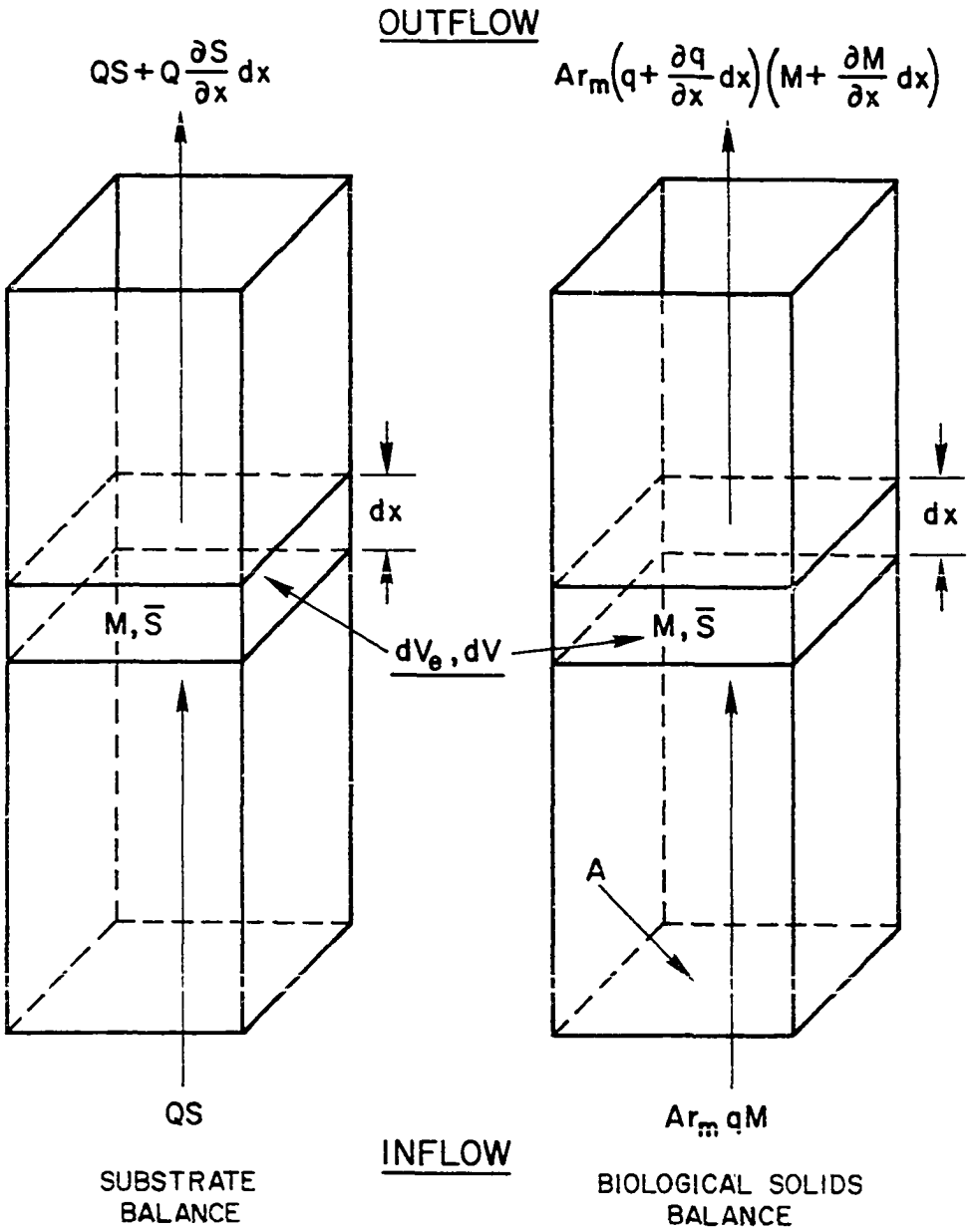

Figure 11. Elemental sections of the anaerobic filter process used for developing a materials balance for substrate and biomass concentrations (65)

individual small intervals of equal thickness. Each of these intervals was considered to perform as an individual reactor in a series of reactors, the total of which make up the anaerobic filter reactor. A reiterative solution technique allowed for continuous accounting of biomass and substrate concentrations throughout the reactor column.

The anaerobic filter model will be discussed again in a later section of this report. All physical and kinetic constants and coefficients will be quantitatively defined and the model's ability to simulate actual anaerobic filter operation will be tested by comparison to actual pilot-plant data obtained during this study.

Effects of Anaerobic Filter Media

As was indicated earlier through the review of previous anaerobic filter applications, a variety of media types have been used in anaerobic filter operation. Most of the media used in these studies were either small quartzite stones (usually 1-1.5 in. (25-38 mm) in diameter) or small plastic or ceramic rings and modules. The effects of media on anaerobic filter performance, therefore, are not very well-documented since no known studies have been reported with that explicit purpose in mind.

Young (65) postulated that higher organic loading rates (higher than this investigator applied) should be possible by using more porous media than the small stones used in his studies. Use of highly porous media would obviously increase the effective volume of the filter and presumably lessen the effects of solids transport and channeling due to the increase in cross-sectional area through which the product gas must flow upwards through the column.

Simulated performance obtained by the anaerobic filter model led Young (65) to estimate that anaerobic filters using plastic media with a porosity of 95 percent should result in about the same (or better) performance when loaded at 424 lb COD/MCF-day (6.8 gm COD/L-day) as anaerobic filters using stone media (porosity of about 42 percent) and loaded at 212 lb COD/MCF-day (3.4 gm COD/L-day). This comparison is based on the assumption that a volatile acids waste is used at an influent COD concentration of 3000 mg/L. It was reported that the results of a laboratory investigation using highly porous media supported the predicted improved performance (65). In this investigation a honey-combed material was placed only in the upper 54 in. (1.37 m) of a reactor column so that the bottom 18 in. (0.45 m) section of the reactor contained no media and its contents were mechanically mixed. The reactor column was fed a volatile acids substrate at a loading rate of 106 lb COD/MCF-day (1.7 gm COD/L-day) and at an influent concentration of 3000 mg/L. The results of this investigation compared favorably with the calculated results using the anaerobic filter model and identical operation conditions (65).

Young (67) suggested that an important factor in medium selection is its ability to capture and hold solids either by surface adhesion or by its ability to effect solids flocculation and entrapment in void spaces. Indications are that a major fraction of the total solids in an anaerobic filter are held in suspension in the media void spaces. These solids tend to become well-flocculated and eventually form granules that are held in suspension in the filter interstitial spaces. Young (67) suggested that anaerobic filter media must permit these flocculated solids to be transported through the media bed or otherwise be wasted from the

anaerobic filter in order for the media bed not to become plugged.

This granulation seems to be an important factor in the filter performance since these granules (or flocs) can increase the total available biological surface area. These biomass granules are expected to settle to the bottom of the filter thus forcing substrate removal to take place at the lower sections of the filter. The degree of solids settling will be greatly influenced by the anaerobic filter media characteristics. However, biomass settleability must be balanced by both hydraulic uplifting and solids transport due to the upwards movement of the product gas, otherwise the lower sections of the filter would soon become plugged, thus leading to possible failures. In this respect, media must be designed so that their pore spaces allow enough solids to migrate upwards to avoid such plugging. Young (67) suggested that media pore spaces, in modular media, having openings of less than 1/2 in. (13 mm) may lead to hampering of solids transport while openings larger than 1 1/2 in. (38 mm) may lead to excessive short-circuiting.

The lower limit on pore space size suggested by Young (67) may have merit since attached biomass growth would contribute significantly to the reduction of effective pore space. However, the upper limit is likely to be controlled by the specific design of the media modules and their ability to minimize short-circuiting. There are currently media available commercially that have designs such that the hydraulic flow pattern through them is of a cross-flow nature, thus keeping reactor contents continuously intermixed on a horizontal plane while maintaining near plug flow in a vertical direction. This cross-flow pattern also can enhance granulated floc settleability and entrapment and thus potentially

increase overall filter performance. Consequently, the media pore size may have to be optimized through either dynamic modeling or more realistically through extensive pilot-plant testing or both.

The concept of biomass granulation is obviously an important characteristic in anaerobic filter treatment. However, it must be realized that such anaerobic floc tends to have specific gravities that are seemingly very close to that of water and thus hydraulic flow rates must be such that excessive biomass transport is minimized.

EXPERIMENTAL STUDY

Test Reactors

In this study, four anaerobic filter reactors each measuring 20 in. (0.51 m) in diameter and 6 ft. (1.83 m) in height were constructed using aluminum sheeting. These columns were surrounded with a water jacket so that constant-temperature water could be circulated around the reactor sections to maintain their contents at a constant temperature. Figure 12 shows a profile of these columns.

The columns were designed so that a variety of column packings could be used as the biological support medium. These columns could be stacked to provide heights greater than six feet. Each column was equipped with an inlet manifold, a medium support grate, and a flat plate (1/2 in.) aluminum cover. Each column also was equipped with a minimum of three dispersion rings (2 in. wide) to reduce the tendency of the liquid inside the reactor to travel along the reactor walls. Sampling taps were provided at 1 ft. (0.3 m) intervals along the reactor height. Because of the difficulty of placing sample taps through the reactor wall due to its double-wall construction, sampling tubes had to be run (from any given height interval) to taps on the reactor cover plate. This scheme allowed the sample tubes to be placed directly at the center of the reactor. These sampling taps were used to collect column profile samples for COD, suspended solids, and volatile acids analyses.

During this study, two to four reactors were operated simultaneously at the same flow rate and at the same organic loading rates. The only difference between these columns was in the biological growth support

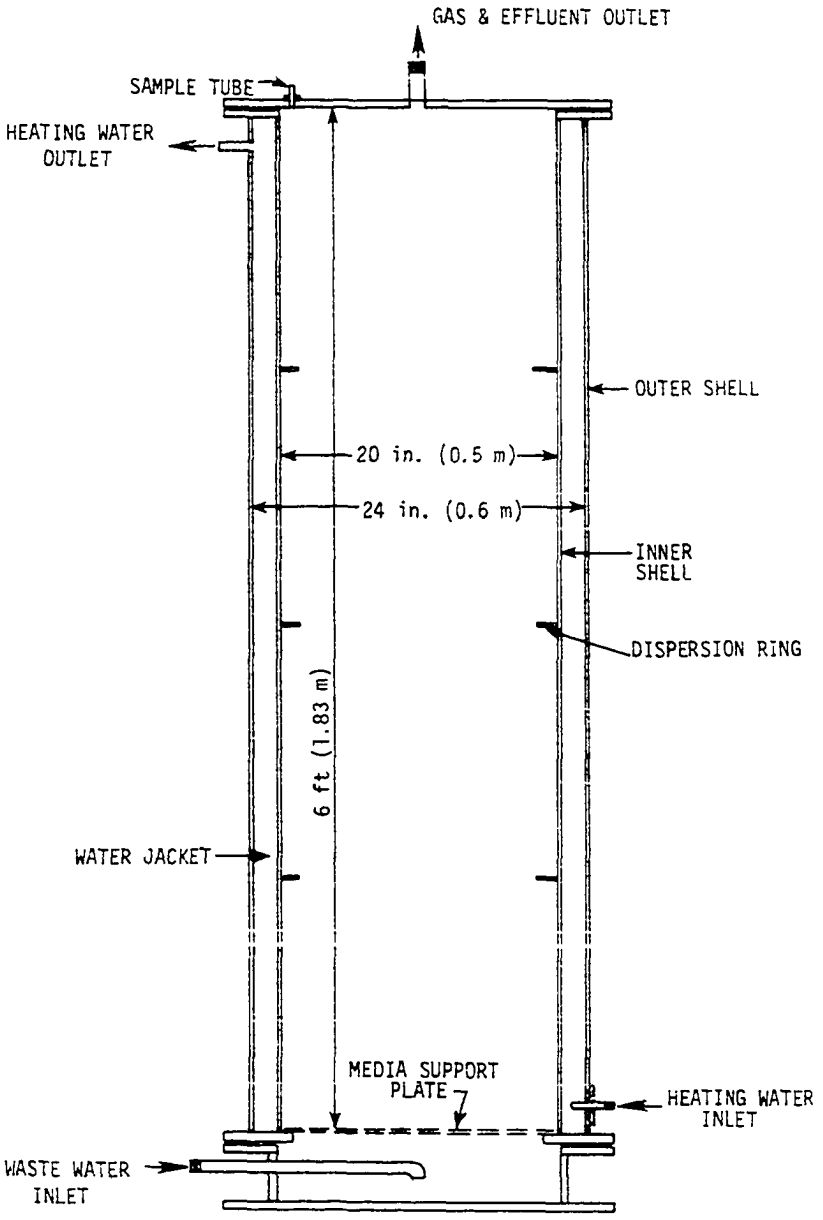

Figure 12. Schematic diagram showing details of anaerobic filter reactors used in this study

medium inside each reactor. The choice of these media will be discussed in detail in a later section.

Feed and Temperature Control System

The size of the pilot plant system necessitated that the feed solution to the system be prepared in a concentrated form and then fed by diluting it with tap water to the proper strength. This system of feedstock preparation eliminated the need to prepare and store large quantities of dilute feedstock material.

The feed and temperature control systems are illustrated schematically in Figure 13. As shown, a 1/3 hp centrifugal pump[1] was used to supply water for temperature control and for feedstock dilution from a single supply tank. The temperature in the supply tank was controlled using electric heater elements to supply heat as needed. The water temperature in the supply tank was regulated electronically using a cycling temperature controller[2] and a platinum probe.[3] Because heated water was pumped through the water jackets and returned to the supply tank at much higher rates than were actually needed, little temperature loss was experienced. In fact under normal operating conditions it was possible to maintain the operating temperature with less than 0.5°C variation. The loss from the supply tank as inlet dilution water was made up continuously using a float-controlled valve connected to the Iowa State University water supply

---

[1]Teel Pump, Model 3P577A, Dayton Electric Manufacturing Co., Chicago, IL 60648.

[2]Versa-Therm Electronic Temperature Controller, Model 2158-4, Cole-Parmer Instrument Company, Chicago, IL 60648.

[3]Series 400 Probe, Cole-Parmer Instrument Co., Chicago, IL 60648.

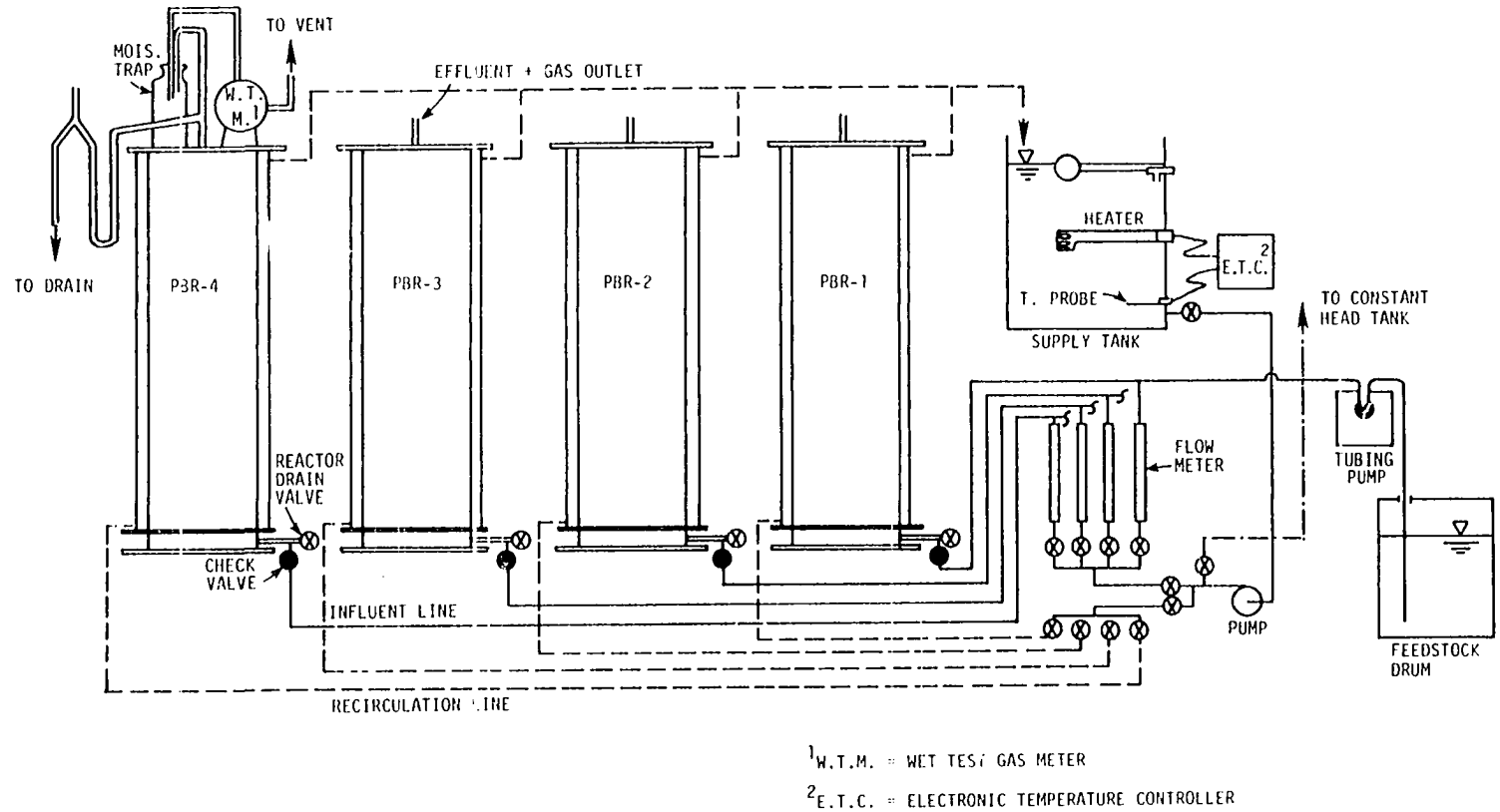

Figure 13. Schematic diagram showing the entire anaerobic filter system used in this study

system. Influent water rates were metered using glass-tube flow meters.[1]

The concentrated feedstock solution was metered using positive displacement tubing pumps[2] and was injected into the influent lines immediately after the glass-tube flow meters so that the combination of both streams provided the desired total influent flow rate and feedstock concentration. The feedstock metering pumps were fairly reliable and accurate within reasonably short calibration intervals.

As shown in Figure 13, all influent lines were equipped with sufficient valves to isolate any individual reactor. In addition, check valves were installed on influent lines to prevent the back flowing of column contents. All influent and supply lines in addition to the supply tank were insulated to minimize heat loss. All influent and temperature recirculation lines were made of nylon reinforced 1/2 in. (13 mm) hose.

Effluent streams

Liquid effluent and product gas were both collected using the same outlet on top of each reactor. The liquid effluent was carried through an inverted siphon which prevented the product gas from escaping through the drain lines (Figure 13) and was discharged to the floor drain.

The product gas was passed through a moisture trap to prevent the movement of any liquid effluent droplets to the gas meters. Gas volume measurements were made using wet-test gas meters.[3] The moisture traps and

---

[1]Rotometer, Model R-6-15-B, Brooks Instrument Division, Emerson Electric Co., Hatfield, PN 19440.

[2]Masterflex Tubing Pumps, Model 7565, Cole-Parmer Instrument Co., Chicago, IL 60648.

[3]Wet-Test Gas Meter, Model 63115, Precision Scientific Co., Chicago, IL 60647.

gas meters were mounted on top of each column. Total gas production was determined on a daily basis.

Feedstock (substrate) material

Background: The recent decline in petroleum supplies has led to a considerable interest in ethyl alcohol (ethanol) as a supplement to or replacement for common hydrocarbon fuels. As a result, terms such as "gasohol" (a mixture of 10% ethanol and 90% unleaded gasoline) have become familiar particularly in the midwestern United States. Ethanol for this use commonly is produced by fermentation of grains such as corn and wheat although sugar cane, sugar beets, and other cellulosic biomass materials can be utilized effectively (3, 4, 18, 45, 52). Fermentation basically involves the enzymatic hydrolysis of long-chain polysaccharides to sugars and the subsequent conversion of these sugars to alcohol and carbon dioxide by yeast in an aqueous medium. Alcohol is then extracted from the water through distillation.

Ethanol production by fermentation and its distillation requires the use of considerable quantities of water throughout the process. Although a portion of this water can be recycled, complete reuse generally is not possible because of the buildup of salts and toxic byproducts of the fermentation reaction. In general, an accepted measure of water use for grain alcohol production is about 16 gallons of water (exclusive of cooling and support function use) per gallon of ethanol produced (61). This figure is often higher depending on the nature of the process by which alcohol is produced (61). Almost all of this water is mixed with the grain solids and becomes "stillage" or the product remaining after

removal of the alcohol by distillation. The solids usually are removed by screening, pressing or centrifugation leaving a "thin stillage" containing a high concentration of soluble and colloidal organic material.

While disposal of stillage at small alcohol production facilities may not pose significant problems, large facilities are faced with considerable quantities that must be treated before discharge or disposal. Because of the relatively high organic content of stillage, its treatment can be a major cost item that can have a measurable impact on the economic viability of grain alcohol production. Therefore, it is important that the cost of stillage treatment is kept at a minimum.

Anaerobic treatment potentially is attractive since a portion of the grain energy remaining in the stillage can be recycled as methane gas to provide heat for the distillation process (which is very energy-intensive). Anaerobic filter treatment, in particular, offers a variety of advantages to grain fermentation operations that make this process extremely attractive. These advantages include the ability to handle high organic loadings, the ability to withstand intermittent operation, and the relative stability compared to other treatment processes. An additional, and equally important, advantage is that anaerobic filter treatment can be more cost effective because of its lower operating costs (20). These advantages make the anaerobic filter process a practical alternative for the treatment of alcohol stillage wastes.

Before waste stillage could be used in this study as the substrate (feedstock) to the anaerobic filter units, the task of arriving at a relatively accurate characterization of typical stillage composition from alcohol production facilities became primary. Consequently, a

number of farm-sized grain alcohol production facilities were visited to document their operational characteristics and to collect wastewater (or stillage) samples. Once a typical "fingerprint" of waste stillage became known, this fingerprint was used to prepare a synthetic stillage which was then used as a feedstock to test the performance of pilot-scale anaerobic filters. Details of the sampling and analyses procedures of waste stillage samples were described elsewhere (12).

A summary of the stillage composition is shown in Tables 1 and 2. Of particular importance to this study are parameters such as BOD_5, COD, nitrogens, alcohols and fatty acids. These parameters best illustrate the magnitude of the pollutional potential of stillage if it were to be discharged with little or no treatment. In all samples, the COD exceeded 23,000 mg/L - a rather high strength when compared to typical domestic wastewater.

As seen from Table 2, most of the stills did not extract all the ethanol from the fermented mash. In addition, a variety of other residual alcohols or fusel oils were detected in measurable concentrations. All of these alcohols exert oxygen demand and therefore are included in the COD measurement. Acetic and propionic acids were the predominant volatile acids although sizeable quantities of butyric and hexanoic (caproic) acids were detected in two samples. All of these volatile acids also are oxidized in the COD test.

Additional analyses were conducted to characterize the stillage samples as to their starch and other carbohydrate content. Although small amounts of starch were detected by the starch-iodine test procedure, the unavailability of reliable procedures for measuring individual carbohydrates

Table 1. Summary of stillage analyses[a]

Parameter	Ethanol Production Facility				
	ECL[b]	CII[c]	ISU[d]	KOC[e]	RCC[f]
BOD	28,400	20,800	38,600	54,400	43,100
COD	36,800	23,100	60,500	98,700	59,400
TS	12,200	(35,000)	52,000	40,400	39,460
VS	9,870	(29,900)	49,000	38,270	30,980
TKN	266	361	224	532	546
NO_2 + NO_3-N	0.45	2.6	0.25	0.08	<0.5
NH_4-N	4.5	10	31.5	0.37	0.05
SO_4	300	--[g]	466	388	299
PO_4	400	--	477	544	700
Ag	<0.002	--	<0.02	0.01	0.004
As	<0.015	--	0.005	NA[h]	<0.005
Ba	0.09	--	0.30	NA	0.39
Cd	0.01	--	0.006	0.006	0.2
Cr	0.02	--	0.006	0.02	0.058
Ka	0.13	--	0.17	0.15	0.38
Hg	<0.002	--	NA	0.0015	0.004
Pb	0.05	--	0.03	0.04	0.1
Zn	4.41	--	5.2	13.8	5.05

[a]All units are in mg/L.

[b]Energy Concepts Limited, Linden, Iowa.

[c]Conrad Industries Inc., Bonaparte, Iowa.

[d]Iowa State University, Department of Agricultural Engineering, Ames, Iowa.

[e]Keith O'dell Company, Leon, Iowa.

[f]Roberts Chemical Company, Audubon, Iowa.

[g]Insufficient sample quantity to complete analysis.

Table 2. Summary of stillage analyses--alcohols and fatty acids[a]

Parameter	Ethanol Production Facility					Range	Composite
	ECL	CII	ISU	KOC	RCC		
Ethanol (%)	1.6	0.6	2.8	1.3	1.1	0.6-1.6	1
Propanol	15.7	7.6	21	66.7	6.5	6.5-66.5	25
2-methyl-1-propanol	8	3.5	-	18.6	48.8	3.5-48.8	20
2-methyl-1-butanol	-	T	-	2.6	14.9	0-14.9	8
Butanol	3.6	-	T[b]	-	-	0-3.6	1
Tert-amyl-alcohol	0.9	2.0	-	-	-	0-2.0	1
Iso-pentyl alcohol	-	21.2	-	12.9	40.1	0-40.1	20
Acetic acid	935	1910	NA	684	557	557-1910	1000
Propionic acid	2	2	NA	134	145	2-145	70
Iso-butyric acid	2	2	NA	-	-	0-2	-
Butyric acid	125	400	NA	-	-	0-400	130
Caproic acid	40	120	NA	6.7	-	0-120	40
Valeric acid	-	-	NA	12	9.6	0-12	5

[a]All units are in mg/L unless otherwise noted.

[b]T = Trace.

(i.e. sugars) made the task difficult and estimates of such carbohydrates had to be made on the basis of overall COD test results.

It was also suspected that stillage may contain higher molecular weight alcohols than shown in Table 2. The nature and typical concentrations of such alcohols are not well established in the literature and therefore the effort to establish their concentrations was limited by the fact that their identity was not known.

Feed Composition: The concentrated synthetic waste used as the feedstock to the anaerobic PBR units was designed based on the fingerprint obtained from the alcohol stillage sampling program as described previously. A mixture of volatile acids and short chain alcohols was prepared to provide the relative amounts of materials as shown in Table 2. Because of their small concentrations and lack of characterization, no high molecular weight alcohols were added to this synthetic wastewater. Sucrose (table sugar - a readily biodegradable material) was added to simulate the carbohydrate fraction of stillage. No starch or other nonsoluble materials were added.

Nutrient and buffering required to sustain an active microbial culture also were added (Table 3). The chemicals used in the feedstock preparation were either reagent grade or the best available technical grade material. The nutrient composition was selected from work by Speece and McCarty (54) and Young (65) and was designed to provide the elements needed for supporting anaerobic biological growth. Alkalinity was added in the form of sodium bicarbonate at levels sufficient to keep the pH at near neutrality throughout the reactor height. All of the ingredients were

mixed together and stored in a 208 L (55 gallon) plastic-lined drum. A mineral analysis of the tap water used to dilute the concentrated feedstock is presented in Table 3.

It should be noted that the feed composition shown in Table 3 was based on a total influent COD of 1500 mg/L. At higher influent COD concentrations the ratios of nutrient and buffer to total COD content were kept constant as long as the known bacterial requirements were satisfied according to established stoichiometric relationships. This particular point is discussed in more detail in the section on experimental design.

Media selection

The choice of reactor media to be placed in the anaerobic filters used in this study was of particular importance to the overall program of experimentation. As pointed out earlier, there currently is a large variety of reactor media available in the market-place particularly in the chemical distillation industry. Few types of media have been thoroughly tested in general municipal treatment wastes particularly in conjunction with trickling filters.

Synthetic reactor media generally are available commercially in two types: 1) modular blocks, and 2) loose-fill. Modular blocks generally are made of polyvinyl chloride (PVC) or other plastic materials in corrugated sheets laminated in a variety of configurations and with and without any slope to the corrugation flutes. Loose-fill type media generally are made of polyethylene, polypropylene, and other plastic resins as well as ceramic and stainless-steel.

The basic requirement in the selection of reactor media was that such media be available commercially and have no physical or chemical

Table 3. Reactor feed composition

Component	Concentration mg/L	COD equivalent[a] gm COD/ml (of mixture)	COD %
CONCENTRATED FEEDSTOCK			
Alcohols[a]	1000	1.593	66.66
Volatile Fatty Acids[b]	100	1.243	6.67
Carbohydrates[c]	400	1.123	26.67
Nutrients:			
$FeCL_3$[d]	60	-	
$CoCL_3 \cdot 6H_2O$	8	-	
Thiamine	2	-	
KOH[e]	70	-	
NH_4Cl	140	-	
$(NH_4)_2HPO_4$	20	-	
Buffer ($NaHCO_3$)	1300[f]	-	
TAP WATER			
Calcium	44.3		
Magnesium	16.5		
Iron	0.1		
Cobalt	0.002		
Zinc	0.016		
Copper	0.005		
Manganese	0.005		
Molybdenum	0.007		

[a] Based on stoichiometric calculations.

[b] See Table 1 for relative make-up.

[c] As sucrose (table sugar).

[d] Discontinued after a period of operation.

[e] Added to neutralize VFAs and provide K.

[f] Equivalent alkalinity measured as $CaCO_3$.

characteristics that would limit their applicability or use in standard environmental engineering practices. A secondary requirement for the media chosen in this study was somewhat matched porosity and specific surface area (surface area/unit volume).

Three types of column packings were chosen for this study; modular corrugated blocks[1], Pall rings[2], and perforated spheres[3] (Figure 14). The modular blocks were made of corrugated PVC sheets counter stacked and welded at the contact points so that the media flutes were slanted at about 60^{o} with respect to the horizontal plane. These media permitted cross-flow in the horizontal direction thus, perhaps, reducing the effects of short-circuiting as the fluid travelled upwards through the reactor. Two reactors (PBR-1 and PBR-4) were packed with this type of media (Table 4).

The modular corrugated media were cut in cylindrical blocks 20 in. (0.50 m) in diameter and 1 ft. (0.30 m) in height and were placed into the anaerobic filters. The larger size of these media, having a specific surface area of 30 ft^2/ft^3 (100 m^2/m^3), a pore size of 3 in. by 2 in. (75 mm by 50 mm), and a porosity in excess of 95 percent, was placed in the first anaerobic filter (i.e. PBR-1). The second size of corrugated media, having a specific surface area of 42 ft^2/ft^3 (140 m^2/m^3), a pore size of 2 in. by 1.5 in. (50 mm by 40 mm), and a porosity of about 95

---

[1]"BIOdek" corrugated media, Manufactured by the Munters Corporation, Ft. Myers, FL 33901.

[2]"ACTIFIL-90", Manufactured by Norton Chemical Products Division, Akron, OH.

[3]Perforated spheres, Manufactured by K and S Manufacturing Co., Freemont, IL for General Filter Company, Ames, IA.

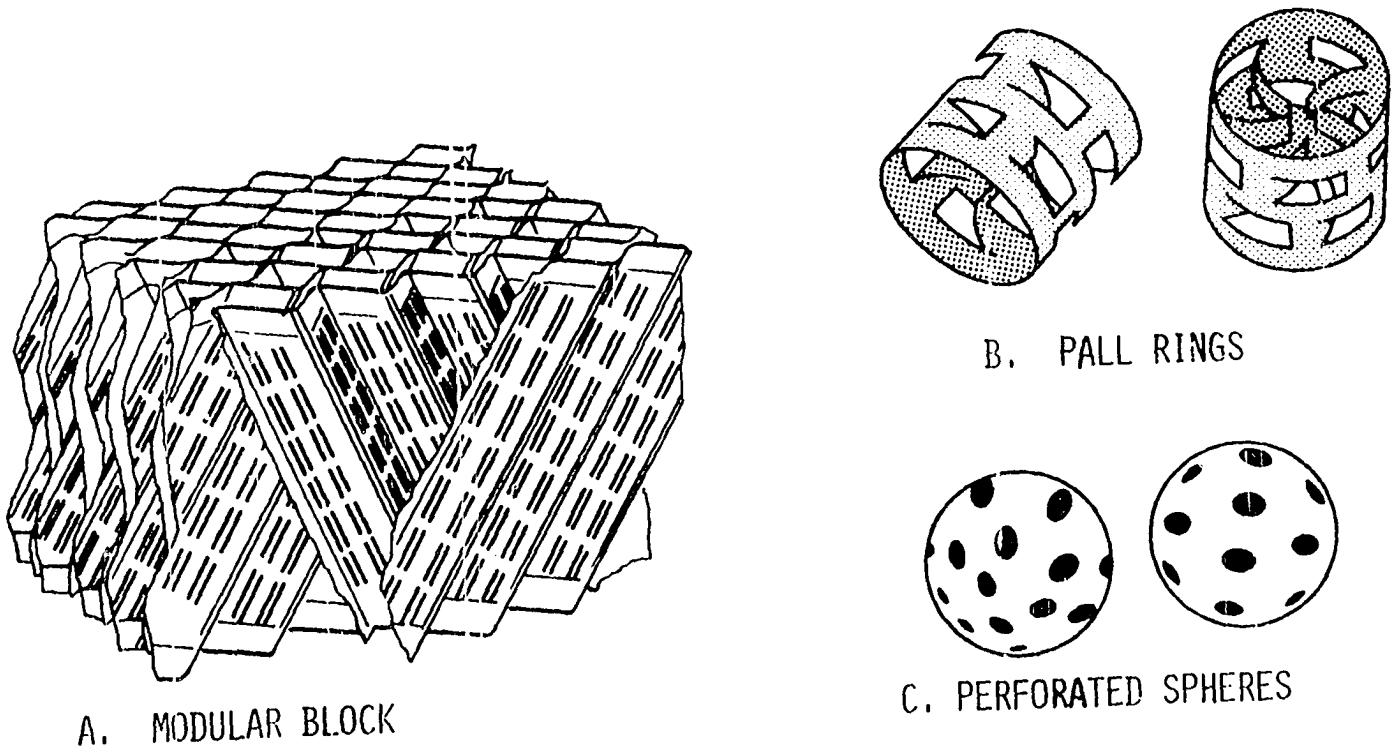

Figure 14. Types and shapes of anaerobic filter media used in this study. (A) Modular blocks, (B) Pall rings, and (C) Perforated spheres

Table 4. Anaerobic filter packing media characteristics

Reactor	Media type	Specific Surface Area m^2/m^3, (ft^2/ft^3)	Porosity %
PBR-1	Modular Blocks	100, (30)	95
PBR-2	Perforated Spheres	82, (25)	95
PBR-3	Pall Rings	103, (31)	95
PBR-4	Modular Blocks	140, (42)	95

percent, was placed in reactor PBR-4. This medium was cut in cylindrical blocks in the same manner as before.

The second type of medium used in this study consisted of polypropylene perforated balls (Figure 14). This medium was 3.5 in. (90 mm) in diameter and had a porosity in excess of 95 percent and a specific surface area of about 25 ft^2/ft^3 (82 m^2/m^3). This medium was placed in reactor PBR-2.

The third type of medium used in this investigation was polyethylene resin Pall rings (Figure 14). Each cylindrical ring was 3.5 in. (90 mm) in diameter and 3.5 in. (90 mm) in height. The in-place porosity of this medium was in excess of 95 percent and its specific surface area was about 31 ft^2/ft^3 (103 m^2/m^3). This medium was placed in reactor PBR-3 (Table 4).

As seen from Table 4, the larger size of the modular blocks media and the other two types had somewhat comparable pore sizes as well as comparable specific surface areas. The decision to fill reactor PBR-4 with the smaller pore sized modular media was based on the desire to

compare the relative performance of two media having the same design but having markedly different specific surface areas.

The modular blocks media had also been used in tube settlers and therefore it was desired to see if this characteristic could have any detectable effects on the performance of anaerobic packed-bed reactors. With its high porosity and its slanted tube design, it is possible that most of the solids settling in the upper sections of the anaerobic filter would eventually migrate to the lower portions of the column. This would result in much higher organic removal rates in the bottom sections of the filter than its higher sections and would help in reducing losses of suspended solids in the effluent.

EXPERIMENTAL DESIGN

Synthetic Waste

As was pointed out previously, the results of the grain alcohol distilling wastewater characterization were used as a fingerprint in formulating the substrate used in this anaerobic filter study. As was shown in Table 3, the basic makeup of the influent feed to the anaerobic filters consisted basically of an alcohol mixture, a volatile acids mixture, and a carbohydrate supplement. Alcohols provided about 66.7 percent, volatile acids about 6.7 percent and table sugar (sucrose) about 26.6 percent of the total COD content of the influent. These major components were mixed together in a large mixing tank after adding the necessary nutrients and buffering chemicals. The concentrated feed solution contained 51.4 gm COD/L and 50 gm of sodium bicarbonate alkalinity (as $NaHCO_3$) per liter. After being thoroughly mixed, this solution was transferred to a plastic-lined, 55 gal. (208 L), drum out of which it was metered to the anaerobic reactors at the desired rates.

Throughout this study the influent substrate was designed to maintain the minimum metabolic requirements of basic nutrients such as nitrogen and phosphorus (Table 5). The proportion of added nitrogen and phosphorous was varied during the study in order to maintain a COD/N/P ratio of 30/2/0.5.

The volatile acids in the feedstock mixture were neutralized using equivalent amounts of potassium hydroxide (KOH). This step not only prevented undesirable alkalinity consumption by volatile acids in the influent, but also provided an antagonistic cation to the sodium cation which was

Table 5. Basic anaerobic filter feedstock components

Loading Rate gm COD/L-day	Influent COD (mg/L)	NH_3-N (mg/L)	PO_4 (mg/L)	Alkalinity (mg/L $CaCO_3$)
0.50	1500	65	5	1300
1.00	1500	65	5	1300
2.00	3000	122	33	2400
4.00	6000	244	66	3500
8.00	6000	244	66	3500
16.00	6000	244	66	3500

added as sodium bicarbonate. At any rate, potassium would have had to be added as a trace element which is necessary for bacterial growth.

While tap water provided some of the necessary trace elements such as calcium, magnesium, and iron, other minerals such as cobalt (added as cobalt chloride) were added in trace amounts according to recommended amounts observed in the literature (54). Trace amounts of thiamine hydrochloride (Vitamin B_{12}) also were added (see Table 3). Iron was added at substantial quantities at the start of the study for a few months. This practice was discontinued since iron floc fouled the feedstock metering pumps and tubing. It was extremely difficult to put ferrous or ferric iron into solution due to the high concentrations of alkalinity in the feedstock concentrate. Instead iron was added (as ferrous sulfate) periodically for short periods of time. No noticeable consequences were observed due to this procedure.

Loading Rates

One of the advantages of the anaerobic filter process is that the reactors can be operated at extremely high organic loading rates as compared to conventional aerobic processes. This characteristic was quite evident from the literature cited earlier. One of the basic objectives of this study was to observe the media design effects on the performance of anaerobic filters operating over a wide range of organic loading rates. Consequently, the anaerobic filters were started at a fairly low loading rate and were operated until steady-state conditions were achieved. The loading rate was then increased by a factor of two. All reactors were operated simultaneously at the same loading rate and input waste concentration.

After an initial start-up period, the organic loadings were set at 0.5 gm COD/L-day (31 lb COD/MCF-day). After steady-state operation was attained, as determined by constant gas production rates and constant effluent COD concentrations, the reactors were operated for a period of time to collect enough data to document performance. The loading rate was then doubled to 1.0 gm COD/L-day (62.4 lb COD/MCF-day). The reactors were operated at this rate for a period of time after steady-state conditions were reached before being switched to the next loading rate (i.e. 2.0 gm COD/L-day (125 lb COD/MCF-day)), and so on (Table 6). The sequence of organic loading rates was continued until a maximum loading rate of 16 gm COD/L-day (1000 lb COD/MCF-day) was reached. The period of operation at each loading rate represents one phase of this study.

The influent COD concentration was varied from an initial concentration of 1500 mg/L at the lower loading rates to 6000 mg/L at the higher rates. The main criterion in selecting these influent COD concentrations was that a reasonable hydraulic retention time be chosen to correspond to a reasonable value under the prevailing conditions. Table 6 summarizes the organic loading rates, influent COD concentrations and corresponding hydraulic retention times. It should be noted that all hydraulic retention times were computed on the basis of empty-tank reactor volumes (i.e. 370 L).

As phase 5 of this study (organic loading rate of 4.0 gm COD/L-day (250 lb COD/MCF-day)) was nearing completion, it was decided to discontinue operation of reactors PBR-2 and PBR-3. These two reactors contained loose-fill media. All data collected to that point had indicated that loose-fill media reactors were resulting in considerably poorer performance as compared to reactors PBR-1 and PBR-4 which contained the modular blocks

Table 6. Organic loading rates, influent COD concentrations, and hydraulic retention times used in this study

Study Phase	Loading Rate (gm COD/L-day)	Influent COD (mg/L)	HRT (hrs)[a]	Duration (weeks)[b]
1	0.50	1500	72	10
2	1.00	1500	36	6
3	2.00	1500	18	7
4	2.00	3000	36	9
5	4.00	6000	36	8
6	8.00[c]	6000	18	8
7	16.00[c]	6000	9	4

[a]Based on empty reactor volume (370 L).

[b]Nominal period of operation.

[c]Only the modular media columns (PBR-1 and PBR-4) were operated at these loading rates.

media. This decision was not only made on the basis of the poorer performance of loose-fill media reactors, but also because of the high cost associated with operating four reactors at such high loading rates.

The procedure by which PBR-2 and PBR-3 were taken out of service was to stop the influent stream (feedstock and dilution water). Constant temperature recirculation water was continued indefinitely to keep the reactor's contents at the same temperature as before shut-down. The gas meters on these two reactors were read daily until gas production virtually stopped. After 4 months of complete shut-down, feedstock metering to reactor 3 was resumed at an influent COD of 3000 mg/L and a loading rate of 2.0 gm/L-day (125 lb COD/MCF-day) to observe its response after such a long period of dormancy.

Temperature of operation

Although anaerobic treatment generally proceeds at faster rates at elevated temperatures, the advantages of such higher rates are offset by the high heating requirements needed to keep the reactor contents at such elevated temperatures. For this reason anaerobic filters generally should be operated at mesophilic temperatures or as near ambient temperatures as practicable. In this study a temperature of 30°C (86°F) was deemed practical.

Sampling and Analysis

Sample collection

A regular sampling schedule was maintained throughout the length of this study. Reactor contents and effluent samples were collected on a regular basis, usually once a week at the lower loading rates. Samples

were collected twice weekly when operating at loading rates of 8 and 16 gm COD/L-day (500 and 1000 lb COD/MCF-day). This schedule was maintained during steady-state operation. During periods of non-steady-state operation (i.e. when loading rate changes were just made) samples were collected more frequently to provide better documentation of the response to the increase of the influent organic loading rates.

Samples were collected periodically from the influent lines and feedstock storage drum (Figure 15). These points were not sampled on a regular basis because the feedstock was carefully prepared and metered to the reactors at precise rates so that the characteristics of the influent waste stream remained relatively constant.

Although there were five points on each reactor in addition to the effluent stream that comprised a complete reactor profile (Figure 15), not all of inner-column sampling ports were always utilized due, in part, to plugging. In particular, after a long period of operation, the one-foot (0.30 m) height sampling ports on PBR-1 and PBR-4 became plugged due to excessive solids accumulations at the bottom of these two reactors.

When samples were collected, 200-250 mls of liquid were usually withdrawn. The sample pH was measured as soon as possible to minimize possible changes due to loss of dissolved carbon dioxide. The samples were then filtered through glass-fiber filter paper. Often it was necessary to centrifuge the sample before it could be filtered. The filtrate was split into two fractions for COD and volatile fatty acids analyses. The COD samples were analyzed as soon as possible. Volatile fatty acids (VFA) samples were usually stored at 3-5^{o}C in small (10 ml) vials after a small drop of concentrated sulfuric acid was added to each vial to fix the sample.

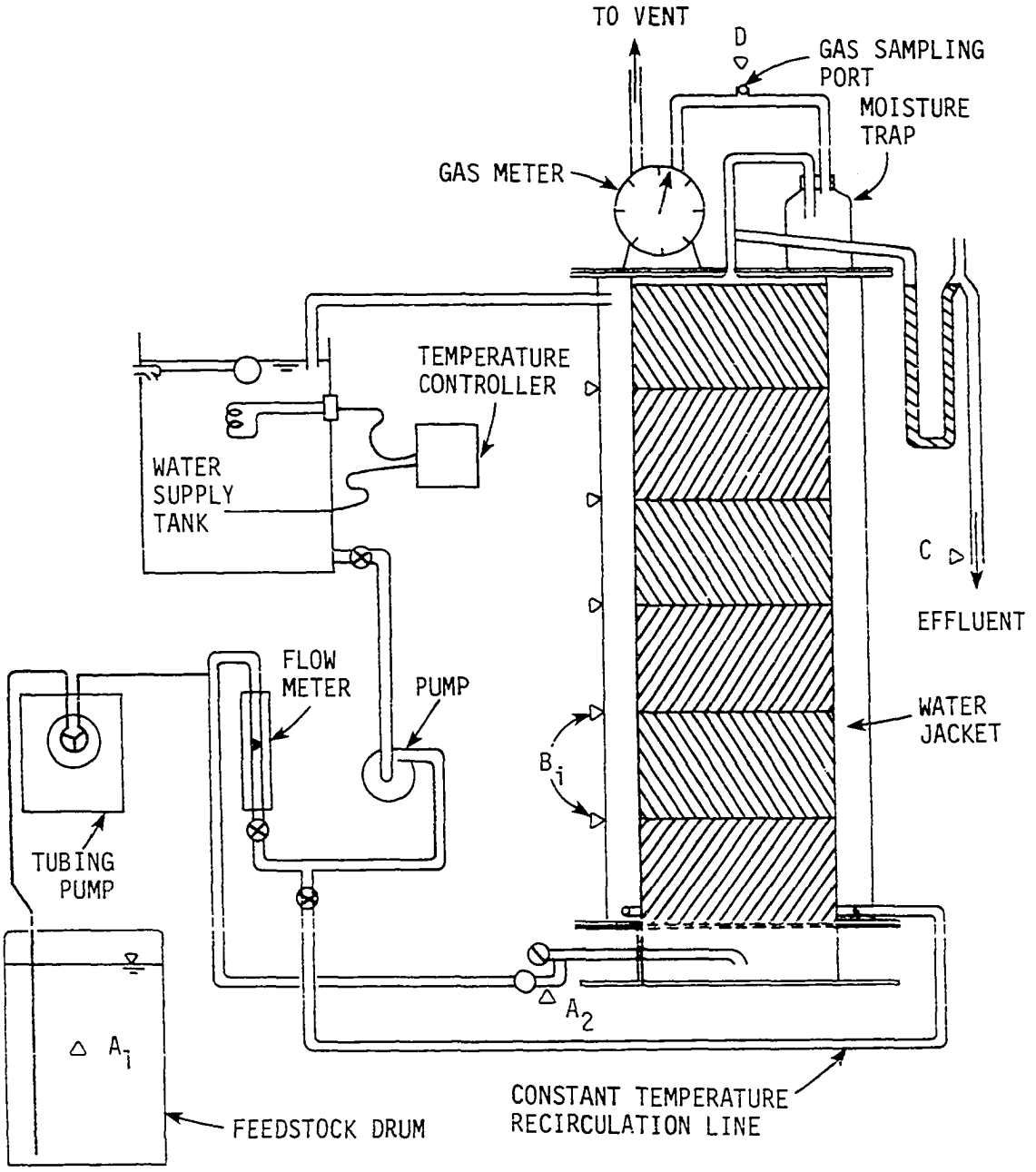

Figure 15. Schematic diagram of pilot-scale anaerobic filter layout showing feedstock metering system and sampling points

Samples for suspended and volatile solids analyses were collected in the same manner as COD and VFA samples. Suspended solids determinations were made immediately after samples were collected.

Effluent samples also were collected periodically for other determinations such as ammonia-N, total nitrogens, and total phosphates. Such analyses were conducted to insure that there were enough residual nutrients so that any possible nutrient deficiencies could be avoided.

Analytical methods

pH: Measurements for pH were made using a pH meter which was equipped with a combination glass electrode. The accuracy of this meter was 0.002 pH units.

Temperature: The temperature throughout the system remained fairly constant due to the large volume of constant-temperature water recirculated around all of the reactors. Temperature was checked periodically at several points in the system using a mercury thermometer. In general the temperature deviated less than 0.5°C from the operational set temperature. No temperature loss was experienced between the influent and effluent points on any reactor.

Suspended and volatile solids: Suspended solids analyses were made using 4.25 cm Whatman GF/C[1] glass fiber filter pads. After a specific volume was filtered through each pad, these pads were dried at 103°C (217.4°F) for at least two hours and then reweighed to determine the suspended solids concentration in the sample. Analyses were run in triplicate.

[1]Whatman Ltd., England.

Periodically the filter pads were ignited at 575°C (1067°F) for about 15 minutes to determine the volatile suspended solids. It should be noted that in the suspended and the volatile suspended solids analysis, long-term averaged blank corrections were applied. When sample suspended solids were too high for direct filtration on the glass fiber pads, smaller samples were used or diluted with distilled water. If the suspended solids concentrations were too high for accurate dilutions to be made, suspended solids determinations were made by evaporating small volumes in evaporating dishes. In such cases dissolved solids blanks were necessary to insure that reasonable suspended solids measurements were made.

Chemical oxygen demand (COD): Chemical oxygen demand (COD) determinations were made using the dichromate reflux technique described by Standard Methods (55). It should be emphasized that during this study only soluble COD measurements were made. All COD determinations were made by the Analytical Services Laboratory of the Engineering Research Institute at Iowa State University.

Volatile fatty acids: Total and individual volatile acids measurements were made using gas chromatographic techniques. A Perkin-Elmer[1] (Sigma I) gas chromatography system which included a data processing station was used in these analyses. A six foot long (1.83 mm) and 0.08 in. (2.0 mm) diameter packed column was used. The gas chromatographic conditions as well as carrier gas flow rate and detector type are listed in Table 7. Some of the samples collected during this study were run on a Hewlett-Packard[2] (Series 5730A) gas chromatograph linked to the

[1]Perkin-Elmer Corporation, Norwalk, CN 06856.
[2]Hewlett-Packard, Avondale, PA 19311.

Table 7. Operating conditions for volatile acids analysis

Gas chromatograph	Perkin-Elmer Sigma I
Column	6 ft x 2 mm ID glass
Packing	10% SP-1200/1% H_3PO_4 on 80/100 Chromosorb W AW
Temperature	115°C
Carrier gas	Nitrogen
Flowrate	35 ml/min
Detector	Flame ionization
Hydrogen flowrate	44 ml/min
Temperature	280° C
Injection port temperature	225° C
Sample size	1.0 µL

Perkin-Elmer system. All gas chromatographic conditions were identical (Table 7). The data station permitted automatic internal calibration and calculation of individual volatile acids found in every sample.

Nitrogen and phosphorus: Nitrogen (ammonia and total Kjeldahl nitrogen (TKN) and total phosphate measurements were conducted using procedures outlined by Standard Methods (55). A Technicon Auto Analyzer[1] was used in these determinations. All of these tests were conducted by the Analytical Services Laboratory at Iowa State University.

Gas analysis: Gas analysis was performed using a Packard (7411S)[2] gas chromatograph. Gas samples were withdrawn from ports placed in the effluent gas line between the moisture trap and the gas meter on the top of each reactor (Figure 15). Gas chromatographic conditions used for these determinations are listed in Table 8.

Daily gas production rates were smoothed using a five-day moving average technique. This smoothing technique allowed for the dampening of variations in total gas flows caused by irregular gas flow rates, errors in meter readings, and changes in local barometric pressure and ambient temperature conditions.

Table 9 provides a summary of sample collection schedules and analytical procedures as well as sampling points. The sampling ports indicated in Table 9 are shown on Figure 15.

---

[1]Technicon Industrial Systems, Tarrytown, NY 10591.
[2]Packard Instrument Company, Downs Grove, IL 60515.

Table 8. Operating conditions for gas analysis

Gas chromatograph	Packard Model 7411S
Column	10 ft X 4 mm glass
Packing	Porapak Q, 80/100 mesh
Temperature	95° C
Carrier gas	Helium
Flowrate	30 ml/min
Column head pressure	29 psig
Detector	Thermalconductivity
Temperature	110° C
Bridge current	250 mA
Sensitivity	10 mV
Injector block temperature	105° C
Sample size	0.5 ml

Table 9. Sample schedule and analytical procedures[a] (see Figure 15 for sampling points)

Test	A_1/A_2	Bi	C	D	Procedure
Flow rate	D	-	-	-	Volumetrically
COD	P.G.	W.G.	W.G.	-	Dichromate oxidation (55)
Sus. Solids	P.G.	W.G.	W.G.	-	Glass fiber filter (55)
Volatile acids	P.G.	W.G.	W.G.		Gas chromatography
Gas production	-	-	-	D	Wet-test meters
Gas analysis	-	-	-	W	Gas chromatography
pH	W	W	W	-	pH meter
Temperature	D	P	P	-	Thermometer
Nitrogens	P.G.	P.G.	P.G.	-	Automatic analyzer (55)
Phosphorus	P.G.	P.G.	P.G.	-	Automatic analyzer (55)
Metals	P.G.	P.G.	P.G.	-	Atomic absorption (55)

[a]D=daily, W=weekly, P=periodically, G=grab sample.

START-UP

Reactor Assembly

During the last week of July, 1980 the four reactor columns were assembled along with influent and effluent lines, temperature control system, and other appurtenances. The system was filled with clear water to test it for leaks and to make sure that the temperature control system worked properly. The media and inner column sampling tubes were placed in three of the reactor columns during the first week of August, 1980. Reactor 1 (PBR-1) was loaded with the larger-sized corrugated media blocks. In this reactor, the top media block measured only 10 in. (0.25 m) in height so as to allow for some free-board space under the column's flat lid for uniform liquid and gas collection. All media blocks were accurately weighed before they were placed in the reactor column.

The second column (PBR-2) was packed with the loose-fill perforated spheres media. Sampling taps were placed inside the column at one foot (0.31 m) intervals in a manner similar to the first column.

The third column (PBR-3) was packed with the plastic Pall rings, and sampling tubes were installed in the same manner as before. All three columns were sealed and filled with clear tap water and prepared for seeding by bringing the system temperature to 30°C (86°F).

Because the modular block media scheduled to be placed in the fourth column (PBR-4) were not ready, this reactor was not loaded and started until the end of August, 1980 (about three weeks later). PBR-4 was then loaded and prepared for seeding in a similar manner. The media blocks placed in this column were also accurately weighed before they were installed.

Reactor Seeding

The first three reactors were seeded using dilute sludge obtained from the primary anaerobic digester at the Ames Water Pollution Control Plant. This plant has a design capacity of about 4.5 MGD and receives mostly domestic waste from the Ames area. The primary sludge digester at this plant is operated continuously at a temperature of about 35°C (95°F). The exact organic loading rate to this digester was not known.

About 10 gallons (40 L) of dilute sludge having a solids content of less than 1 percent were obtained and pumped to each of the anaerobic reactor columns. Synthetic feedstock solution had been metered to each reactor at low concentrations (about 500 mg/L) for a few days before seeding to allow the reactors to become anaerobic before seeding. Feedstock metering to all reactors was stopped for about 24 hours after the columns were seeded to help prevent washout of seed organisms.

Some gas production was observed in all seed reactors about 24 hours after seeding. Feedstock metering was then restarted at a concentration of about 1000 mg/L and an organic loading rate of about 0.3 gm COD/L-day (20 lb COD/MCF-day). This feeding rate was continued for a few weeks to make sure that all reactors were not stressed during the sensitive period of starting. Gas production during this period was observed to fluctuate and seemed to decline consistently. A few days after starting, the alkalinity in the waste was increased to correct a deficiency in the sodium bicarbonate addition rates. As soon as alkalinity was restored to about 1300 mg/L (as $CaCO_3$), gas production increased considerably.

After about four weeks of operation, gas production in reactors PBR-2 and PBR-3 seemed to stabilize. However, gas production in PBR-1

declined to near zero and reseeding was deemed necessary. This reactor was therefore reseeded using about 10 gallons (40 L) of slightly thicker sludge (about 1.0 to 1.5 percent solids) from the Ames primary anaerobic digester. At the same time PBR-4 was seeded using the same type of sludge and the same seeding procedure as used previously with the other reactors. After PBR-1 was reseeded, gas production increased significantly from this reactor. All other reactors (including the newly started PBR-4) demonstrated fairly consistent gas production rates. A few weeks later it was decided that no further reseeding was necessary and active regular sampling and data collection were initiated.

The starting period for these reactors was complicated to some extent by frequent plugging of the influent flow meters and occasional failures of the feedstock and bicarbonate metering pumps. These difficulties were partially responsible for inconsistent gas production rates during the first few months of operation as will be discussed later. After about two months, most operational difficulties and problems were corrected and the entire system operated with considerable consistency and reliability.

RESULTS

Anaerobic Filter Performance During Start-up

As was pointed out earlier, the anaerobic packed-bed reactors were initially operated at both low loading rates and low influent concentration. The purpose was to allow the filter biological mass to become acclimated to the new environmental conditions with as little stress as possible. This was deemed necessary since the seed material was fairly dilute resulting in somewhat lightly seeded reactors.

The responses of the individual anaerobic filters to an influent COD concentration of about 1000 mg/L and an influent organic loading of about 0.3 gm COD/L-day (20 lb COD/MCF-day) were markedly different from each other. This response could not be related to any physical or environmental factors except, perhaps, to how well the seed material became adjusted to the new reactor conditions. Figure 16 summarizes total gas production data during the starting period. As shown, reactor PBR-1 (large modular media) did not respond well to starting conditions, and total gas production was extremely low during most of this period. Once this reactor was reseeded (and perhaps more properly), total gas production increased gradually and the reactor began to respond in a satisfactory manner.

Unlike PBR-1, reactors PBR-2 (perforated spheres) and PBR-3 (Pall rings) seemed to have received adequate amounts of seed material since gas production reached equilibrium rapidly. The response of reactor PBR-2 was somewhat more variable than was the response of PBR-3 as evidenced by the more fluctuating gas production data. Reactor PBR-4 (smaller-sized modular medium) responded satisfactorily to seeding. As shown in Figure 16, gas production rates climbed steadily, although

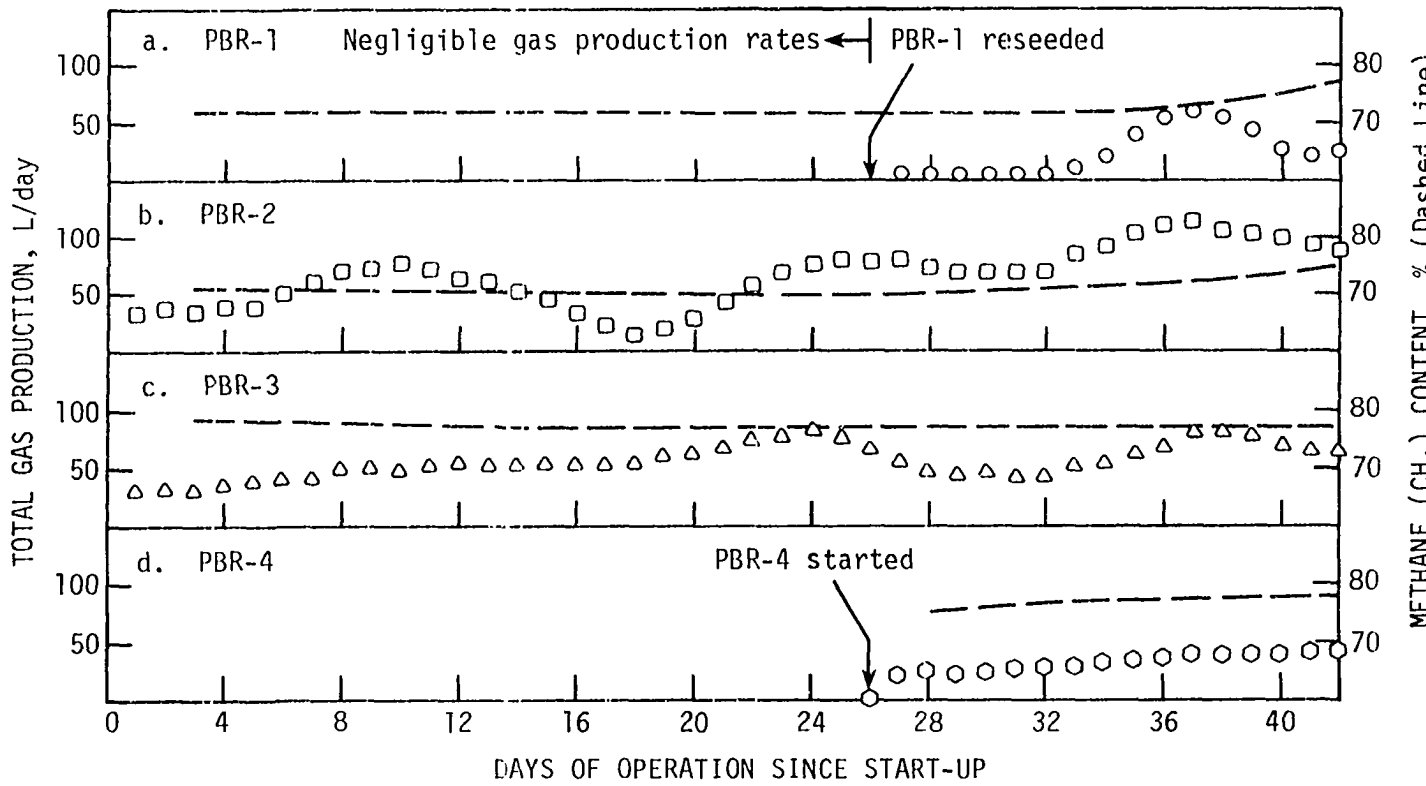

Figure 16. Total gas production rates (L/day) and methane (CH_4) content (%) during start-up of PBR reactors

gradually, with time. In all cases the methane content of the product gas ranged from 72 to 78 percent by volume.

It is estimated that all reactors would have probably responded to starting conditions in a much better fashion than experienced in this study if these columns were seeded more heavily and if the operational difficulties encountered during start-up could have been avoided. It would have been more expedient to start with heavy seed concentrations since some problems with pH adjustment were anticipated. However, small amounts of seed were used in these tests to preclude the addition of excessive solids not related to the waste being treated.

Performance at Low Organic Loading Rates

Immediately after reactor PBR-4 was started and seeded and after reactor PBR-1 was reseeded, the loading rate to all columns was increased to 0.5 gm COD/L-day (31 lb COD/MCF-day) and the influent COD concentration was set at 1500 mg/L. At this loading rate the empty-bed hydraulic retention time (HRT) was 72 hours.

In the discussion to follow, performance will be evaluated in terms of COD removal, total daily gas production, effluent gas methane content, volatile acids concentrations, and effluent suspended solids concentrations. It should be noted, however, that effluent suspended solids concentration is a highly unreliable parameter in anaerobic filter performance evaluation due to several factors that contribute to its variability. Such factors include intermixing and short-circuiting caused by the product gas as it rises through the column and the subsequent nonuniform hydraulic flow pattern through the reactor packing. Stated differently, effluent

suspended solids concentrations are highly dependent on the degree of solids transport brought about by inner reactor hydraulics dictated by the gas and liquid flow through the packing medium.

The anaerobic filters were operated at the 0.5 gm COD/L-day (31 lb COD/MCF-day) loading rate until steady-state conditions were reached. After a few weeks of apparent steady-state operation, the organic loading rate was doubled to 1.0 gm COD/L-day (64 lb COD/L-day) by doubling the flow rate while keeping the influent COD concentration constant at 1500 mg/L. Once steady-state conditions had become apparent again, the reactors were operated for about four more weeks. The organic loading rate was then doubled again to 2.0 gm COD/L-day (125 lb COD/L-day) while keeping the influent COD concentration at 1500 gm/L. This resulted in doubling the flow rate to each reactor or decreasing HRT by one-half.

The sequence of operating conditions thus far had resulted in the lowering of the hydraulic retention time (HRT) from 72 hours to 36 hours and then to 18 hours. In order to observe the effect of HRT on anaerobic filter performance at low loading conditions, the next step was to increase the hydraulic retention time and keep the organic loading rate constant at 2.0 gm COD/L-day (125 lb COD/MCF-day). This was done by increasing the influent COD concentration to 3000 mg/L and decreasing the hydraulic flow rate by a factor of two. The reactors were operated at these conditions for about four weeks after steady-state conditions became apparent.

The next sequence of operating conditions was geared to observing anaerobic filter performance at much higher organic loading rates and significantly higher influent COD concentrations. After the period of operation at the loading rate of 2.0 gm COD/L-day (125 lb COD/MCF-day)

was terminated, the loading rate to all reactors was doubled to 4.0 gm COD/L-day (250 lb COD/MCF-day). This was accomplished by increasing the influent COD concentration to 6000 mg/L at a hydraulic retention time (HRT) of 36 hours (Table 6). Once again all reactors were operated for about six weeks after steady-state conditions had become apparent.

As the period of operation at the loading rate of 4.0 gm COD/L-day (250 lb COD/MCF-day) approached termination, the performance data were examined carefully so that a decision could be made as to whether or not to operate all reactors at loading rates of 8.0 and 16.0 gm COD/L-day (500 and 1000 lb COD/MCF-day). As it will be discussed later, all performance data collected to this point of operation indicated that reactors PBR-2 and PBR-3 (packed with perforated balls and Pall rings, respectively) were less efficient than were reactors PBR-1 and PBR-4 (packed with plastic modular media) and little utility was seen in continuing to operate these reactors at higher loading rates. This decision was also made on the basis that chemical costs, mixing requirements, and equipment capabilities would become practically limiting considering the relatively large size of the anaerobic filter system. Therefore, only the reactors containing modular media (i.e. PBR-1 and PBR-4) were kept in service.

Reactors PBR-1 and PBR-4 were operated at a loading rate of 8.0 gm COD/L-day (500 lb COD/MCF-day) and an influent COD concentration of 6000 mg/L for a period of about six weeks. The loading rate to these two reactors was then doubled to 16.0 gm COD/L-day (1000 lb COD/MCF-day) and the influent COD concentration was kept constant at 6000 mg/L. The hydraulic retention time was 18 and 9 hours, respectively, at these loading rates. After a period of operation of slightly over four weeks

at the 16.0 gm COD/L-day (1000 lb COD/MCF-day) loading rate a failure of one of the feedstock metering pumps forced termination of operation at this loading rate. The feed rate to these two reactors was then reduced to about 2.0 gm COD/L-day (125 lb COD/MCF-day) for a short period of time until the reactors were dismantled and the contents were removed for close examination of biological growth patterns and biomass distribution within the columns.

During the entire period of operation of these anaerobic filters steady-state conditions were primarily determined by the total daily gas production from each reactor. Another measure of steady-state conditions was the effluent COD from each reactor. However, effluent COD results were considered as a secondary parameter due to the lag period in obtaining COD data from the testing laboratory.

Performance during phase I

Phase I designates the period of operation at the loading rate of 0.5 gm COD/L-day (31 lb COD/MCF-day). During this period, the microbial culture in the anaerobic filters was not well-established and the reactors perhaps should be considered in a continuing period of system start-up. Despite some of the mechanical difficulties encountered during this "start-up" period, the anaerobic filters reached what could practically be considered steady-state conditions. This fact is demonstrated by total gas production data as shown on Figure 17.

As shown, total gas production typically increased until it reached a maximum level, declined somewhat for a few days, and then increased and leveled off for the rest of the operational period. The latter period of

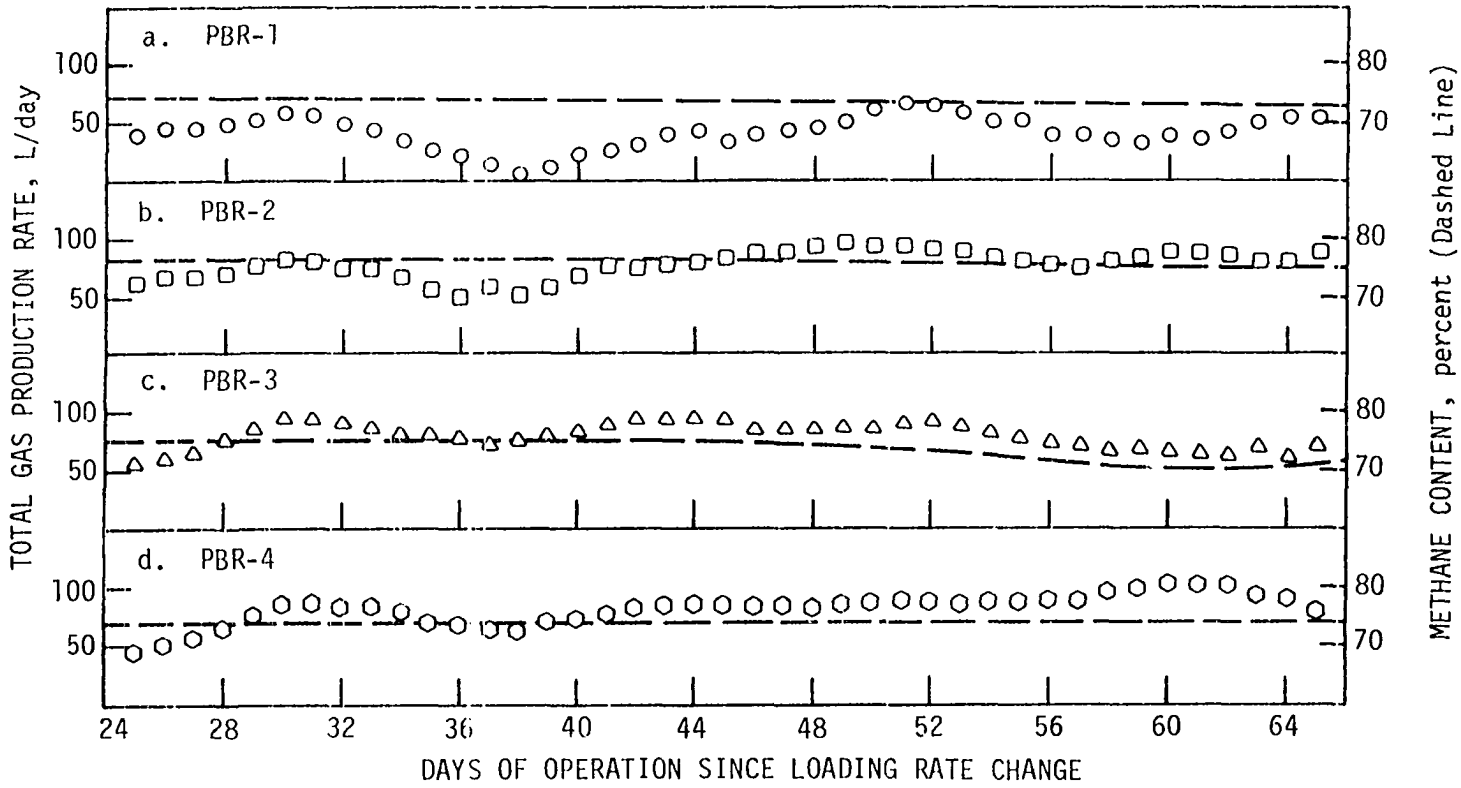

Figure 17. Total gas production rates (L/day) and methane content (%) during operation at a loading rate of 0.5 gm COD/L-day. Influent COD = 1500 mg/L

operation during which gas production became essentially constant was generally considered that of steady-state operation.

The general pattern of total gas production from PBR-1 shown on Figure 17-a was marred by a failure in the feedstock metering pump to this reactor due to plugging in the feeding tubes on about day 32. A similar problem occurred on day 56 (Figure 17-a). However, this latter problem was discovered before the reactor was forced into a serious decline in gas production. This pattern shows the relative quickness at which the anaerobic filter recovered from the accidental state of starvation caused by feedstock cut-off. Actually, the reactor recovered more quickly than Figure 17-a suggests due to the dampening effect caused by the data smoothing technique used in constructing this graph.

The same general pattern of total gas production showing an initial increase followed by decrease and subsequent stabilization was also demonstrated by reactors PBR-2, -3, and -4 as shown in Figure 17-b, c, and d. The total gas production rate in these reactors was generally more uniform (particularly with PBR-4) than experienced with reactor 1. This improved stability undoubtedly was due to minimal interruptions caused by mechanical failures and in part due to, perhaps, better seed adaptation.

Total methane gas production rates in all columns as shown in Figure 17 (dashed lines) generally seemed to reflect a relatively constant fraction of total gas production usually ranging between 70 to 75 percent. The balance of the product gas consisted of carbon dioxide (CO_2) (20-22 %) and a small fraction (usually 1 to 2 percent) of nitrogen gas. Because total sulfate in the substrate was limited to that fraction contained in tap water (less than 50 mg/L as $SO_4^=$), hydrogen sulfide production was

extremely low and both reactors' effluent streams (liquid and gas) were relatively odor free.

Total gas production rates (Figure 17) suggest that, in general, all reactors seemed to produce somewhat equal performance characteristics at this loading rate. This observation is supported by effluent as well as inner-reactor COD determinations. Figure 18 represents typical chemical oxygen demand (COD) profiles in all reactors. As shown, effluent COD results indicate that total COD removal efficiency was in excess of 80 percent with PBR-1 showing slightly, but consistently, better COD removal than the remaining reactors. Figure 18 also indicates that most of the COD removal had occurred in the first (lower) 1 ft. (0.3 m) of height with little or no removal taking place past the 2.0 ft. (0.61 m) height. This pattern is thought to reflect the settling of active biomass floc to the bottom of the highly porous packing medium. This pattern is also probably attributable, in part, to the relatively limited amounts of active biomass that had accumulated in the anaerobic filters up to this time.

Figure 19 shows typical individual volatile acids concentration profiles through all reactors. All volatile acids components shown are expressed as acetic acid for simplification in comparing concentrations. As shown, acetic and propionic acids make up the bulk of volatile acids produced during the anaerobic fermentation process. Smaller quantities of higher molecular weight volatile acids were usually present but their concentrations usually declined to near zero in the effluent. These higher molecular weight volatile acids consisted mainly of normal butyric and valeric acids. However, trace concentrations of iso-butyric and iso-valeric acids as well as smaller fractions of caproic acid also were present.

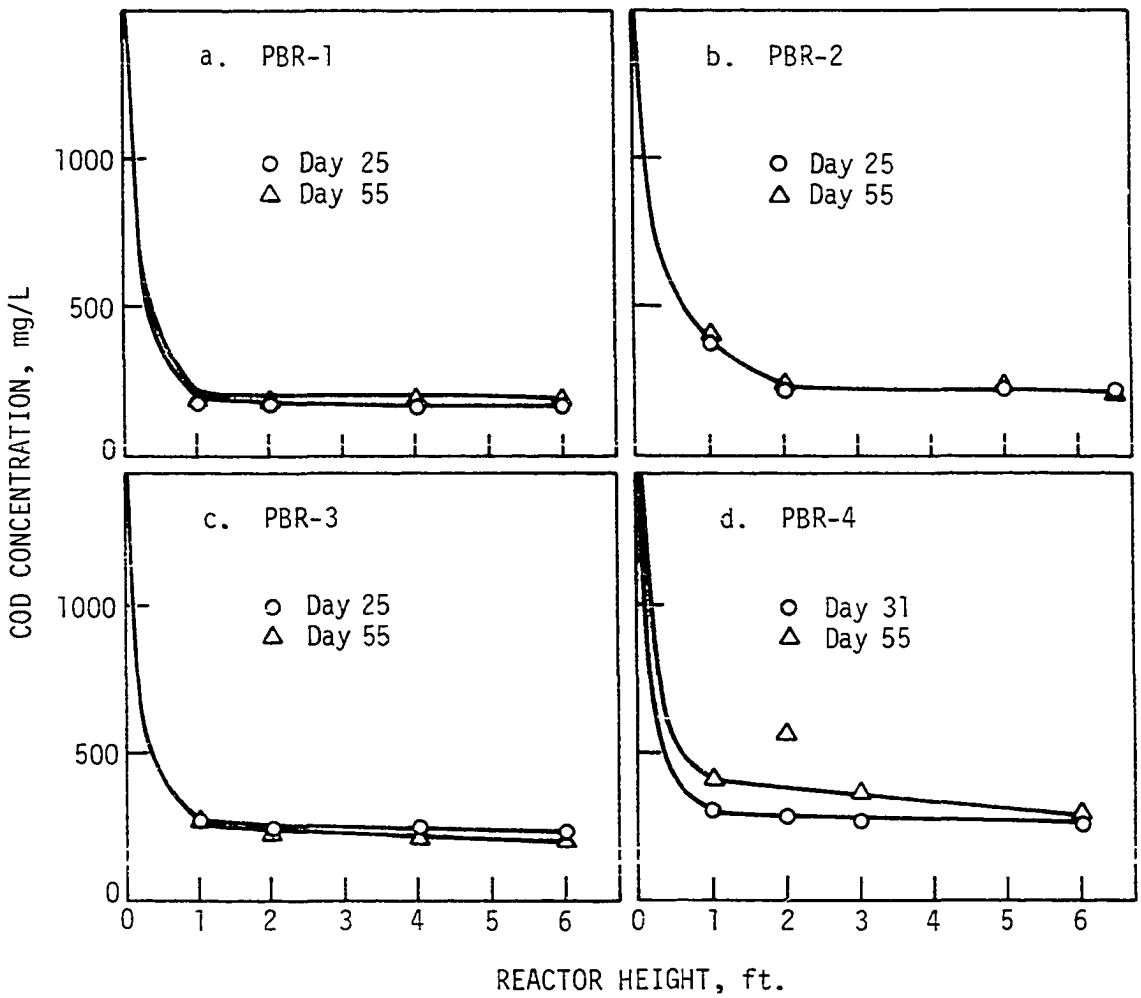

Figure 18. Measured COD concentrations (mg/L) in all reactors at a loading rate of 0.5 gm COD/L-day

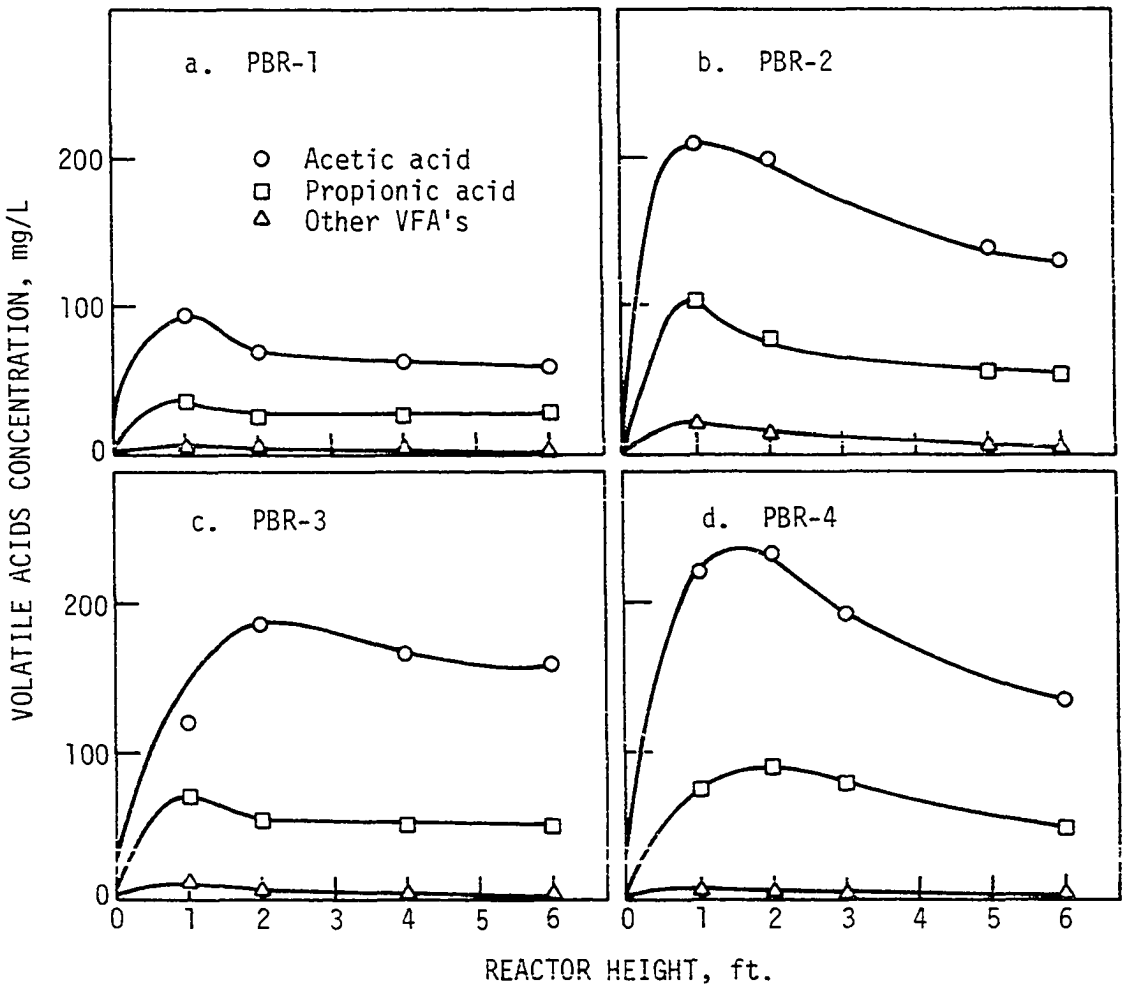

Figure 19. Volatile fatty acids (VFA) concentrations (mg/L as acetic acid) in all reactors at a loading rate of 0.5 gm COD/L-day

At low organic loading rates, the total COD equivalent of volatile acids usually corresponded to the total COD in the reactors effluent indicating complete conversion, or utilization, of the alcohol and carbohydrate components of the influent stream. As will be discussed later, the total COD equivalent of volatile acids in the effluent did not correspond to the total measured COD of these effluents at higher organic loading rates indicating that a fraction of the alcohols and carbohydrates in the influent stream either escaped treatment or were converted to organic materials other than monocarboxylic volatile fatty acids.

Comparison of the data used in constructing Figures 18 (COD) and 19 (volatile acids) indicates that, on the average, acetic acid comprised about 50 to 60 percent of the total equivalent COD at the 1.0 ft. (0.3 m) reactor height. At the same point, propionic acid comprised about 30 to 40 percent of the total COD content. It must be emphasized that the above proportions were based on the assumption that volatile acids utilization was assumed negligible in the first increment of filter height and that the rate of alcohol and carbohydrate conversion at this level was assumed to reach maximum steady-state conditions. These proportions are similar to those obtained in tests conducted by Young (65).

Effluent suspended solids concentrations during phase I are summarized in Table 10 below. As shown, effluent suspended solids concentrations from all reactors were essentially equivalent indicating that no superiority in performance among the anaerobic filters was apparent at this loading rate. The volatility of the suspended solids typically ranged from 85 to 90 percent (of the total) at this loading rate.

Table 10. Suspended solids (SS) concentrations during phase I of anaerobic filter operation

Reactor number	Average SS (mg/L)	Range (mg/L)	Standard Deviation (mg/L)
PBR-1	83	58-104	23
PBR-2	81	70-92	11
PBR-3	84	68-96	14
PBR-4	90	48-120	37

Performance during phase I:

Phase II denotes the period of operation at a loading rate of 1.0 gm COD/L-day (62.4 lb COD/MCF-day). The pattern of total gas production rate observed earlier at the lower loading rate of 0.5 gm COD/L-day (31 lb COD/MCF-day) was observed again at this loading rate (Figure 20). As shown, in all reactors, gas production increased rapidly until it reached a maximum, declined somewhat for a few days, and then stabilized at, or near, the maximum rate. Steady-state operation, as evidenced by constant daily gas production, generally was reached after about 3 weeks of operation. Even reactor PBR-1, which was the subject of somewhat unstable starting conditions at the lower loading rate, demonstrated excellent steady-state operation after only about 3 weeks (Figure 20-a). The most stable response was demonstrated by reactor PBR-4 (Figure 20-d).

The methane (CH_4) content of the product gas remained basically constant during steady-state operation as was expected. However, methane content increased from about 70 percent during non-steady-state conditions

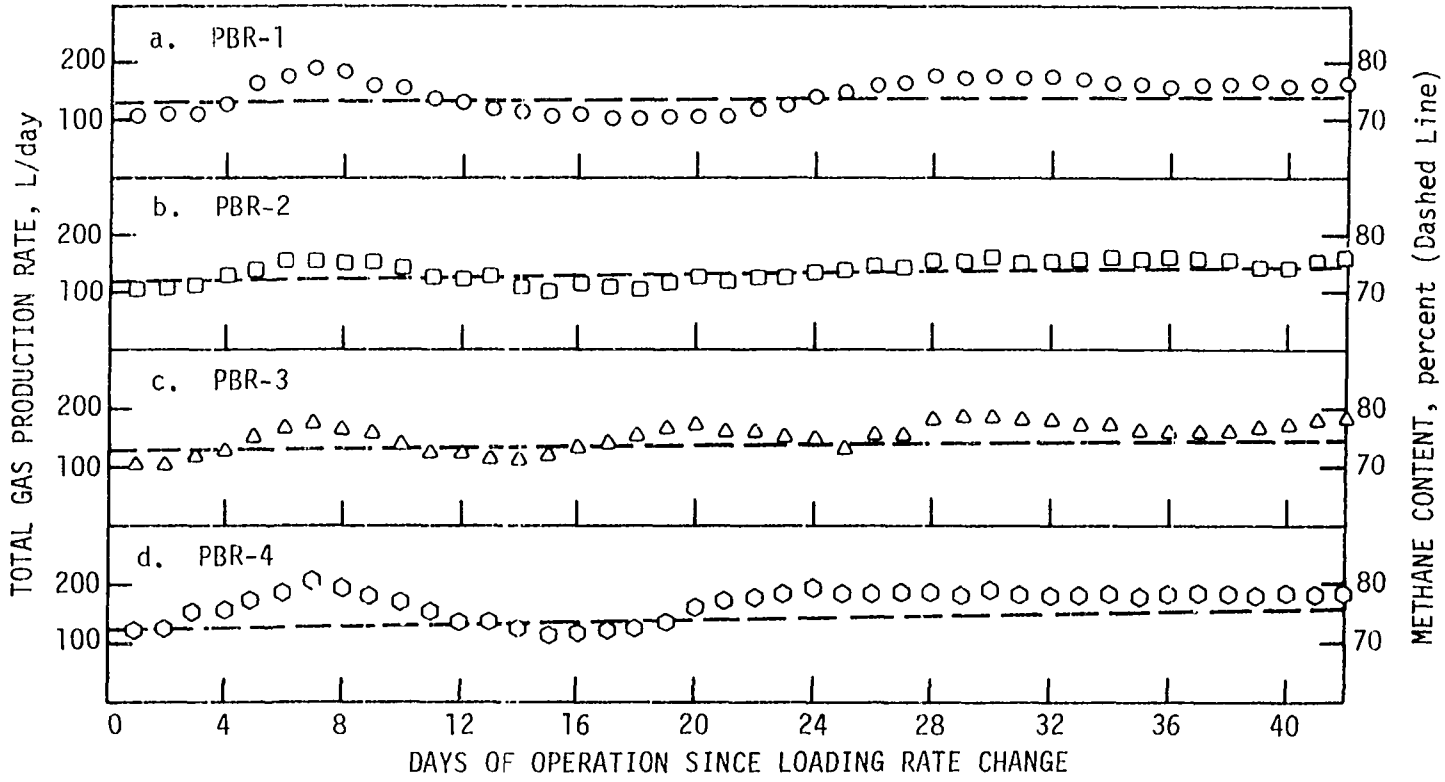

Figure 20. Total gas production rates (L/day) and methane content (%) during operation at a loading rate of 1.0 gm COD/L-day. Influent COD = 1500 mg/L.

(i.e. immediately after the change in loading rate) to about 74 to 75 percent after steady-state conditions were reached.

Figure 21 shows COD profiles through all reactors. The COD data obtained at this loading rate begin to show the relative superiority of reactor PBR-1 over the other reactors. The next best COD removals were obtained with reactor PBR-4. Therefore, the best performance results at this loading rate were associated with the modular block media. The reactor containing the Pall rings (PBR-3) showed some marginal superiority over the unit containing the perforated spheres media (i.e. PBR-2). Figure 21 also shows that steady-state conditions were reached quickly in all reactors. This point is evident by comparing the COD profile data for day 14 with that of day 40 after the loading rate change.

The same performance patterns observed with COD removal were duplicated by individual volatile acids concentrations through each reactor (Figure 22, a-d). On the average reactor PBR-1 demonstrated the best volatile acids removal and was followed by reactor PBR-4. Reactor PBR-3 consistently showed somewhat better volatile acids removal than PBR-2 (Figure 22, b and c). Once again the total COD of all individual volatile acids components in all reactors corresponded closely to the total COD in the reactors effluent indicating near total conversion of the alcohol and carbohydrate components of the influent feed.

Effluent suspended solids concentrations during this period of operation are summarized in Table 11 below. As shown, effluent suspended solids concentrations were markedly lower in reactors PBR-1 and PBR-4 than they were in reactors PBR-2 and PBR-3. This trend differs from that observed earlier at the lower organic loading rate.

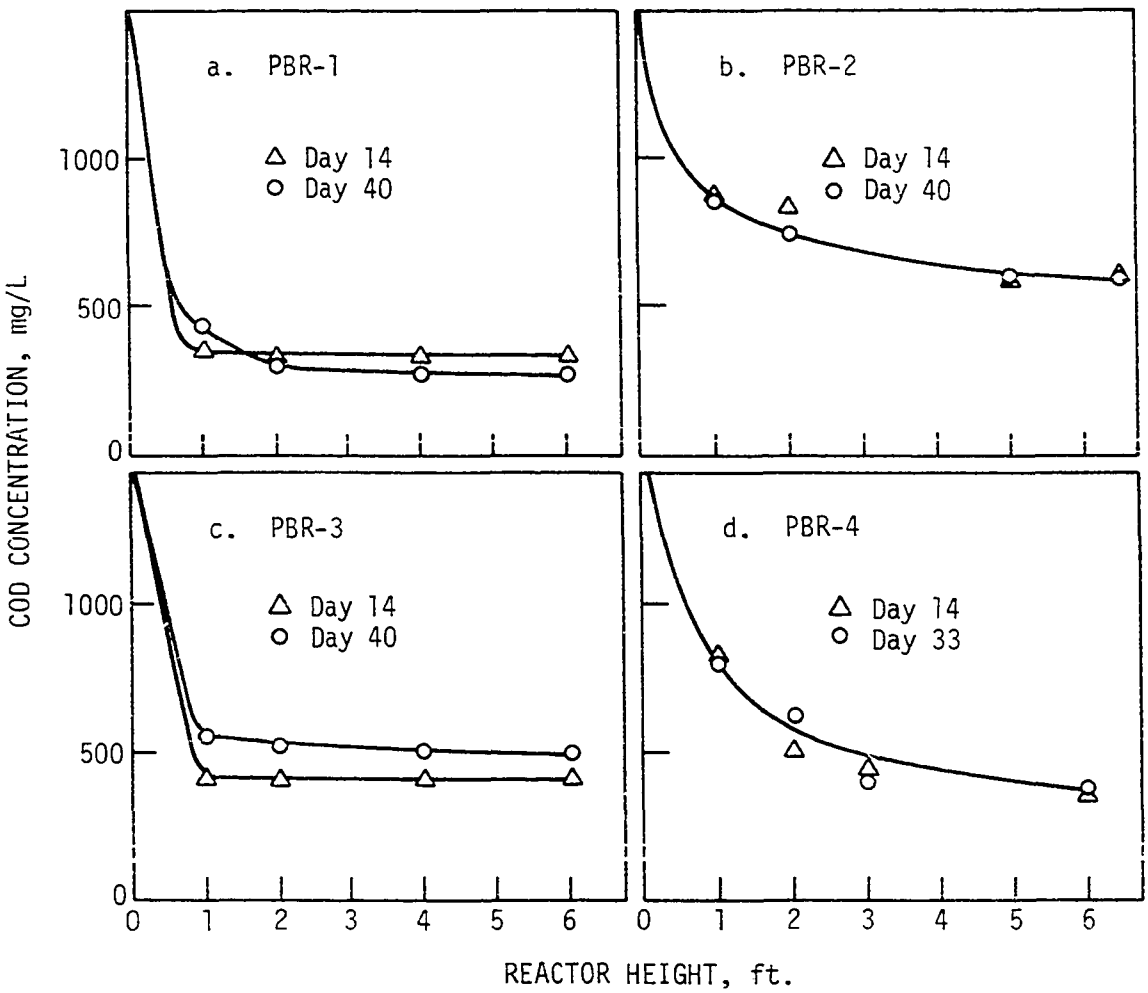

Figure 21. Measured COD concentrations (mg/L) in all reactors at a loading rate of 1.0 gm COD/L-day

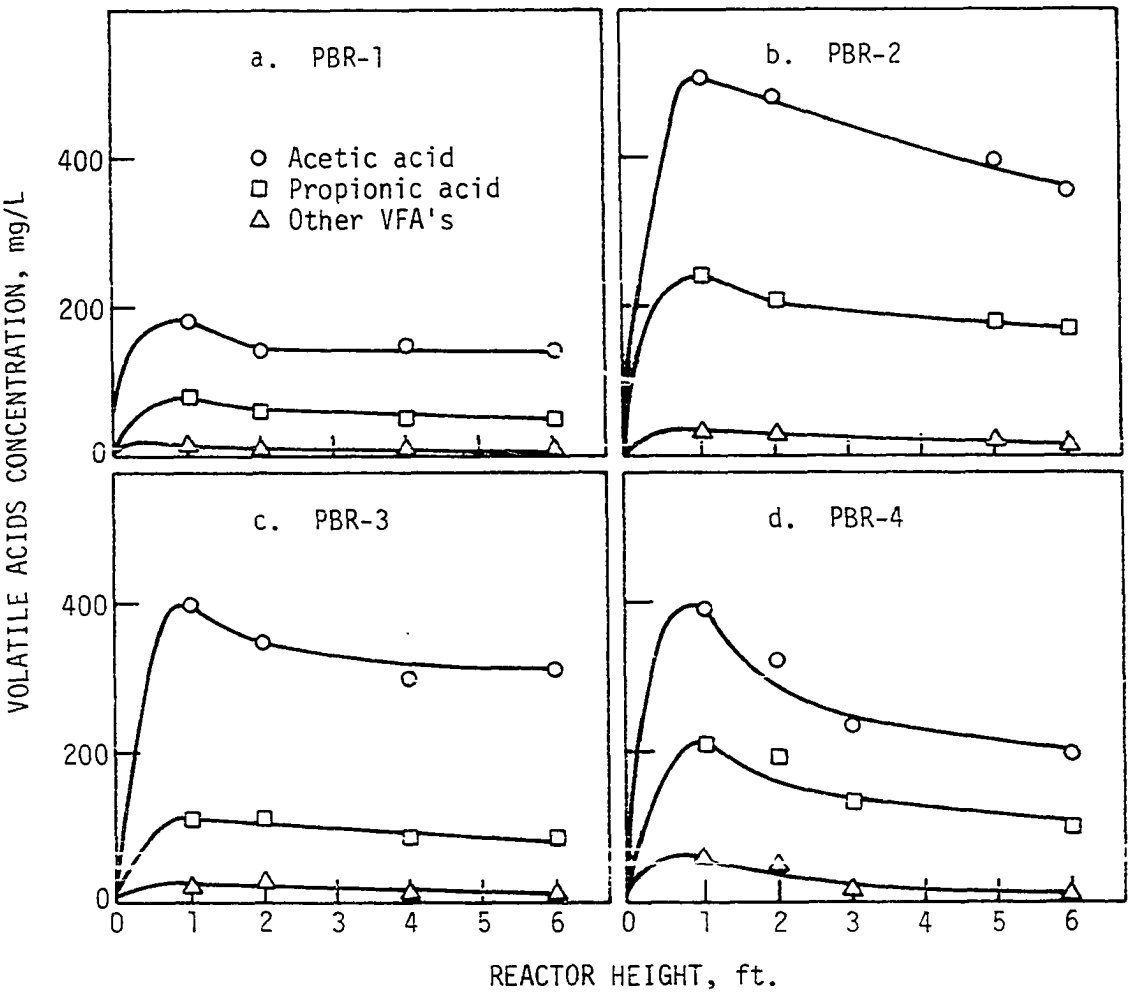

Figure 22. Volatile acids concentrations (mg/L as acetic acid) in all reactors at a loading rate of 1.0 gm COD/L-day

Table 11. Suspended solids (SS) concentrations during phase II of anaerobic filter operation

Reactor Number	Average SS (mg/L)	Range (mg/L)	Standard Deviation (mg/L)
PBR-1	96	52-144	38
PBR-2	106	64-140	34
PBR-3	129	120-148	10
PBR-4	74	66-80	6

Performance during phases III and IV

Phases III and IV refer to the period of operation at an organic loading rate of 2.0 gm COD/L-day (125 lb COD/MCF-day) and influent COD concentrations of 1500 and 3000 mg/L. The influent COD concentration was increased to 3000 mg/L to observe the effects of increased hydraulic retention time on anaerobic filter performance.

Figure 23(a-d) summarizes total gas production data during these phases. When operating at an influent COD concentration of 1500 mg/L, total daily gas production rates followed principally the same overall patterns observed at lower loading rates. Once again steady-state operation generally was reached within about 3 to 4 weeks of operation. As shown in Figure 23, the gas production rate from reactors PBR-1 and PBR-4 seemed to vary more than in PBR-2 and PBR-3 after steady-state conditions were reached. This departure was caused by a drift in the feedstock metering pumps on about day 35 after the loading rate change. During this period of operation, PBR-4 seemed to have higher total gas production rates than the remaining columns particularly reactors PBR-2 and PBR-3.

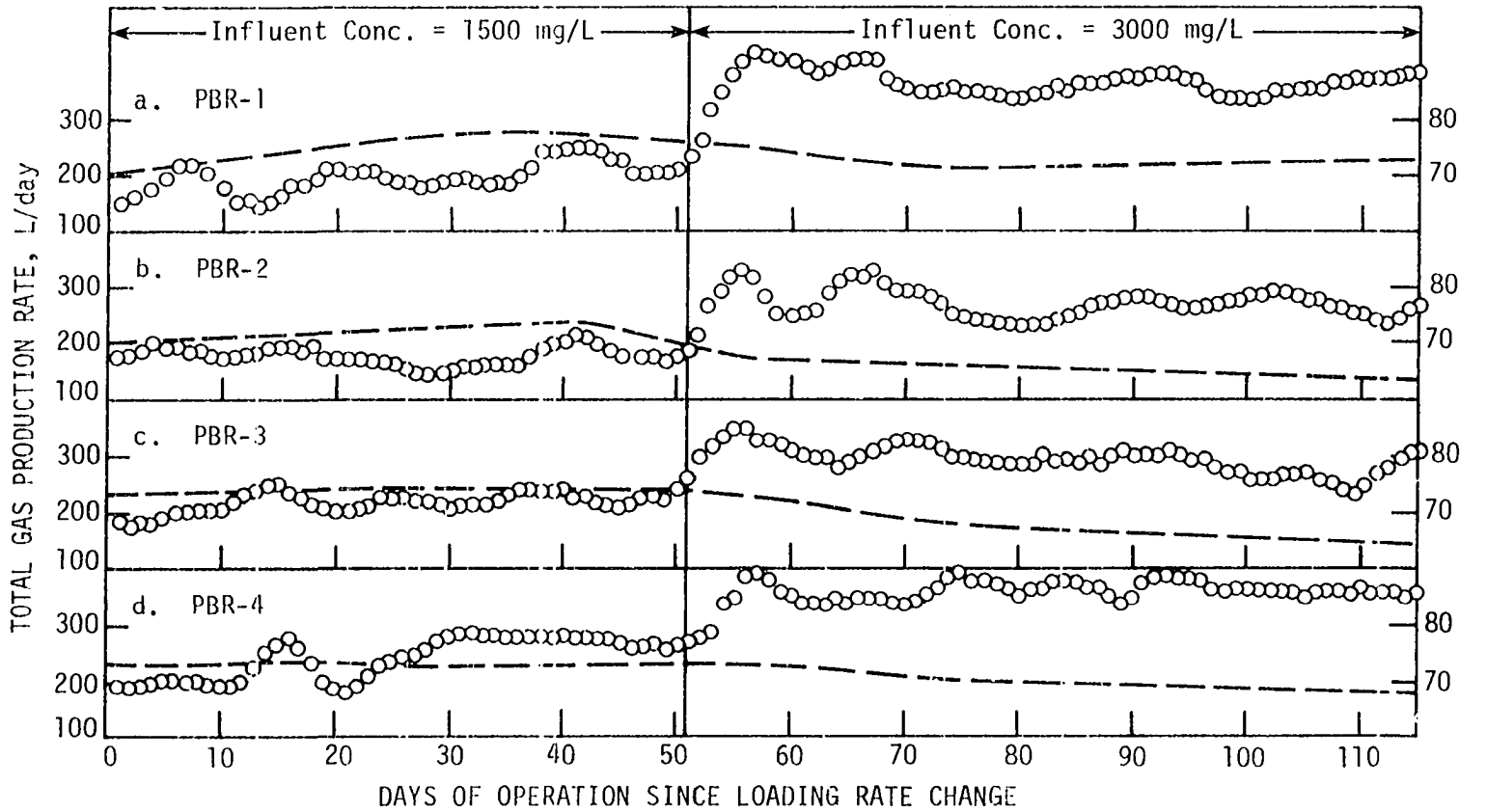

Figure 23. Total gas production rates (L/day) and methane content (%) during operation at a loading rate of 2.0 gm COD/L-day

After 50 days of operation at an influent COD of 1500 mg/L, the influent COD concentration was doubled to 3000 mg/L without changing the organic loading rate. This produced an increase in the hydraulic retention time from 18 to 36 hours. Examination of total gas production rates in Figure 23 shows a rapid increase immediately after the substrate concentration was changed. After a period of three weeks of operation, steady-state gas production rates were reached. Figure 23 also shows that reactors PBR-1 and PBR-4 produced consistently higher total daily gas production rates indicating the superiority of these two reactors over reactors PBR-2 and PBR-3.

The change to a higher influent COD concentration seemed to produce a somewhat lower methane gas content. This obviously reflects a higher consumption of alkalinity due to increased volatile acids concentrations. This observation is supported by a slight decrease in system pH (from 7.1 to 6.8) after the influent feed concentration was increased.

Figures 24 and 25 show COD concentration profiles through each reactor at the loading rate of 2.0 gm COD/L-day (125 lb COD/MCF-day). The COD profiles shown in Figure 24 indicate that reactor PBR-1 typically produced the best overall COD removal followed by PBR-4. Reactors PBR-2 and PBR-3 generally had higher effluent COD concentrations and thus lower overall COD removal. Figure 24 also indicates that more of the reactor height, particularly in PBR-1 and PBR-4 (corrugated modular media), was utilized in COD removal. This phenomenon was observed at a lesser extent in the loose-fill media units (PBR-2 and PBR-3).

When the influent COD concentration was doubled to 3000 mg/L (thus changing the hydraulic retention time from 18 to 36 hours), the superior

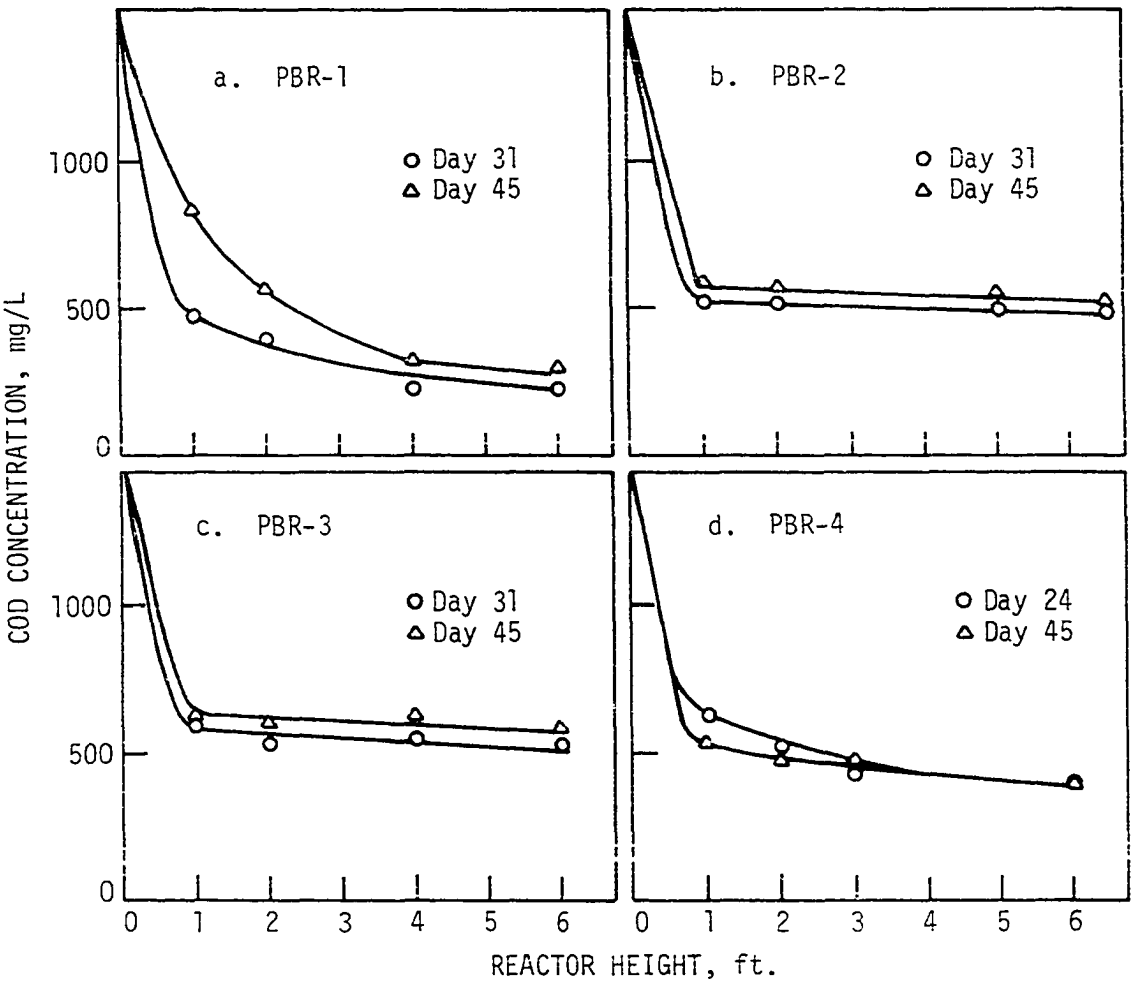

Figure 24. Measured COD concentrations (mg/L) in all reactors at a loading rate of 2.0 gm COD/L-day. Influent COD = 1500 mg/L

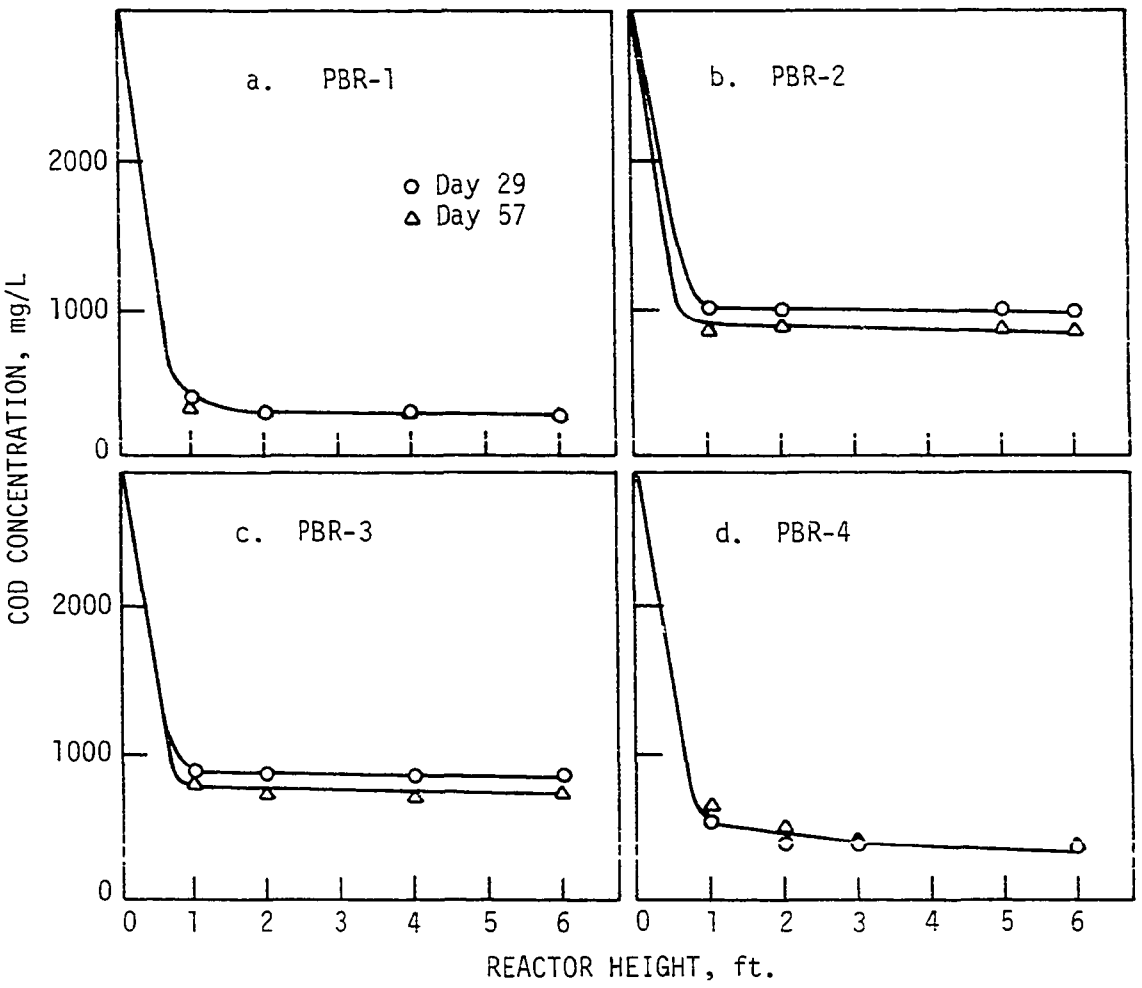

Figure 25. Measured COD concentrations (mg/L) in all reactors at a loading rate of 2.0 gm COD/L-day. Influent COD = 3000 mg/L

performance of reactors PBR-1 and PBR-4 became more evident (Figure 25). Despite the doubling of influent COD, effluent COD concentrations during phase IV remained essentially the same as they were during phase III, thus reflecting considerably higher COD removal efficiencies. This demonstrates that at a given organic loading rate, COD removal efficiency increased as the hydraulic retention time increased. As was observed at previous loadings, COD removal seemed to take place at the lower levels of the reactors as shown in Figures 24 and 25. This perhaps reflects the effect of higher concentration of biological solids settling in the bottom of the filters. This took place despite the increased tendency of solids to move upwards due to increased gas production rates.

Figures 26 and 27 show typical volatile acids profiles through all reactors when operating at a loading rate of 2.0 gm COD/L-day (125 lb COD/MCF-day). Figure 26 shows typical volatile acids profiles when the influent COD concentration was set at 1500 mg/L and Figure 27 with an influent COD concentration of 3000 mg/L. Reactors PBR-1 and PBR-4 demonstrated a better ability to utilize volatile acids thus resulting in markedly lower VFA concentrations not only in the effluent stream but also throughout the reactor height (Figures 26 and 27). Once again, the total COD equivalent of all individual volatile acids components was about equal to the total chemical oxygen demand in the reactors effluents.

Table 12 provides a summary of effluent suspended solids concentrations measured during phases III and IV. Upon close examination of these data, two basic conclusions can be drawn. First, effluent suspended solids concentrations were somewhat better in reactors PBR-1 and PBR-4 than in the remaining reactors when the influent COD concentration was set at

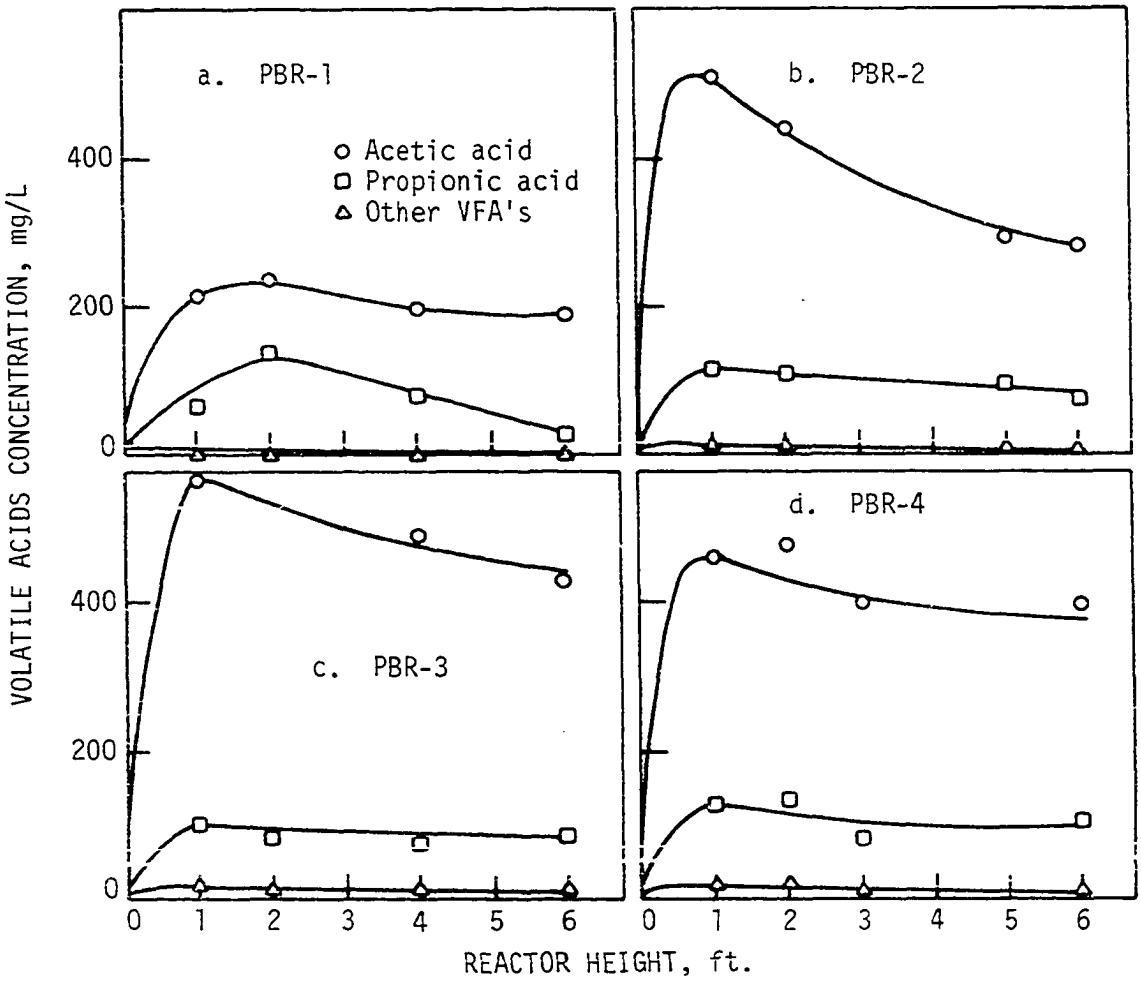

Figure 26. Volatile acids concentrations (mg/L as acetic acid) in all reactors at a loading rate of 2.0 gm COD/L-day. Influent COD = 1500 mg/L

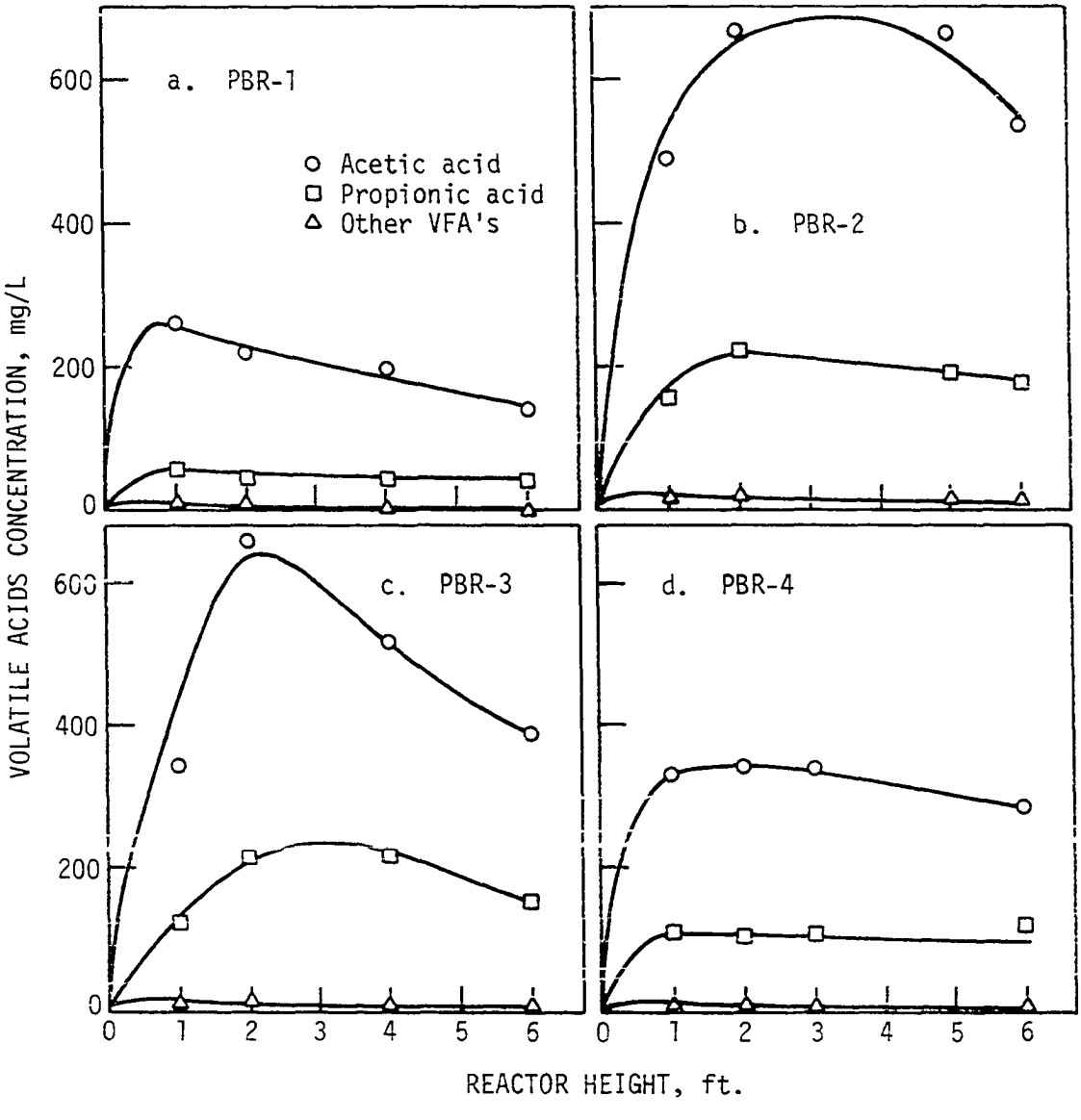

Figure 27. Volatile acids concentrations (mg/L as acetic acid) in all reactors at a loading rate of 2.0 gm COD/L-day. Influent COD = 3000 mg/L

Table 12. Suspended solids (SS) concentrations during phases III and IV of anaerobic filter operation at a loading rate of 2.0 gm COD/L-day (125 lb COD/MCF-day)

Phase of Operation	Reactor Number	Influent COD (mg/L)	Average SS (mg/L)	Range (mg/L)	Standard Deviation (mg/L)
III	1	1500	59	28-84	24
III	2	1500	71	54-88	18
III	3	1500	76	28-96	32
III	4	1500	70	40-92	22
IV	1	3000	200	116-300	76
IV	2	3000	274	84-360	106
IV	3	3000	246	136-320	59
IV	4	3000	237	128-380	50

1500 mg/L. After the influent COD was increased to 3000 mg/L, PBR-1 and PBR-4 demonstrated significantly lower effluent suspended solids concentrations than did PBR-2 and PBR-3. Second, the increase in influent COD resulted in a uniform across the board increase in suspended solids concentrations in all reactors regardless of the media type. This increase in suspended solids took place despite the increase in hydraulic retention time and the subsequent improvement in suspended solids settling opportunities. The dramatic increase in total gas production rates from all reactors as a result of the influent loading rate change appeared to be the main reason for the increase in effluent suspended solids concentrations.

The anaerobic filter performance data discussed so far lead to two basic conclusions. First, COD removals are a strong function of hydraulic retention times within the filter matrix. Second, anaerobic filter effluent suspended solids are clearly dependent on total gas production rates due to the vertical transport of biological solids effected by gas movement through the media. Similar conclusions were drawn by Young (65).

Performance during phase V

Phase V denotes the operational period at a loading rate of 4.0 gm COD/L-day (250 lb COD/MCF-day). During this phase, the influent COD concentration was increased to 6000 mg/L resulting in a hydraulic detention time (HRT) of 36 hours to all reactors (Table 6).

Total daily gas production data (Figure 28) show that all anaerobic filters responded slowly to the loading rate change. Although the total gas production rates seemed to follow the same general patterns observed previously at lower loading rates, steady-state operation was not generally

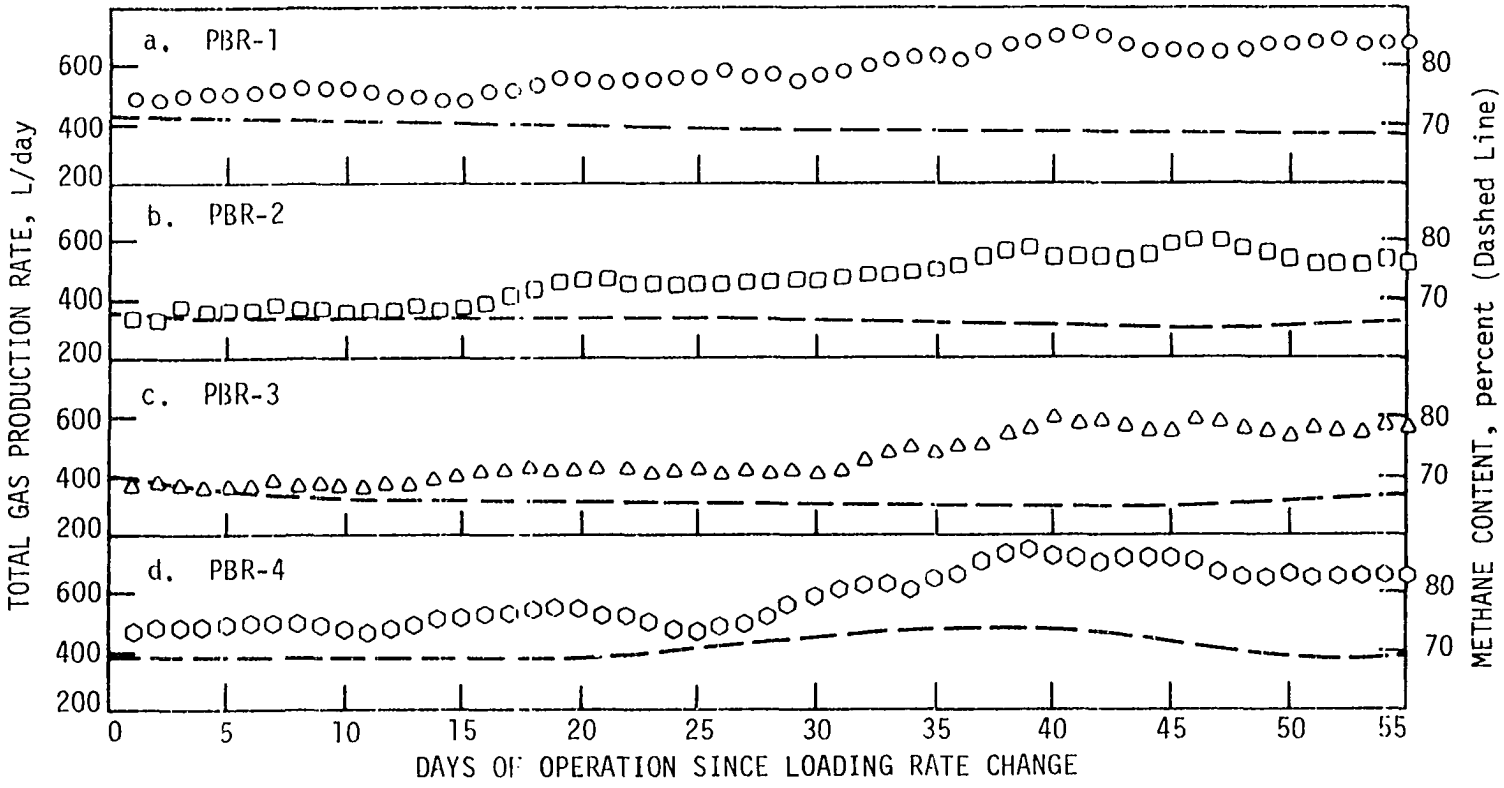

Figure 28. Total gas production rates (L/day) and methane content (%) during operation at a loading rate of 4.0 gm COD/L-day. Influent COD = 6000 mg/L

apparent until after about one month after making the loading rate change. This response could be attributable, at least in part, to some difficulties in obtaining precise settings on the feedstock metering pumps.

During the period of steady-state operations the superiority of reactors PBR-1 and PBR-4 again was clearly demonstrated through significantly higher daily gas production rates (Figure 28, a through d). Comparison of gas production rates from reactors PBR-2 and PBR-3 indicates that the former demonstrated slightly better performance during steady-state conditions.

During this period of operation the methane content of the effluent gas generally ranged from 68 to 70 percent in all reactors. This methane content was slightly lower than was observed when operating at lower loading rates and reflected a higher alkalinity consumption due to increased volatile acids production. It should be noted, however, that despite this alkalinity consumption, the pH through the height of each reactor remained between 6.5 and 7.0.

Figure 29 shows typical COD profile data when operating during phase V. Two important characteristics are easily identified upon examination of these COD profiles. First, PBR-1 and PBR-4 (modular corrugated media reactors) continued to produce better COD removal efficiencies than either PBR-3 or PBR-2. COD removal efficiency exceeded 85 percent in PBR-1 and PBR-4 while averaging slightly better than 70 percent in both PBR-2 and PBR-3. Second, most of the COD removal was achieved within the first 1.0 ft. (0.30 m) of height. Again this trend seemed to be directly related to the high porosity of the packing materials.

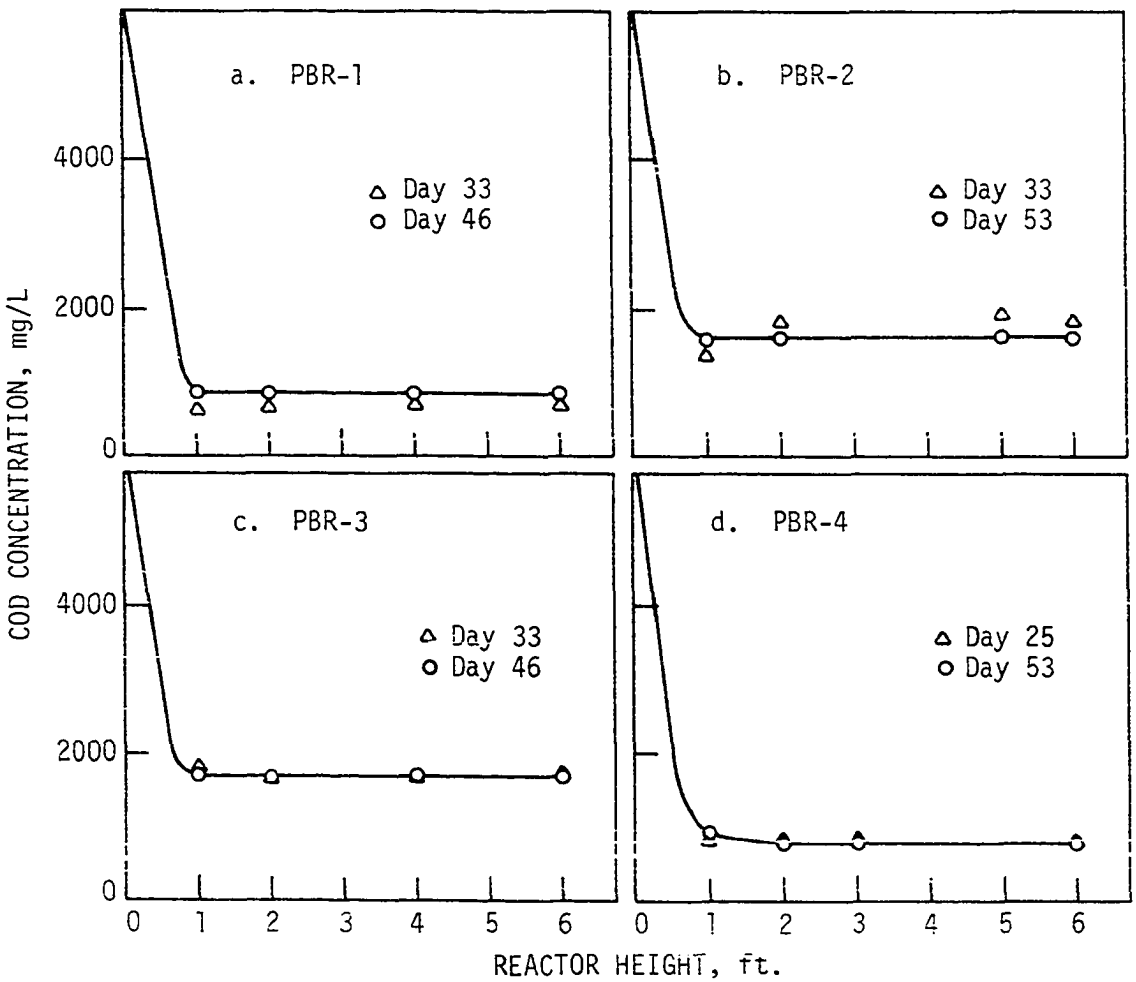

Figure 29. Measured COD concentrations (mg/L) in all reactors at a loading rate of 4.0 gm COD/L-day

Volatile acids concentrations within each of the four reactors during this period of operation are illustrated in Figure 30. The VFA concentrations followed the same general pattern exhibited previously by COD profiles at other organic loading rates. These profiles not only demonstrate the relative superiority of reactors PBR-1 and PBR-4 but indicate, as also was observed earlier, that reactor PBR-1 generally produced better overall performance characteristics than its counterpart (i.e. PBR-4) which contained the same type of modular media but having a larger specific surface area.

Figure 30 also indicates that the general proportions of individual volatile acids had not changed appreciably at higher organic loading rates with acetic and propionic acids making up the major fraction of total volatile acids at all reactor heights. Higher molecular weight volatile acids continued to be present throughout the reactor height although at the same general low concentrations as was observed previously. Again, volatile acids basically accounted for the total COD in the effluent stream indicating total conversion of influent alcohol and sugar components to volatile acids.

Table 13 summarizes effluent suspended solids concentrations during phase V of operation. During this period, effluent suspended solids concentrations from reactors PBR-1 and PBR-4 basically were equivalent and significantly lower than effluent suspended solids concentrations from reactors PBR-2 and PBR-3. This difference in effluent suspended solids concentrations was perhaps related to the ability of the modular media to effect better solids settling and to an increased amount of solids transport caused by short-circuiting in the reactors containing loose-fill media.

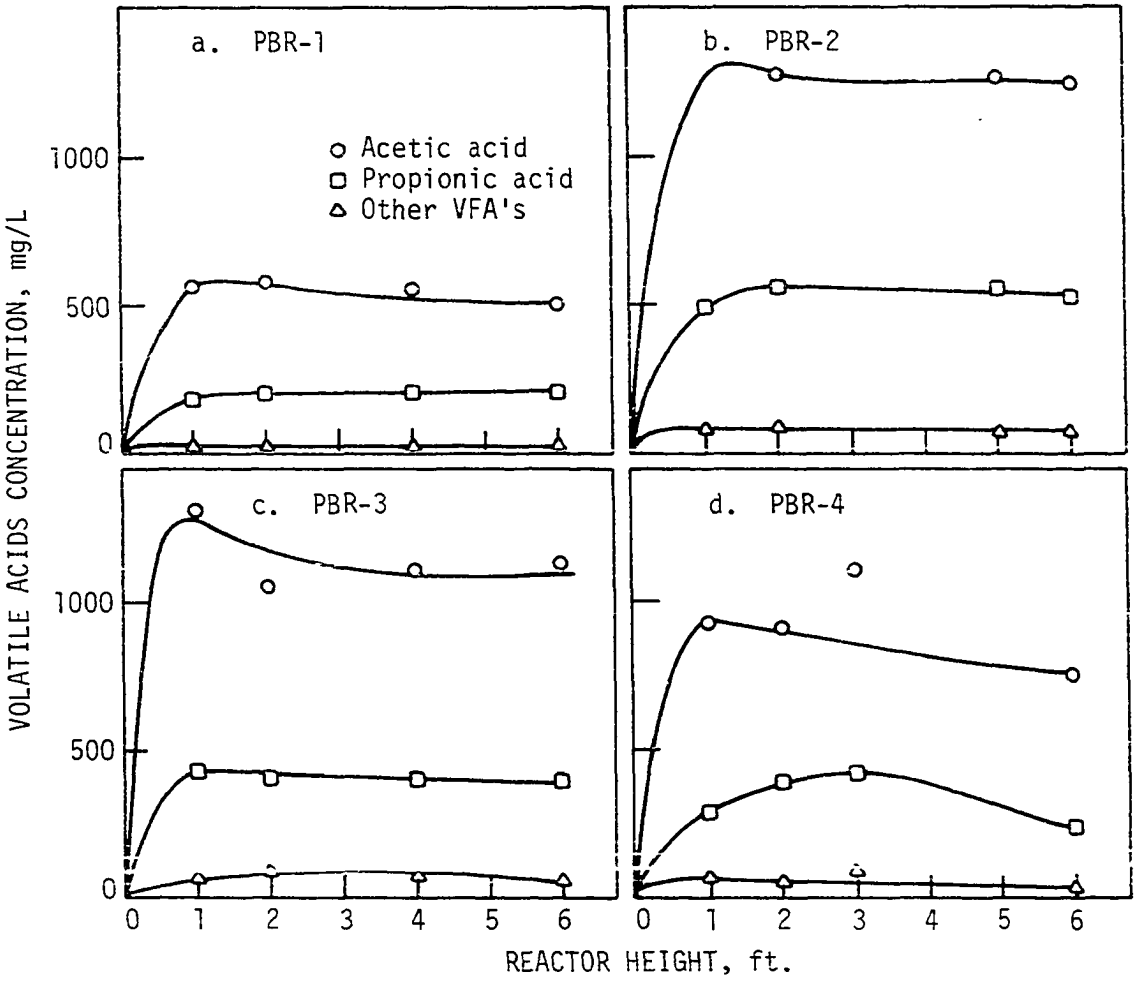

Figure 30. Volatile acids concentrations (mg/L as acetic acid) in all reactors at a loading rate of 4.0 gm COD/L-day. Influent COD = 6000 mg/L

Table 13. Suspended solids (SS) concentrations during phase V of anaerobic filter operation

Reactor Number	Average SS (mg/L)	Range (mg/L)	Standard Deviation (mg/L)
PBR-1	330	210-460	84
PBR-2	548	460-640	75
PBR-3	472	310-650	140
PBR-4	313	230-400	66

Based on the representative performance data shown on Figures 29 and 30 and Table 13, it is obvious that despite the difference in chemical oxygen demand removal efficiencies between the reactors packed with modular corrugated media (PBR-1 and PBR-4) and those packed with loose-fill media (PBR-2 and PBR-3) little or no COD removal took place past the 1 ft. (0.3 m) increment of reactor height. In this case the discrepancy in COD removal was not related to either media surface area or media type. If media surface area was a controlling factor, as might have been anticipated, then reactor PBR-4 would have produced noticeably better COD removal efficiency than the remaining reactors since its media had the highest specific surface area (i.e. area per unit volume). If porosity was a controlling factor, then all reactors should have resulted in somewhat equivalent COD removal since all of the media used had porosities in excess of 95 percent (based on clean bed basis). The question remains then, why was the corrugated modular media almost consistently associated with better overall COD removal rates?

Although the answer to the above question is not quite evident from the data collected to this point of operation, examination of effluent suspended solids data (Table 13) reveals that a larger amount of solids transport took place in the loose-fill media (reactors PBR-2 and PBR-3) as compared to the reactors with the modular corrugated media (PBR-1 and PBR-4). This greater solids transport was considered to be related to a greater extent of short-circuiting that apparently was taking place in PBR-2 and PBR-3. Short-circuiting not only is expected to result in higher effluent suspended solids concentrations but also would result in deterioration of effluent quality as measured by COD removal.

Performance at High Organic Loading Rates

All of the data presented and discussed earlier clearly pointed to the inability of the loose-fill media packed in reactors PBR-2 and PBR-3 to perform as well as the modular corrugated media packed in reactors PBR-1 and PBR-4 under the loading conditions used in this study. In addition, comparative performance between reactors PBR-1 and PBR-4 indicated, almost consistently, that the former had responded slightly better while operating under identical loading conditions.

As it was pointed out previously, reactors PBR-2 and PBR-3 were taken out of service completely after the period of operation at a loading rate of 4.0 gm COD/L-day (250 lb COD/MCF-day). This decision was based both on the comparatively poor performance as well as the fact that operating all reactors at high loading rates was quite costly and required more equipment and personnel capabilities than were available. It was therefore decided to keep only the two reactors containing the modular corrugated media in

service to observe their performance characteristics when operating at significantly higher loading rates.

The organic loading rate to PBR-1 and PBR-4 was increased to 8.0 gm COD/L-day (500 lb COD/MCF-day) while the influent COD concentration was held at 6000 mg/L. These loading conditions resulted in an empty-bed hydraulic retention time of 18 hours.

The resulting total gas production rate pattern was similar to that observed when operating at lower loading rates although seemingly lagging by a period of about 2 weeks (Figure 31). Steady-state operation was achieved after about 28 days of operation. Total gas production rates during steady-state operation were, on the average, slightly better from PBR-1 than from PBR-4. However, PBR-4 demonstrated slightly more stable daily gas production rates than did reactor PBR-1. The reason behind this slight variability may be attributable to some drifting in the calibration of the feedstock metering pumps supplying substrate to PBR-1.

The methane content of the product gas generally ranged between 62 to 64 percent. This relatively low methane content of the product gas was undoubtedly the result of more carbon dioxide being forced out of solution than before due to increased volatile acids production rates.

Figure 32 shows typical COD and volatile acids profiles through both reactors. The COD profiles indicate quite clearly that little or no removal is achieved past about 2.0 ft. of reactor height. Reactor PBR-1, however, showed COD removal efficiency averaging better than 80 percent as compared to about 70 percent in PBR-4.

Volatile acids profiles (Figure 32) clearly show the relatively better performance characteristics obtained with the larger size modular

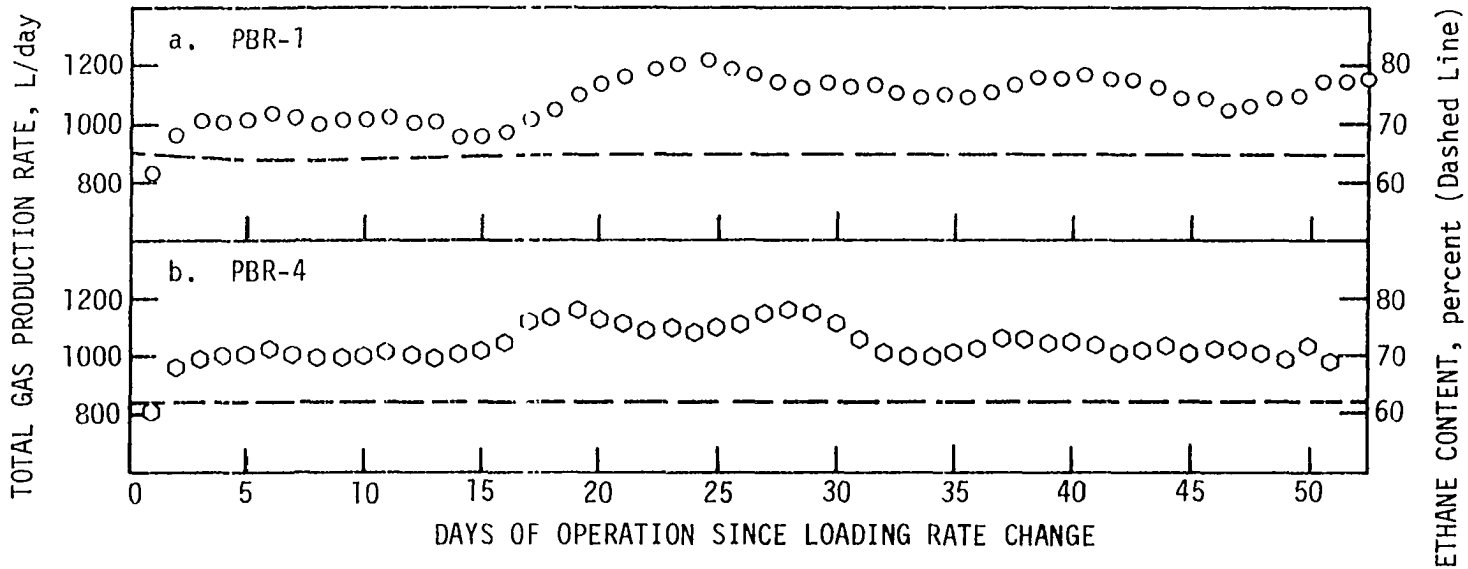

Figure 31. Total gas production rates (L/day) and methane content (%) during operation of PBR-1 and PBR-4 at a loading rate of 8.0 gm COD/L-day. Influent COD = 6000 mg/L

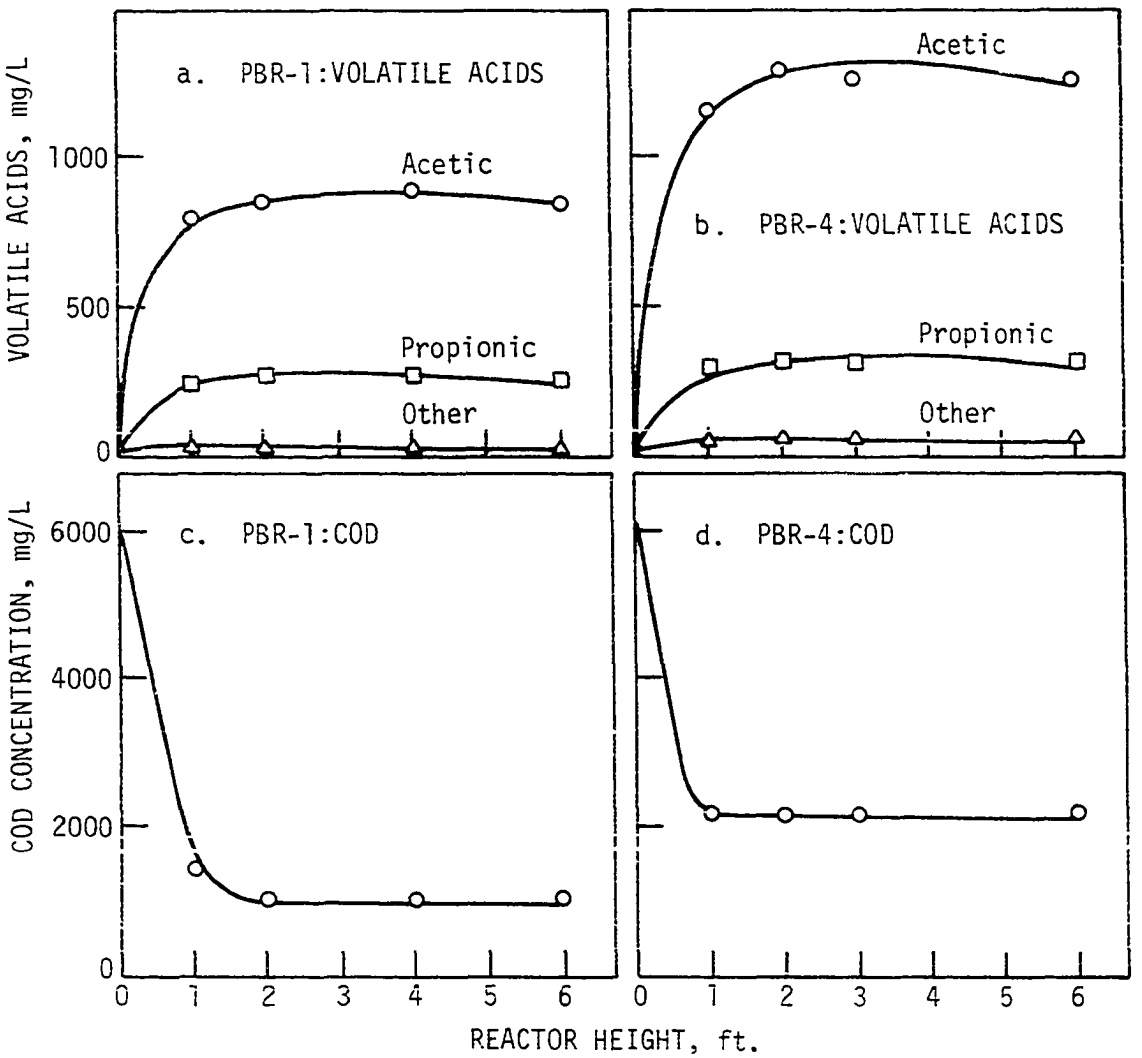

Figure 32. Measured COD and volatile acids (as acetic acid) in PBR-1 and PBR-4 at a loading rate of 8.0 gm COD/L-day. Influent COD = 6000 mg/L

corrugated media (PBR-1). Comparison of volatile acids data with COD data indicated that volatile acids accounted for about 85 percent of the total COD in the effluent stream. The exact make-up of the remaining fraction of effluent COD (i.e. 15 percent) was not known.

After a period of 54 days of operation at 8.0 gm COD/L-day (500 lb COD/MCF-day) the loading rate to these two reactors was doubled to 16.0 gm COD/L-day (1000 lb COD/MCF-day). The influent COD concentration was maintained at 6000 mg/L thus resulting in an empty-bed hydraulic retention time of 9.0 hours. This loading rate could not, however, be maintained for a long period of time due to a failure in substrate metering equipment. This phase of operation was therefore terminated after a period of only four weeks.

Figure 33 shows total daily gas production data during the period of operation at the loading rate of 16.0 gm COD/L-day. The gas production patterns observed earlier at low loading rates (i.e. gas production increase to a maximum value, decrease, and subsequent stabilization) were repeated again at this high loading rate. Figure 33 indicates that apparent steady-state operation was reached only after about three weeks of operation. Because operation at this loading rate had to be terminated, only one week of operational data at what appeared to be steady-state operation was collected.

In general, average daily gas production rates indicated that reactor PBR-1 was once again superior to its counterpart PBR-4. Methane gas content in both reactors was about 60 percent of the total effluent gas reflecting the lowest proportion encountered during this anaerobic filter study.

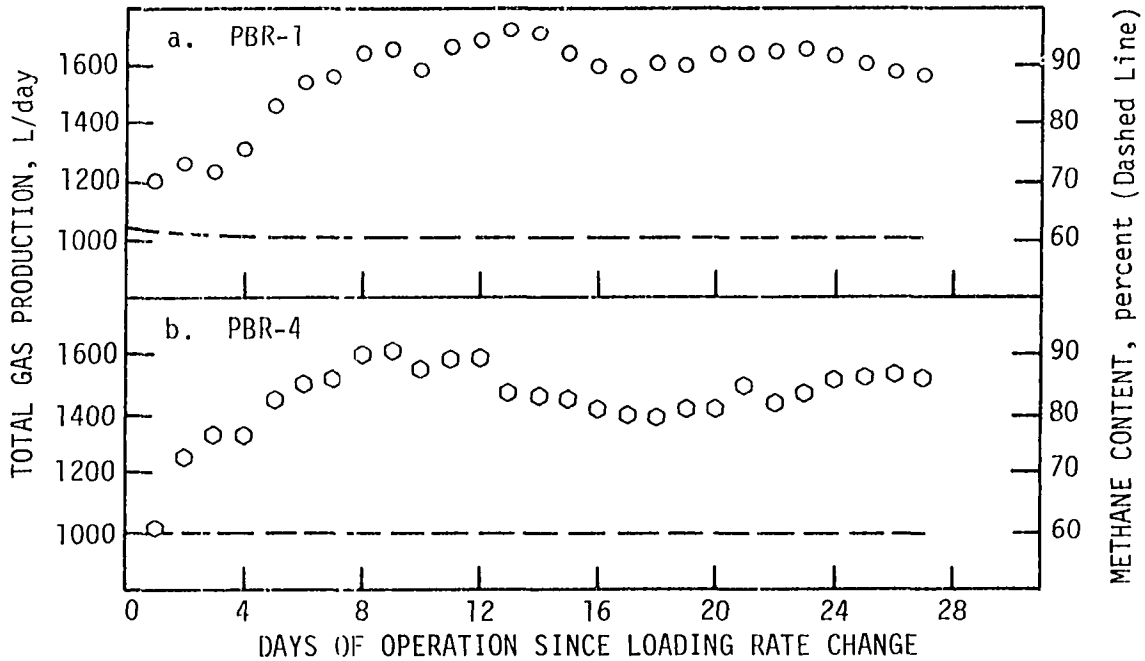

Figure 33. Total gas production rates (L/day) and methane content (%) during operation of PBR-1 and PBR-4 at a loading rate of 16.0 gm COD/L-day. Influent COD = 6000 mg/L

Figure 34 shows measured COD and volatile acids profiles during this phase of the study. The general pattern of COD profiles shows that for all practical purposes no COD removal took place past the 2.0 ft. (0.61 m) height. The sampling taps at the 1 ft. (0.3 m) height interval became plugged due to excessive solids accumulation in the bottom of both reactors shortly after the loading rate was changed indicating the high concentration of interstitial solids present.

The COD profiles clearly indicate that PBR-1 produced better overall removal efficiencies than did PBR-4. On the average, PBR-1 resulted in about 60 percent COD removal while PBR-4 resulted in generally less than 50 percent removal. The volatile acids profiles shown on Figure 34 underscore the relatively better performance characteristics obtained with reactor PBR-1. Comparison of the COD and volatile acids data indicated that only about 80 percent of the effluent COD was accounted for as volatile acids.

Table 14 provides a summary of suspended solids data collected during phases VI and VII. As can be seen from this Table, the two reactors resulted in basically equal effluent suspended solids concentration while operating at a loading rate of 8.0 gm COD/L-day (500 lb COD/MCF-day). At 16.0 gm COD/L-day (1000 lb COD/MCF-day), reactor PBR-4 produced better average suspended solids concentrations than did PBR-1 despite its normally lower performance in terms of COD removal and volatile acids measurements. The difference in effluent suspended solids concentrations is most likely the result of higher total gas production rates from PBR-1 which tended to force more of the biomass solids out into the effluent stream. It also is interesting to point out the higher relative stability in effluent suspended

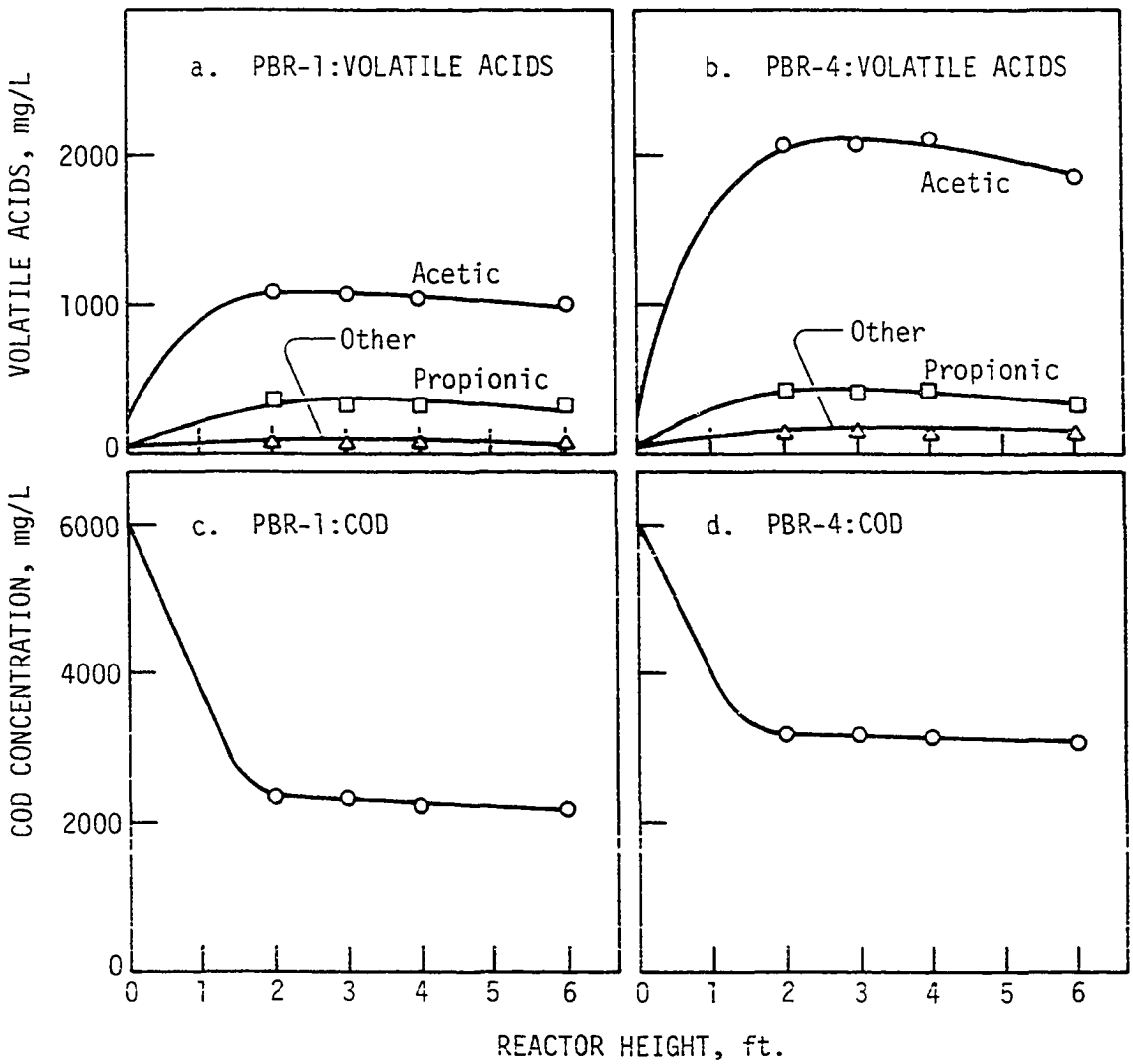

Figure 34. Measured COD and volatile acids (as acetic acid) (mg/L) in PBR-1 and PBR-4 at a loading rate of 16.0 gm COD/L-day. Influent COD = 6000 mg/L.

solids concentrations from PBR-4, compared to PBR-1, as indicated by the significantly lower standard deviations in suspended solids measurements. One may recall that this reactor generally was also more stable than PBR-1 in terms of total gas production rates and COD measurements (Figures 31 and 33).

Table 14. Suspended solids (SS) concentrations during phases VI and VII of anaerobic filter operation

Phase of Operation	Reactor Number	Loading Rate (gm/L-day)	Average SS (mg/L)	Range (mg/L)	Standard Deviation (mg/L)
VI	PBR-1	8.0	435	230-550	177
VI	PBR-4	8.0	433	260-550	100
VII	PBR-1	16.0	392	220-475	149
VII	PBR-4	16.0	317	290-340	25

Anaerobic Filter Performance Analysis

Anaerobic filter effluent quality is measured by two basic parameters; COD removal efficiencies and effluent suspended solids concentrations. Effluent suspended solids concentrations were summarized in Tables 10 through 14 and were discussed in some detail earlier in this report. Effluent COD removal efficiencies are summarized in Tables 15 and 16 and are shown graphically on Figure 35.

Figure 35 shows COD removal efficiencies observed when all four anaerobic filters were operated simultaneously under the same operational conditions. In general, these COD removal efficiencies demonstrate a relative superiority of the modular block media over the loose-fill media. The reactors containing loose-fill media resulted in nearly

Table 15. Chemical oxygen demand removal efficiencies during phases I, II, and III of anaerobic filter operation

Phase of Operation	Reactor Number	Loading Rate gm/L-day	Influent COD mg/L	Average Efficiency %	Range (%)	Standard Deviation	n[a]
I	PBR-1	0.5	1500	85	80-88	3	10
I	PBR-2	0.5	1500	81	72-89	5	10
I	PBR-3	0.5	1500	86	75-96	6	10
I	PBR-4	0.5	1500	83	72-94	6	10
II	PBR-1	1.0	1500	75	68-86	6	10
II	PBR-2	1.0	1500	60	56-68	4	10
II	PBR-3	1.0	1500	71	65-80	6	10
II	PBR-4	1.0	1500	72	62-79	6	10
III	PBR-1	2.0	1500	78	72-85	5	8
III	PBR-2	2.0	1500	56	44-69	9	8
III	PBR-3	2.0	1500	53	34-64	11	8
III	PBR-4	2.0	1500	68	56-84	8	8

[a] n=number of COD measurements.

Table 16. Chemical oxygen demand removal efficiencies during phases IV-VII of anaerobic filter operation

Phase of Operation	Reactor Number	Loading Rate (gm/L-day)	Influent COD (mg/L)	Average Efficiency (%)	Range (%)	Standard Deviation	n[a]
IV	PBR-1	2.0	3000	88	82-90	3	13
IV	PBR-2	2.0	3000	61	46-74	9	13
IV	PBR-3	2.0	3000	71	60-77	5	13
IV	PBR-4	2.0	3000	83	73-89	4	13
V	PBR-1	4.0	6000	89	84-94	3	10
V	PBR-2	4.0	6000	72	64-86	6	10
V	PBR-3	4.0	6000	78	71-88	5	10
V	PBR-4	4.0	6000	86	74-93	6	10
VI	PBR-1	8.0	6000	82	72-89	6	11
VI	PBR-4	8.0	6000	69	62-83	7	11
VII	PBR-1	16.0	6000	60	54-67	4	8
VII	PBR-4	16.0	6000	48	39-65	7	8

[a] n=number of COD measurements

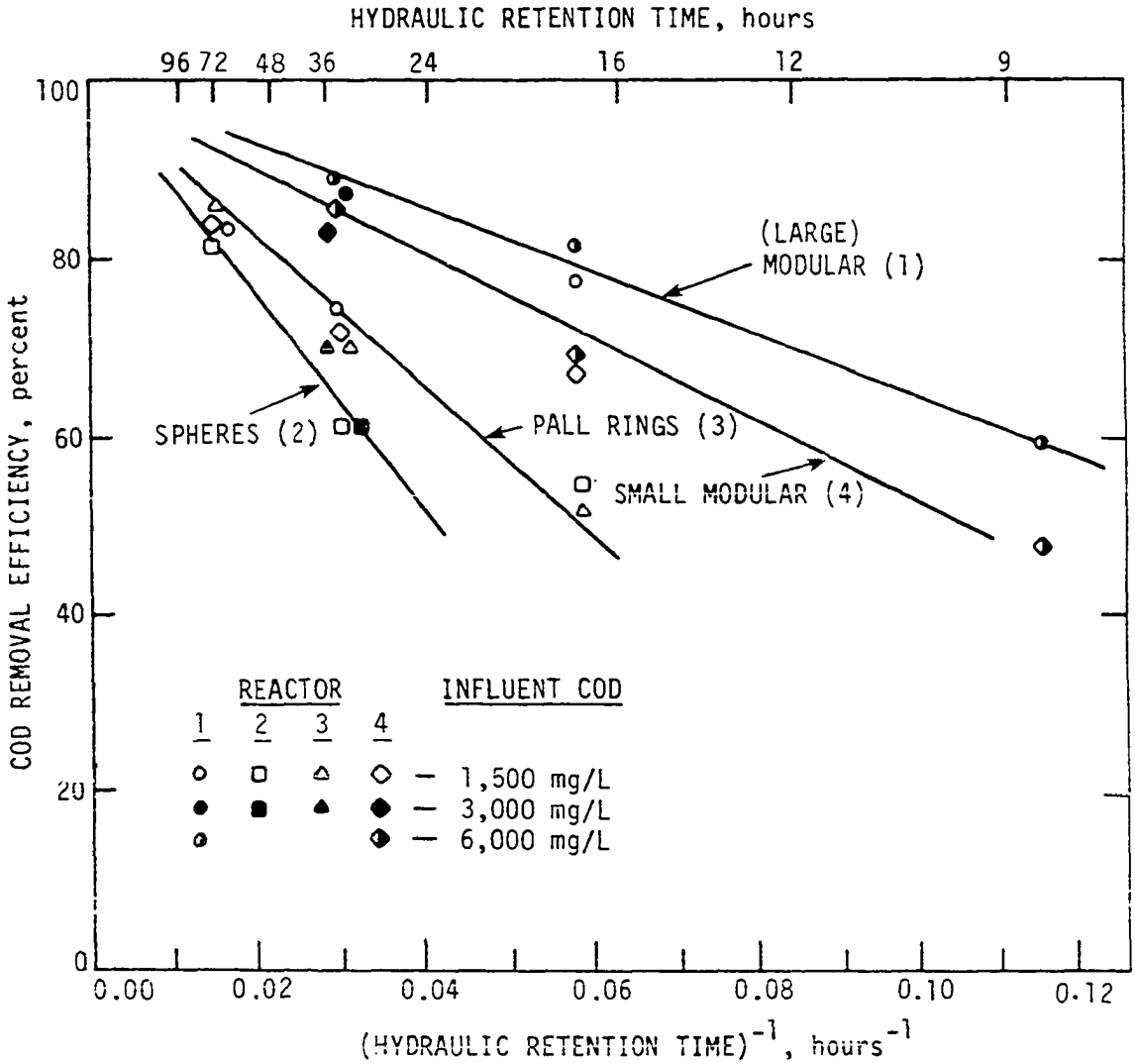

Figure 35. Anaerobic filter treatment efficiency (%) vs. the inverse of the hydraulic retention time (hours^{-1})

identical performance efficiencies with the Pall ring media showing only marginally better overall COD removal characteristics.

The modular media reactors resulted in substantially better COD removal characteristics with the larger sized medium (PBR-1) having a pronounced relative superiority over the smaller counterpart (PBR-4). This trend continued at high organic loading rates as seen on Figure 35.

Figure 35 suggests that COD removal efficiency is a linear function of the inverse hydraulic retention time. This trend is more evident at high organic loading rates and high influent COD concentrations as shown on Figure 35 for the corrugated media units (PBR-1 and PBR-4). Examination of Figure 35 suggests that the hydraulic retention time (HRT) is a more significant parameter than either the influent waste strength or the organic loading rate. A similar conclusion was made by other researchers (65, 69). Young (65) suggested an empirical relationship based on data similar to that shown in Figure 35. If COD removal efficiency is denoted by E, then

$$E = 100\ (1 - e/T) \tag{30}$$

where

T = Theoretical hydraulic retention time, hours, and

e = A proportionality constant, hours.

It is obvious from the data shown in Figure 35 that $\underline{e}$ is a strong function of media characteristics (i.e. design and size). Due to the variability of effluent COD concentrations, even at constant organic loading rates, Equation 30 appears to have somewhat limited practical use in anaerobic filter performance prediction due to the difficulty in estimating $\underline{e}$ for a variety of media.

Gauged in terms of qualitative observations, the effluent from all anaerobic filters generally had a grayish dark hue characteristic of its suspended solids. Once an effluent sample was centrifuged or filtered, the centrate or filtrate was consistently color-free.

Variability of effluent quality

Tables 15 and 16 show the ranges and standard deviations of COD removal efficiencies at each loading rate. As shown, the standard deviations were generally less than 10 and frequently less than 5 percentage units. Examination of anaerobic filter performance data in the literature (8, 65) indicates that the variability shown in these tables was generally low and reflects a high degree of consistency given the large number of factors that could contribute to daily fluctuations in anaerobic filter treatment efficiency.

The variability of anaerobic filter performance is affected by such parameters as the variability in influent feedstock metering (i.e. changes in organic load and influent COD concentrations) and changes in environmental conditions such as temperature and pH. Another important parameter contributing to the variability of effluent quality is the accuracy of chemical oxygen demand determinations in the laboratory (i.e. analytical errors). Standard methods (55) reported that a coefficient of variability of 8 percent in COD determinations was common.

COD-CH_4 balance during steady-state operation

A chemical oxygen demand-methane balance is shown on Tables 17 through 20 for reactors PBR-1 through PBR-4, respectively. These tables were constructed on the basis of average performance during apparent

Table 17. $COD-CH_4$ conversion during steady-state anaerobic filter treatment. Reactor PBR-1 (large modular media)

L.R. (gm/L-day)	Influent COD (mg/L)	Avg. COD Removal (%)	Total Gas Production (L/day)	Methane content (%)	COD Equiv. of CH_4 (gm/day)	Act. COD Removed (gm/day)	Conversion of COD to CH_4 (%)
0.5	1500	85	70	75	145	158	92
1.0	1500	75	160	74	320	278	115
2.0	1500	78	240	75	500	579	86
2.0	3000	87	370	72	700	650	108
4.0	6000	89	670	70	1225	1323	93
8.0	6000	82	1150	65	1960	2430	81
16.0	6000	60	1650	60	2618	3560	74
						Average =	93

Table 18. $COD-CH_4$ conversion during steady-state anaerobic filter treatment. Reactor PBR-2 (perforated balls media)

L.R. (gm/L-day)	Influent COD (mg/L)	Avg. COD Removal (%)	Total Gas Production (L/day)	Methane content (%)	COD Equiv. of CH_4 (gm/day)	Act. COD Removed (gm/day)	Conversion of COD to CH_4 (%)
0.5	1500	81	70	75	145	150	97
1.0	1500	60	150	74	305	223	136
2.0	1500	56	175	72	363	416	87
2.0	3000	61	250	67	449	453	99
4.0	6000	72	500	66	866	1068	81
						Average =	100

Table 19. COD-CH_4 conversion during steady-state anaerobic filter treatment. Reactor PBR-3 (Pall ring media)

L.R. (gm/L-day)	Influent COD (mg/L)	Avg. COD Removal (%)	Total Gas Production (L/day)	Methane content (%)	COD Equiv. of CH_4 (gm/day)	Act. COD Removed (gm/day)	Conversion of COD to CH_4 (%)
0.5	1500	86	75	74	152	160	95
1.0	1500	71	150	74	304	263	115
2.0	1500	53	220	73	451	393	114
2.0	3000	71	280	68	508	527	96
4.0	6000	78	550	66	970	1157	84
						Average =	100

Table 20. COD-CH_4 conversion during steady-state anaerobic filter treatment. Reactor PBR-4 (smaller modular media)

L.R. (gm/L-day)	Influent COD (mg/L)	Avg. COD Removal (%)	Total Gas Production (L/day)	Methane content (%)	COD Equiv. of CH_4 (gm/day)	Act. COD Removed (gm/day)	Conversion of COD to CH_4 (%)
0.5	1500	83	75	74	152	154	99
1.0	1500	72	150	74	304	267	113
2.0	1500	68	260	73	525	504	104
2.0	3000	83	350	70	648	516	125
4.0	6000	86	640	70	1169	1276	92
8.0	6000	69	1050	62	1709	2047	83
16.0	6000	48	1470	60	2342	2849	82
						Average =	100

steady-state conditions. The COD equivalent of the product methane gas was calculated using a theoretical amount of COD consumed per unit of product methane of 0.390 gm CH_4/gm COD at 30°C. The total product methane included the portion normally measured in the effluent gas and the amount dissolved in the liquid effluent stream. The latter amount was calculated on the basis of the theoretical solubility of methane in water at 30°C (0.032 L CH_4/L water).

On the average, as seen from Tables 17-20, essentially all of the COD removed during steady-state operation was accounted for as methane gas. Only PBR-1 deviated slightly resulting in an average COD to methane conversion of about 93 percent. This deviation is probably the result of higher biomass synthesis rates in this reactor and the fact that steady-state conditions perhaps were not fully reached.

In general, COD conversion to methane declined with increasing organic loading rate. This downward trend is shown in Figure 36 for units PBR-1 and PBR-2 although the same trend is apparent for the other two reactors as well (Tables 18 and 19). The decline in COD conversion to methane gas at high organic loading rates was probably due to the increased loss of COD as biological solids (i.e. suspended solids) in the effluent stream.

Biomass Growth Characteristics

At the end of phase VII of this study PBR-1 and PBR-4 were dismantled and the modular media blocks were taken out to observe the general patterns of both suspended and attached growth within these two reactors. The general procedure by which these two reactors were taken apart was designed

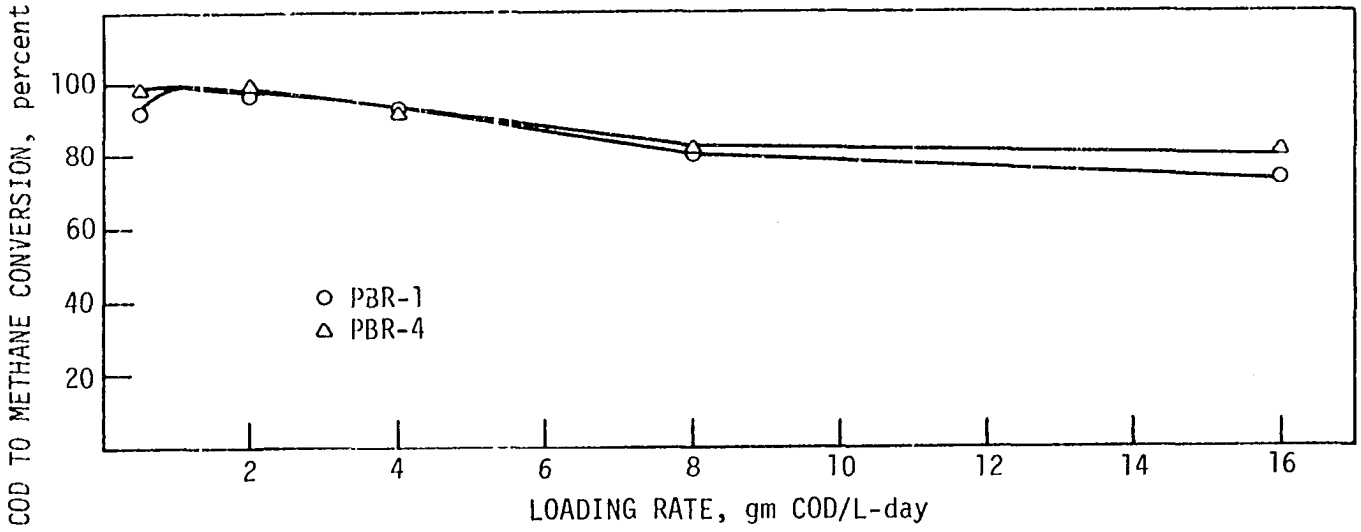

Figure 36. COD to methane conversion (%) vs. organic loading rates (gm-COD/L-day) for PBR-1 and PBR-4

to minimize the intermixing of suspended solids or the shearing and sloughing of attached solids.

The first step in the dismantling procedure involved disconnecting the effluent manifolds and gas meters and removing the reactor lid. The next step was to extract the top media module (block) using steel tongs. The media block was then set aside to drain away excess liquid. The mixed liquor left behind in the top one foot of the reactor was gently stirred and samples from this portion were collected for solids analysis. The remainder of the liquid left behind was siphoned out to the level of the next media block. The next media block was removed gently, samples were collected, and the remainder of the liquid was siphoned out. This procedure was continued until all media modules were removed and the reactor was completely drained.

Examination of the suspended biological mass indicated, as expected, that these solids were generally well-flocculated and readily settleable under quiescent conditions. Typical floc particles were rounded and resembled coarse sand in appearance and were grayish-black to deep black in color. Although it was difficult to estimate the size of these solids particles, visual examination indicated that such sizes were generally between 1 and 3 mm in diameter with occasional larger granules.

When put under quiescent settling conditions, the particles settled quickly and only an extremely fine layer of pin-point sized solids were left at the surface. The smaller sized particles that settled to the bottom occasionally would rise due to the accumulation and growth of tiny gas bubbles on them. Once the gas bubbles were released, the particles settled quickly. The action of rising gas bubbles was observed to cause

larger solids particles to roll until the gas bubble was released. This gas-induced motion could contribute to the flocculation and growth of suspended solids particles on one hand and it could cause biomass to be lifted upward through the reactor, on the other.

After the modular media blocks were removed from the reactors, these blocks were examined and photographed to document attached growth patterns and thicknesses. These blocks were then placed in a constant temperature room and left to dry over a period of a few days at 40°C (104°F). Figure 37 shows typical media blocks after being removed from the bottom of PBR-1 and PBR-4.

The characteristics of attached growth solids were nearly identical in both PBR-1 and PBR-4. The biological film consisted of extremely slimy and often filamentous growth that was grayish black to deep black in color. The film was highly variable in thickness with solids globules attached to the media surface at frequent locations regardless of where the original media blocks were placed in the column. However, film thickness decreased with reactor height and ranged from about 3 to 5 mm on the bottom media block (first 1-foot (0.30 m) height) to about 1 to 3 mm in the top media block (i.e. 6-foot (1.83 m) height). The attached growth was extremely fragile and could easily be sloughed off the surface of the media. Therefore, the media blocks had to be handled with care.

Typical distribution of biological growth

Suspended growth: Figure 38 shows the concentrations of suspended solids in PBR-1 and PBR-4 obtained as the media were removed from these reactors. As expected from an assessment of the COD removal profiles, the

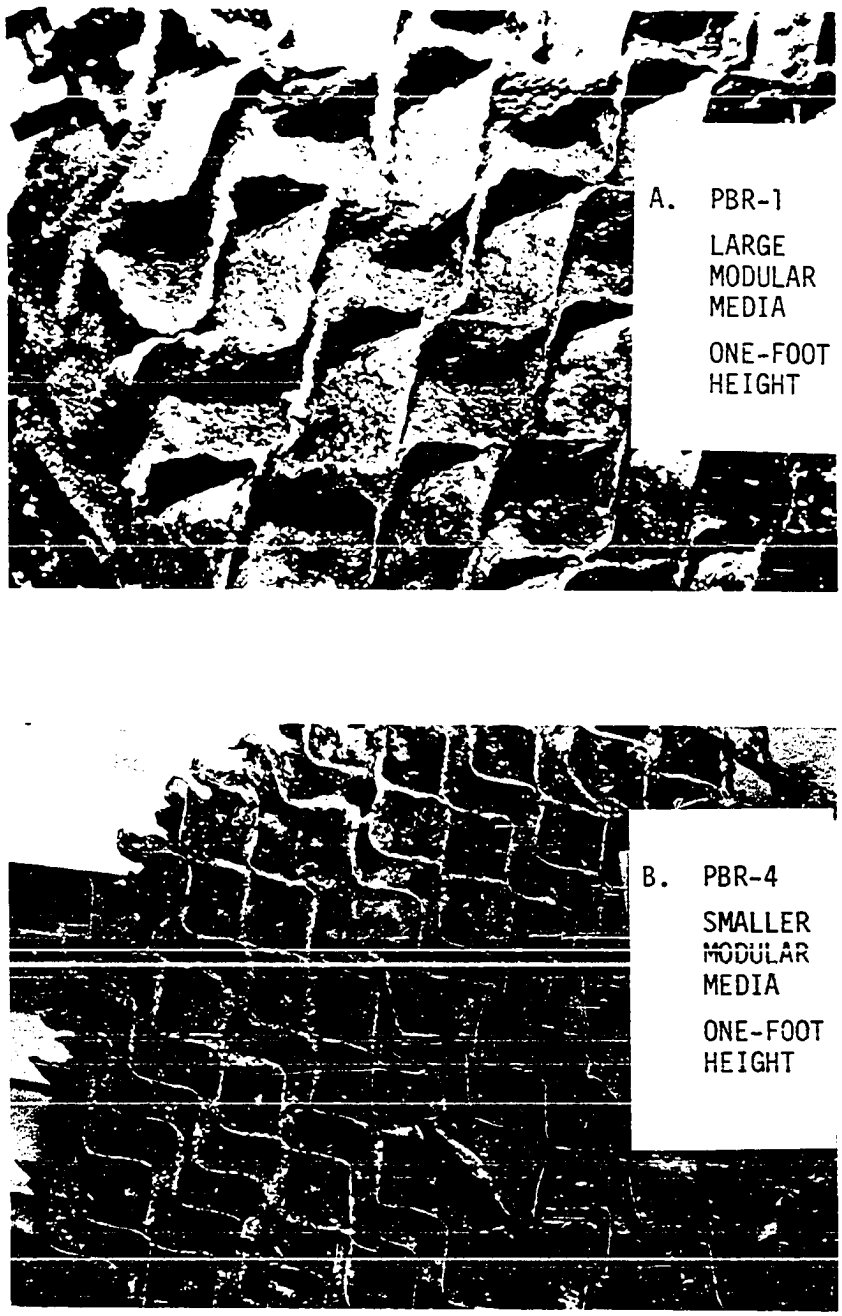

Figure 37. Modular media blocks after being removed from anaerobic filters. (A) Bottom blocks from PBR-1, and (B) bottom blocks from PBR-4

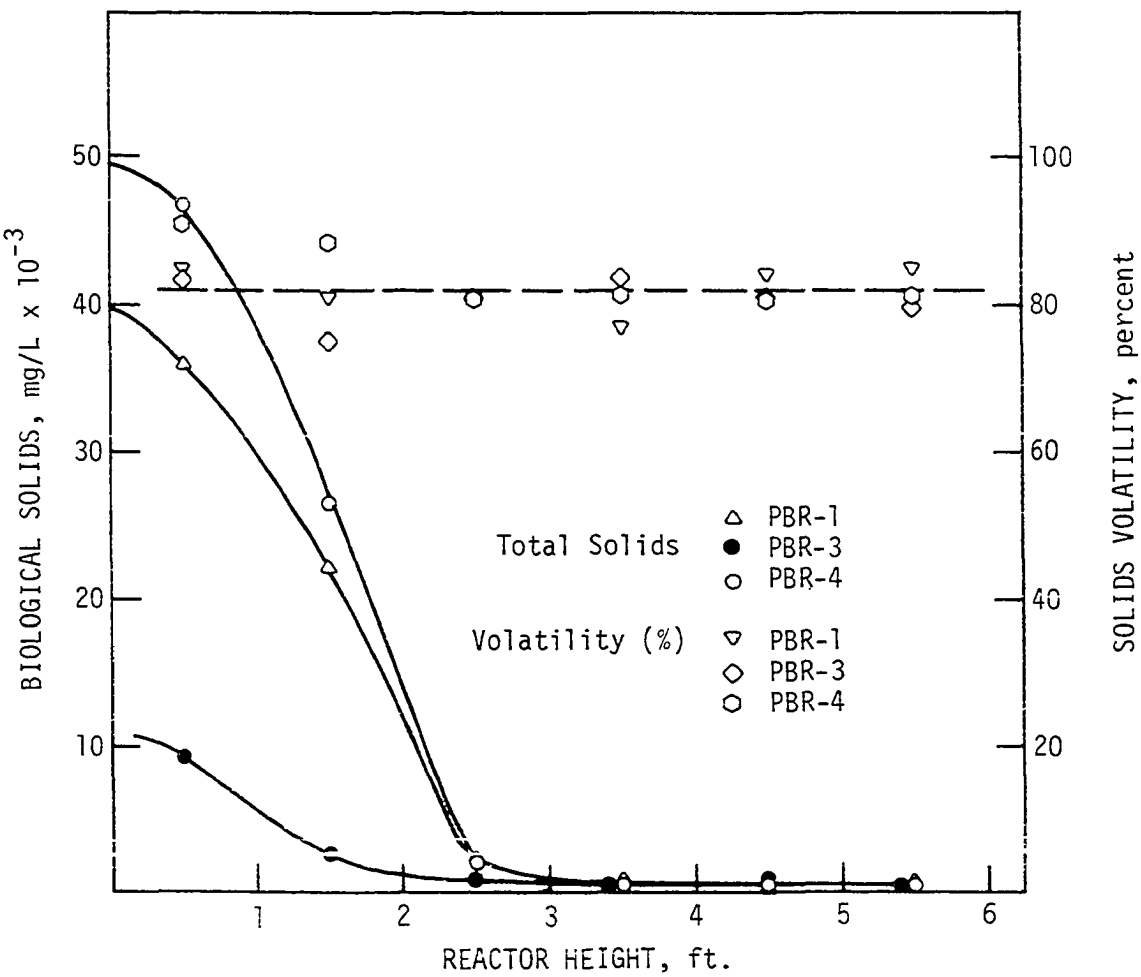

Figure 38. Total suspended solids (mg/L) and percent volatile solids in PBR-1, PBR-3, and PBR-4 at the end of study

bulk of suspended solids were in the lower two feet (0.61 m) of each reactor. The suspended growth was practically negligible in the top half of each reactor as compared to the concentrations of solids in the lower sections. These solids profiles support the lack of COD and volatile acids removal in these reactors past two feet (0.61 m) of height. Figure 38 also shows the relatively high volatility of the suspended solids. In general, suspended solids volatility was consistently better than 80 percent in both reactors and did not seem to change with reactor height.

The suspended growth patterns shown in Figure 38 were most likely the result of the media characteristics that allowed solids to settle to the bottom of the reactors. These solids profiles also indicated that little net upwards solids transport took place within the reactors to force a more even distribution of solids throughout the reactor media. A long period of operation would be expected to cause a shift of the suspended solids profiles.

After about four months of dormancy, reactor PBR-3 (Pall ring media) was restarted by resuming feedstock metering to this unit at an estimated organic loading rate of 2.0 gm COD/L-day (125 lb COD/MCF-day) to observe its response. The reactor responded very quickly, as will be discussed later in more detail, and gas production was observed almost immediately. The unit was operated for a period of about three weeks and then it was shut down again during the holiday season. After about one month of shut-down, this reactor was dismantled in a manner similar to PBR-1 and PBR-4. The suspended solids concentrations measured during dismantling are shown in Figure 38. The extended period of inactivity of PBR-3 prior to dis-mantling makes it difficult to compare these data with data from the

modular media units. It is evident, however, that there were no dramatic differences in suspended solids profiles between these reactors.

Attached growth: As shown in Table 21, despite the fact that the biofilm thickness on the media blocks was greater on the lower media modules in both PBR-1 and PBR-4 than it was on the top sections, the attached solids were significantly more evenly distributed than were the suspended growth solids. In fact, with the exception of the bottom two sections of modular media, attached growth was quite evenly distributed as seen in Figure 39.

Specific biomass growth (kg biomass per unit media surface area) was significantly different between PBR-1 and PBR-4 contrary to what one may have expected since the units were operated under identical conditions throughout this study (Figure 40). The difference in specific growth between the two sizes of media was likely due to the larger number of corrugated sheets and subsequently the larger number of intersections of media flutes. This larger number of intersections apparently caused larger amounts of biomass to become lodged at these intersections (i.e. angles) thus causing the specific growth to be much higher than in PBR-1.

Apparently a larger fraction of attached solids that died off and decayed were not readily transported out of the reactors. This phenomenon was evident by the lower volatile fraction of attached solids as shown in Table 21. The volatile fraction was essentially the same in both reactors and did not seem to vary with height within either unit. The mean volatility of attached solids (about 67 percent) was lower than the mean volatility of the suspended solids (about 83 percent) in both reactors.

Examination of the attached growth pattern in PBR-3 (Pall rings)

Table 21. Summary of attached growth data from modular media blocks in reactors PBR-1 and PBR-4

Media Block Number	Reactor Height ft (m)	Media Block Weight (gm)	Total Attached Solids (Dry) (gm)	Solids Volatility (%)	Total Attached Solids (gm/L)[a]
PBR-1-1	1 (0.30)	2500	690	68	11.76
1-2	2 (0.61)	2570	236	66	4.02
1-3	3 (0.91)	2605	244	65	4.16
1-4	4 (1.22)	2510	241	67	4.11
1-5	5 (1.51)	2580	292	67	4.98
1-6	6 (1.83)[b]	1980	218	66	3.72
PBR-4-1	1 (0.30)	1345	1357	69	23.13
4-2	2 (0.61)	1400	1575	67	26.84
4-3	3 (0.91)	1430	478	67	8.15
4-4	4 (1.22)	1337	568	67	9.68
4-5	5 (1.51)	1400	576	64	9.82
4-6	6 (1.83)[b]	975	542	68	9.24

[a]Computed on the basis of available void volume within each media block.

[b]Short blocks, block thickness = 10 in. (0.25 m).

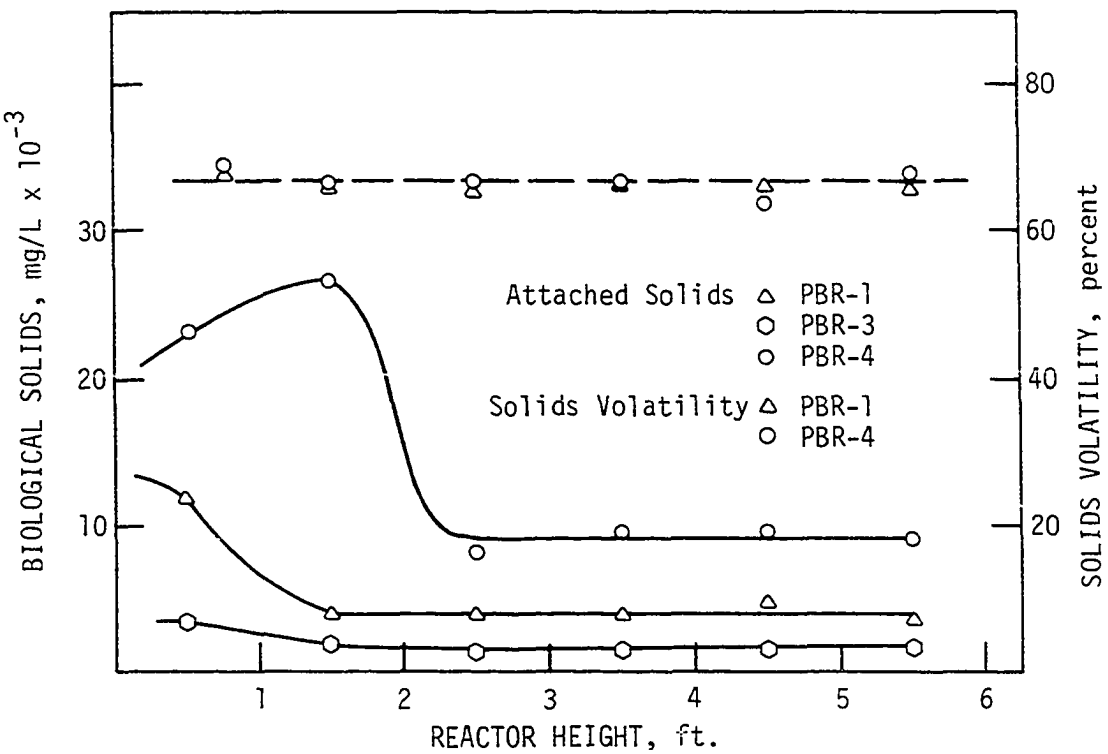

Figure 39. Attached solids (expressed as mg/L) and attached solids volatility in reactors PBR-1, PBR-3, and PBR-4 at the end of study

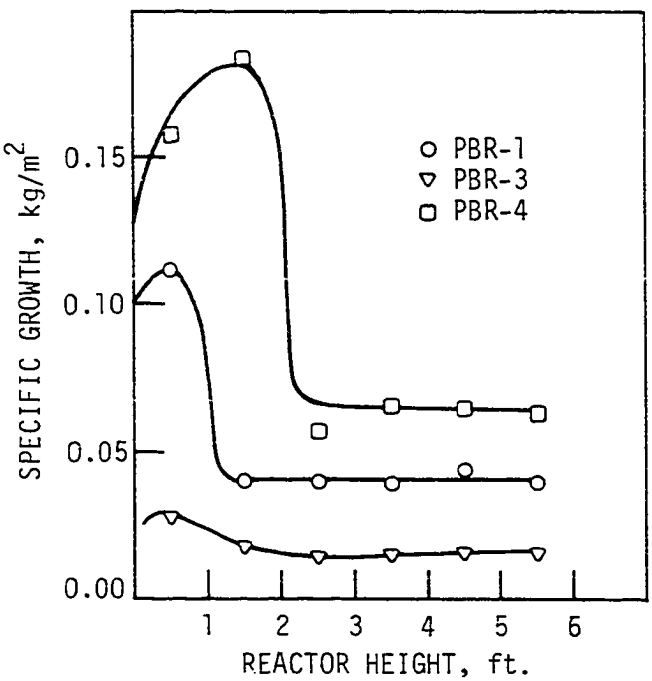

Figure 40. Specific biomass growth (kg/m^2) vs. reactor height in reactors PBR-1, PBR-3, and PBR-4 at the end of study

indicated that these solids were evenly distributed throughout the reactor height (Figure 39). Specific growth in this reactor was quite uniform even in the lower section of the column in contrast to the modular media units (Figure 40). The extended period of inactivity of this reactor and the fact that it was not operated at high organic loading rates as in PBR-1 and PBR-4 precludes drawing concrete conclusions concerning growth patterns in this reactor. Indications are, however, that specific growth may not have followed the same patterns observed with PBR-1 and PBR-4 had this unit been operated at the same high organic loading rates as were PBR-1 and PBR-4.

Biomass activity

The volatile fraction of biological mass, as determined by the ignition procedures described in Standard Methods (55), is often used as a measure of active solids in biological waste treatment systems. This procedure, however, is nonspecific and, at best, is an approximation since cell matter is highly volatile regardless of whether such cells are active or not. A practical indication of biomass activity in anaerobic systems is the measurement of methane gas production rates under highly controlled conditions. Biomass activity in this case could be expressed in terms of the amount of methane produced per unit weight of volatile solids per unit time (e.g. mls CH_4/gm VSS-hr).

After reactor PBR-4 was dismantled, the suspended growth samples collected at each increment of filter depth were used to determine biomass activity in these anaerobic systems. The procedure used for this test was a modification of a procedure used by Johnson and Young (30) in the study

of the toxicity of priority chemical pollutants in anaerobic waste treatment systems. In this procedure, samples containing suspended solids were placed in sterile (250 ml) serum bottles after these bottles were filled with pure nitrogen gas to eliminate the presence of oxygen. Known quantities of substrate (normal anaerobic filter feedstock) were added to these serum bottles after the suspended solids samples had sat overnight in a 30°C (86°F) constant temperature room. Total gas production (and methane content) was monitored frequently particularly at the start of this experiment. All suspended solids activity measurements were carried out in triplicate with a correction blank that contained a solids sample and no added substrate. The basic procedure is described in more detail by Johnson and Young (30).

At the conclusion of this experiment the suspended and volatile suspended solids concentrations were determined in order to estimate the relative amount of biological growth that took place during the test period. It was basically found that such growth was negligible given the relatively short test period over which actual activity measurements were made (less than 24 hours). The total amount of gas production, its methane content, and volatile suspended solids concentrations, were used to arrive at a measure of solids activity in terms of the volume of methane gas produced per unit volatile solids per unit time as shown on Figure 41.

As shown, biomass activity was fairly high in the solids removed from the first one-foot (0.61 m) of anaerobic filter height. This activity reached a maximum value of about 0.30 mls CH_4/gm VSS-hr in the second one-foot increment of reactor height, declined quickly in the third one-foot increment of height, and leveled off past that point. The biomass activity

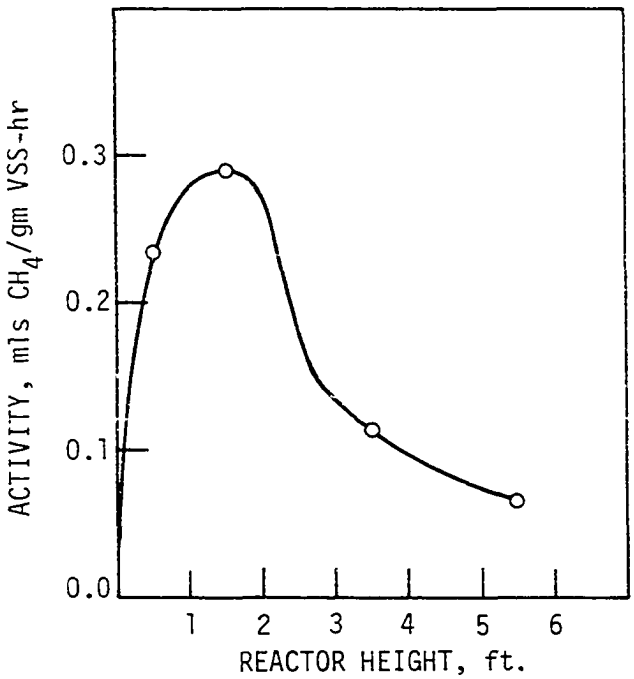

Figure 41. Suspended solids activity (mls CH_4/gm VSS-hr) vs. reactor height (ft.) (reactor PBR-4)

as shown on Figure 41 is in agreement with the specific growth profiles shown on Figure 40 and provided further justification of the basic pattern of COD removal rates observed earlier.

Examination of Figure 38, which shows the total suspended solids concentrations and volatile fraction for reactor PBR-4, indicates that for all practical purposes, biomass volatility was basically constant despite the drastic difference in total suspended solids concentrations between the lower and upper sections of the reactor. Yet, despite this apparent constant suspended solids volatility, volatile solids activity, as measured and shown on Figure 41, indicates that most of the solids activity was in the bottom sections of the reactor. This leads to the conclusion that the volatile suspended solids in the upper sections of the reactor were primarily composed of decaying cell matter.

In their studies using small diameter anaerobic filter reactors, van den Berg and Lentz (59) reported results similar to those shown in Figure 41 leading these investigators to arrive at similar conclusions about removal of organic materials in anaerobic filters containing high porosity packing materials. Van den Berg and Lentz (59) also concluded that most of the organic removal in this type of anaerobic filters is attributed to suspended growth and not to attached growth.

Because of the difficulties encountered in devising a realistically true activity test for attached growth solids, no such test was conducted. A valid test would require a procedure in which the solids remain attached to the support medium in order to simulate actual conditions within the anaerobic filter reactor. This could not be done particularly with the loose-fill media used in this study. Additionally, any attempt to remove

the attached biomass so that it could be used in the 250 ml serum bottle test described above would have been inappropriate.

Anaerobic Filter Response to Intermittent Operation

After reactor PBR-3 was taken out of service at the end of phase V of this study, gas production from this unit declined steadily until it reached no apparent activity after about two weeks. No gas production was observed in this reactor for the remainder of a four-month period of complete shut-down. At the conclusion of this entire study, feedstock metering to PBR-3 (Pall ring media) was restarted at an approximate loading rate of 2.0 gm COD/L-day (125 lb COD/MCF-day) and an influent COD concentration of 3000 mg/L.

The response of reactor PBR-3 to resumed operation was almost immediate. As shown in Figure 42, total daily gas production rate increased steadily until steady-state conditions were reached at the end of two weeks of operation.

The data shown graphically in Figure 42 clearly demonstrate the resilience of the anaerobic filter process and its ability to recover after long periods of dormancy. This characteristic is not matched by conventional mixed-culture biological waste treatment processes where continuous operation is required to maintain an active microbial population for removal of organic wastes. The ability of the anaerobic filter process to withstand intermittent operation with no harmful results to the process is extremely advantageous to industries producing wastewater streams that are intermittent or perhaps even seasonal.

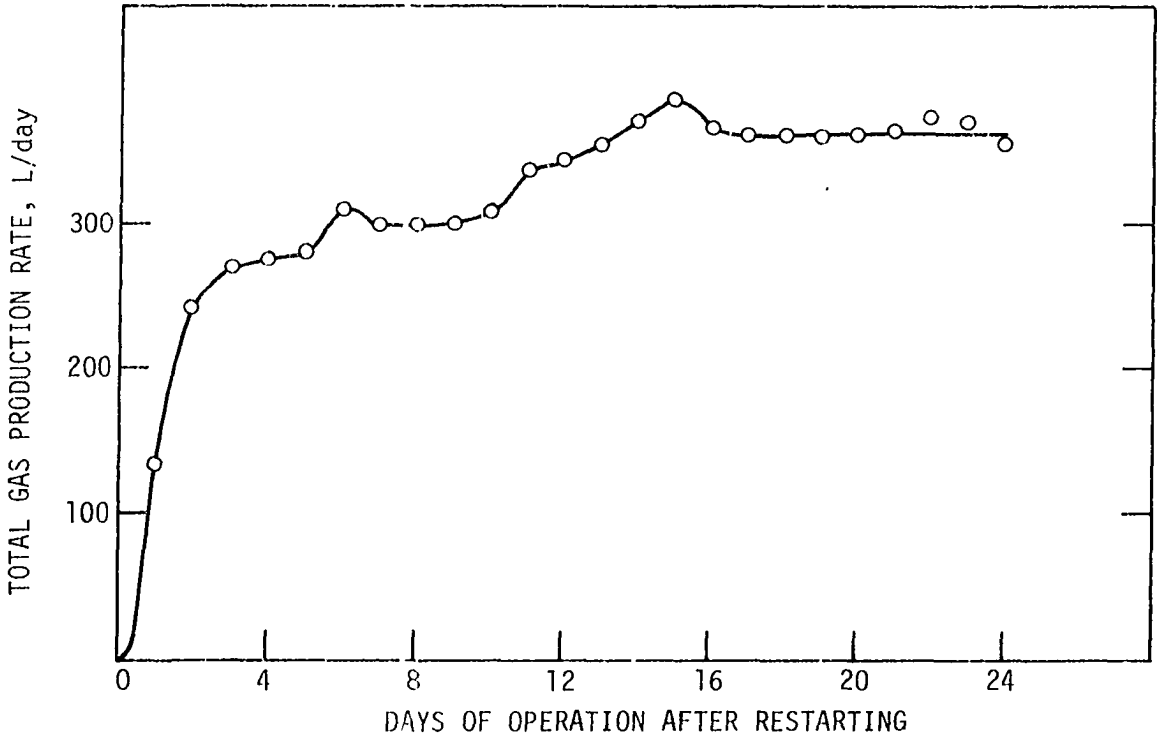

Figure 42. Total gas production rates (L/day) upon restarting of PBR-3 after four months of complete shut-down at a loading rate of 2.0 gm COD/L-day. Influent COD = 3000 mg/L

MATHEMATICAL SIMULATION OF ANAEROBIC FILTER PERFORMANCE

As was discussed earlier, a dynamic model was formulated by Young (65) to simulate the operation and performance of the anaerobic filter process. This model was tested using data obtained from laboratory-scale anaerobic filters that were operated under a variety of loading conditions and was able to simulate anaerobic filter performance with a reasonable degree of accuracy.

Young's model (65) was used in its basic form to simulate the results of this anaerobic filter study. Before this model could be used successfully, biological growth, substrate utilization, and other physical coefficients had to be re-evaluated to fit the conditions and characteristics of this study. In addition, some modifications were made in an attempt to account for the effects of differing media designs on anaerobic filter performance.

Coefficients of the Anaerobic Filter Model

Coefficients of growth and substrate utilization

Growth yield: As was shown in Table 3, the basic composition of the feedstock used in this study consisted of a volatile acids mixture, an alcohols mixture, and a sugar additive. The COD contributions of these components were 6.7, 66.6, and 26.7 percent, respectively. The alcohol and sugar fractions comprise complex waste components that are decomposed anaerobically in a two-stage process, similar to that illustrated by Figure 1, in which the components are converted to volatile acids, principally acetic and propionic.

Growth yield coefficients for the decomposition of volatile acids to methane gas range from 0.04 to 0.054 mg VSS/mg COD converted to CH_4 and cells (65). These values were based on measurements by Lawrence and McCarty (32) and Speece and McCarty (54).

For the first-stage conversion of proteins and carbohydrate wastes, Young (65) calculated average yield coefficients for these wastes using the following expression:

$$a_c = (a_s - a_v)/(1 - 1.42a_v) \quad (31)$$

where

a_c = Growth yield coefficient for the first stage conversion of complex waste, mg VSS/mg COD,

a_v = Growth yield coefficient for volatile acids decomposition, mg VSS/mg COD, and

a_s = Growth yield coefficient for the complete stabilization of complex waste, mg VSS/mg COD.

Equation 31 also was used for estimating the biological growth coefficients for the complex waste components used in this study. For typical carbohydrate wastes, growth yield coefficients are expected to be about 0.20 mg VSS/mg COD converted to methane (42, 65) and for short chain alcohols to be about 0.15 mg VSS/mg COD (28). Based on equation 31, first-stage yield coefficients for these two components are expected to be in the range of 0.1 to 0.17 mg-VSS/mg-COD converted to methane. Based on actual mixtures of carbohydrates and alcohols used as feedstock in this study, an overall growth yield coefficient of 0.14 mg VSS/mg COD was determined to be the best available approximation for use in the anaerobic filter model.

Biomass decay: For volatile acids wastes, biological decay coefficients range from about 0.01 to 0.04 day^{-1} at temperatures of 25 and

35°C, respectively (65). Because the effects of temperature on biological decay rates have not been firmly established, a conventional value of 0.04 day^{-1} was chosen for the volatile acids waste fraction used in this study.

For the carbohydrate-alcohols waste fractions, a first stage decay coefficient of 0.08 day^{-1} was selected. This value represents a conservative estimate of this parameter based on data cited in the literature (33, 54, 65).

Maximum waste utilization rates: The maximum rate of waste utilization, k, (Equation 2) for acetic acid is about 5.0 gm COD/day/mg VSS at 25°C and 18.3 mg COD/day/mg-VSS for propionic acid (65). Only about 43 percent of the propionic acid COD is converted directly to methane gas and cell matter and the remainder, 57 percent, is released as acetic acid which then undergoes methanogenesis. The value of k increases to about 6.1 mg COD/mg VSS-day at 30°C. However, the value of k reportedly remains constant between 25 and 35°C for propionic acid (65).

Half-velocity coefficients: Values of the half-velocity coefficient, K_s, (Equation 2) for both acetic and propionic acids COD used in the anaerobic filter model were 355 and 205 mg/L, respectively, at 30°C (65). The value of K_s for propionic acid represents an estimate based on graphical analysis of data presented by Lawrence and McCarty (33).

Rate of complex waste conversion: In the development of the anaerobic filter model, Young (65) and Young and McCarty (69) used a value of 24 gm COD/L day for the first-stage conversion rate of complex waste (i.e. protein-carbohydrate). This value was arrived at through examination of anaerobic filter performance data obtained from their laboratory

studies. The rate of complex waste first-stage conversion is dependent on a variety of operational factors such as loading rates, operational temperatures, the concentration of first-stage complex waste utilizing biomass, and the composition of the complex waste itself. Therefore, an accurate estimate of this parameter was extremely difficult. However, examination of chemical oxygen demand profiles throughout this study, as was shown earlier, indicated that this first stage conversion rate was equivalent to values suggested by Young (65). A value of 25 gm COD/L-day was estimated through trial runs of the filter model. At this rate the entire complex waste fraction used in this study was converted entirely to volatile acids in the first one-foot (0.30 m) increment of anaerobic filter height. This conclusion was supported by the COD and volatile acids data collected during this study. Table 22 provides a summary of the coefficients of growth and substrate utilization rates used in this study.

Total gas production

Total gas production in the anaerobic filter model was determined using the following relationship (65):

$$q = \frac{Cf_g Q}{P} (\Delta S/1000) \qquad (32)$$

where

q = Total gas moving through an increment of filter height, L/day-ft^2

C = Potential volume of methane produced per unit of substrate converted to methane = 0.390 L/gm COD at 30^{o}C and one atmosphere

f_g = Fraction of removed substrate COD converted to methane COD

Q = Hydraulic flow rate, L/day

Table 22. Biological growth and substrate utilization coefficients used in the anaerobic filter model

Coefficient	Substrate	Label[a]	Value	Units	Source
Growth yield	Acetic acid	a_a	0.05	gm VSS/gm COD	32, 54, 65
	Propionic acid	a_p	0.05	gm VSS/gm COD	32, 65
	Complex waste	a_c	0.14	gm VSS/gm COD	42, 65
Decay rate	Acetic acid	b_a	0.04	day^{-1}	65
	Propionic acid	b_p	0.04	day^{-1}	65
	Complex waste	b_c	0.08	day^{-1}	65
Active mass synthesis (fraction)	All substrate components	e	0.80	gm active VSS/gm VSS synthesized	65
Conversion rate	Complex waste	R_c	25	gm COD/L-day	This study, 65
Production rates	Complex waste to acetic acid	r_a	0.35	gm acetic acid COD/ gm complex waste COD	This study, 65

[a]As used in the anaerobic filter model. See the Appendix.

Table 22. Continued

Coefficient	Substrate	Label[a]	Value	Units	Source
Production rates	Complex waste to propionic acid	r_p	0.44	gm propionic acid COD/gm complex waste COD	This study, 65
	propionic acid to acetic acid	$(1-f_p)$	0.57	gm acetic acid COD/ gm propionic acid COD	65
Maximum[b] utilization rate	Acetic acid	k_a	6.1	mg COD/mg VSS-day	32, 65
	Propionic acid	k_p	18.3	mg COD/mg VSS-day	32, 65
Half-velocity coefficients	Acetic acid	K_{sa}	355	mg COD/L	32, 65
	Propionic acid	K_{sp}	205	mg COD/L	32, 65

[b]Uncorrected for inactive biomass production.

P = Fraction of methane in gas

ΔS = Difference in COD concentration between the bottom and top of an increment of filter height, mg/L.

The value of f_g in Equation 32 was assumed to be near 100 percent based on the actual methane COD balance shown on Tables 17 through 20 for low organic loading rates. At high organic loading rates the fraction of COD converted to methane was often significantly lower than 100 percent and therefore adjustments were made to account for this fact. Realistically the value of f_g must be somewhat lower than 100 percent regardless of the loading rate to account for the fraction of substrate converted into cell matter. The difference is, however, small so that the error introduced by the use of the 100 percent value should be small.

Hydraulic and other physical coefficients

Table 23 provides a summary of the physical factors relating to biomass accumulation, channelling and short-circuiting, mass transport, and the substrate gradient factor as used in the anaerobic filter model. These values represent estimates determined through trial runs of the model and thus are the best available estimates under the given operational conditions listed in Table 22.

It may be recalled that the effects of channelling and short-circuiting were incorporated in the anaerobic filter model by using the following expression (i.e. Equation 25):

$$V_e = \alpha V_o(1-k_v M_t)(1-r_s q) \qquad (33)$$

Equation 33 is used to calculate the effective void volume, V_e, of the

Table 23. Physical operational coefficients used in the anaerobic filter mmodel

Coefficient	Label[a]	Value	Units
Mass accumulation	k_v	0.02	$(\text{gm VSS})^{-1}$
Channelling or short circuiting	r_s	0.0025	$(\text{liters of gas flow/day-ft}^2)^{-1}$
Mass transport	r_m	0.0006	$(\text{liters of gas flow/ft}^3)^{-1}$
Substrate gradient factor (SGF)	SGF	4.0	Unitless
	k_g[b]	1.5	$(\text{gm COD/L})^{-1}$

[a] As used in the anaerobic filter model. See the Appendix.

[b] See Equation 18.

anaerobic filter corrected for the effects of biomass accumulation and short circuiting as induced by gas flow. As such, Equation 33 does not incorporate any effects that may result due to the physical configuration or shape of the filter media.

It was shown previously that reactors PBR-1 and PBR-4, which contained media of the same design and shape produced markedly different performance characteristics. Such differences can only be explained in terms of physical characteristics that may affect the hydraulics of flow through the media.

In Equation 33 the effects of biological growth as well as the effects of gas production on the effective void volume of anaerobic filter media were accounted for. However, this expression does not account for the effect of the physical shape or configuration of the media on the hydraulics of flow. This effect can be accounted for by adding a packing shape factor (PSF) as follows:

$$V_e = \alpha V_o(1-k_v M_t)(1-r_s q)(PSF) \quad (34)$$

The packing shape factor (PSF) relates the effects of system hydraulics and as such is a function of the medium's geometry. Due to the uniformity in the configuration of modular media, an effective pore diameter can generally be measured or calculated. For loose-fill media such equivalent diameter may have to be estimated.

The results obtained during this study suggest that media pore diameter is an important factor to anaerobic filter performance. As the media effective diameter is decreased and the flow is maintained constant, the boundary layer effects are expected to become greater thus

resulting in a reduction in the effective cross-sectional area of the media pore. The net result is a decrease in the effective void volume available for the anaerobic reaction. This phenomenon is illustrated by considering as an example the modular media blocks used in this study to be made up of slanted tubes. Since the flow through this media is well within the laminar range (i.e. the Reynolds number at the highest loading rate applied during this study was about 35), then it follows from basic fluid dynamics that the flow through each media tube should approach boundary layer conditions. In this situation the velocity profile through each tube increases from near zero at the wall of the tube to some peak velocity at the center of the tube. It is thus seen that such flow conditions not only tend to reduce the effective void volume when the media pore diameter is decreased but also tend to diminish the possible advantage of increased media surface area associated with decreased media pore spaces.

By considering the preceding development concerning the effects of media pore diameter on anaerobic filter performance, the media packing shape factor (PSF, Equation 34) is expressed as follows:

$$PSF = 1 - k_{sf}Q/d^n \qquad (35)$$

In Equation 35 k_{sf} is a media design coefficient (TL^{-2}), Q is the waste flow rate (L^3T^{-1}), d is the media effective pore diameter (L) and n is a dimensionless exponent. The values of k_{sf} and n must be determined experimentally. In this study the value of n was estimated to be unity and the media design coefficient to be about 2.0 min/ft^2.

The value of the media pore diameter varies with the shape and configuration of such media. For the media used in this study, measured

values of this parameter are shown in Table 24. It should be pointed out that the equivalent pore diameter of the perforated spheres media was calculated on the basis of the interstitial openings between the individual media particles with some adjustment for the perforations in these spheres. In the case of the Pall rings, an estimate of equivalent pore diameter was difficult to obtain due to the multiplicity of openings in individual media particles. The value shown in Table 24 represents an estimate which is specific to the type of Pall rings used in this study. The equivalent pore diameters (Table 24) for the modular media were based on data provided by the manufacturer.

Table 24. Equivalent pore diameter estimates for media used in this study

Reactor	Media Type	Porosity (%)	Equiv. Pore Diameter (in.)
PBR-1	Modular Blocks	95	1.80
PBR-2	Perforated Spheres	95	0.60
PBR-3	Pall Rings	95	0.80
PBR-4	Modular Blocks	95	1.25

Operation of the Anaerobic Filter Model

The Appendix provides a listing of the anaerobic filter model computer program used in this study. This program is a modified version of the original listing formulated by Young (65). By substituting the proper biological growth and physical factors discussed earlier, simulated

solutions describing the performance and characteristics of the anaerobic filter process were obtained for a range of organic loading rates and influent substrate concentrations.

The model was run for as long a period of time as desired and printed output was obtained for every operational day or number of days as specified in the program. Although the actual anaerobic filters used in this study were operated for a maximum period of about two months at each loading rate, the anaerobic filter model usually was run for a longer period of time to observe the disparity between long-term simulated steady-state operation and actual anaerobic filter operation.

In this model, a continuous updating of substrate concentrations, volatile acids and complex waste decomposing biomass, and total mass accumulations was carried out throughout the height of the filter column. Once starting conditions were specified, the program was run for the desired period of time, and the calculated results (i.e. volatile acids COD, accumulated active and total biomass concentrations, etc.) were re-entered into the program as the starting parameters for subsequent changes in operating conditions.

Despite the fact that the anaerobic filters used in this study were operated under virtually identical conditions, major differences in performance were apparent. These performance differences were the result of the differing media characteristics between these reactors. Thus, in the operation of the anaerobic filter model the only variable input parameters were those relating to the design and hydraulic characteristics of the media used in this study. Therefore, an attempt was made to simulate the performance of each of the four reactors used in this study.

Comparison between measured and calculated results

Figure 43 shows measured and calculated gas production rates for reactor PBR-1 during steady-state operation. As shown, fairly good agreement between actual pilot-plant data and simulated results is evident at all loading rates although measured values tended to be slightly higher than calculated values when operating at a loading rate of 4.0 gm COD/L-day (250 lb COD/MCF-day). As expected, although not graphically shown, the calculated total gas flow rates when depicting the conditions in PBR-2 and PBR-3 were generally better than measured values. Similar results to those shown in Figure 43 were obtained with PBR-4 indicating the ability of the anaerobic filter model to reproduce measured results in this case.

A comparison between calculated and measured COD profiles when operating at an organic loading rate of 1.0 gm COD/L-day (64 lb COD/MCF-day) is shown in Figure 44. In general, the anaerobic filter model predicted considerably better COD removal than was actually measured in the laboratory units although the disparity between calculated and measured results was less in the case of PBR-1 and PBR-4 than it was with PBR-2 and PBR-3. The difference between measured and calculated results in this case was obviously due to the fact that the anaerobic filter units had not reached maturity yet at this phase of operation.

At the higher loading rate of 2.0 gm COD/L-day (125 lb COD/MCF-day) fairly good agreement between measured and calculated COD profiles was obtained particularly with reactors PBR-1 and PBR-4 (Figure 45). The difference between calculated and measured values in the cases of PBR-2 and PBR-3 was less at this loading rate than it was with the lower loading

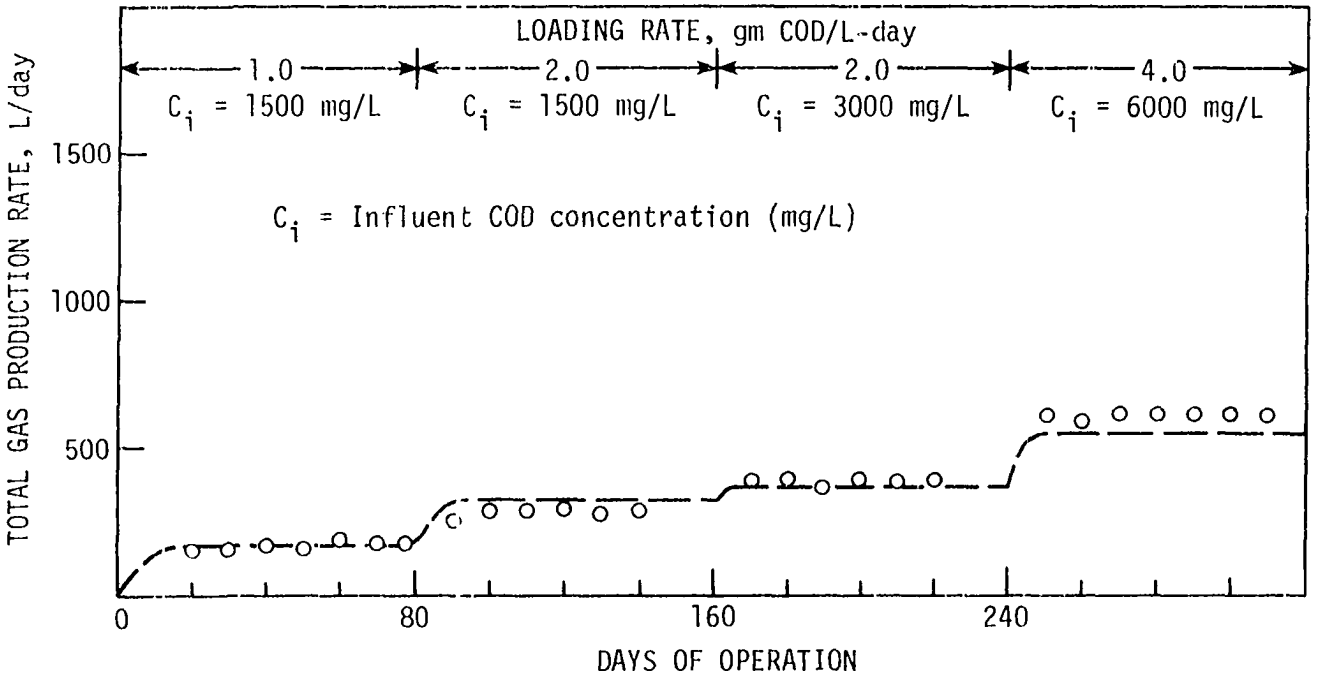

Figure 43. Measured and calculated (dashed line) gas production rates during steady-state operation of PBR-1

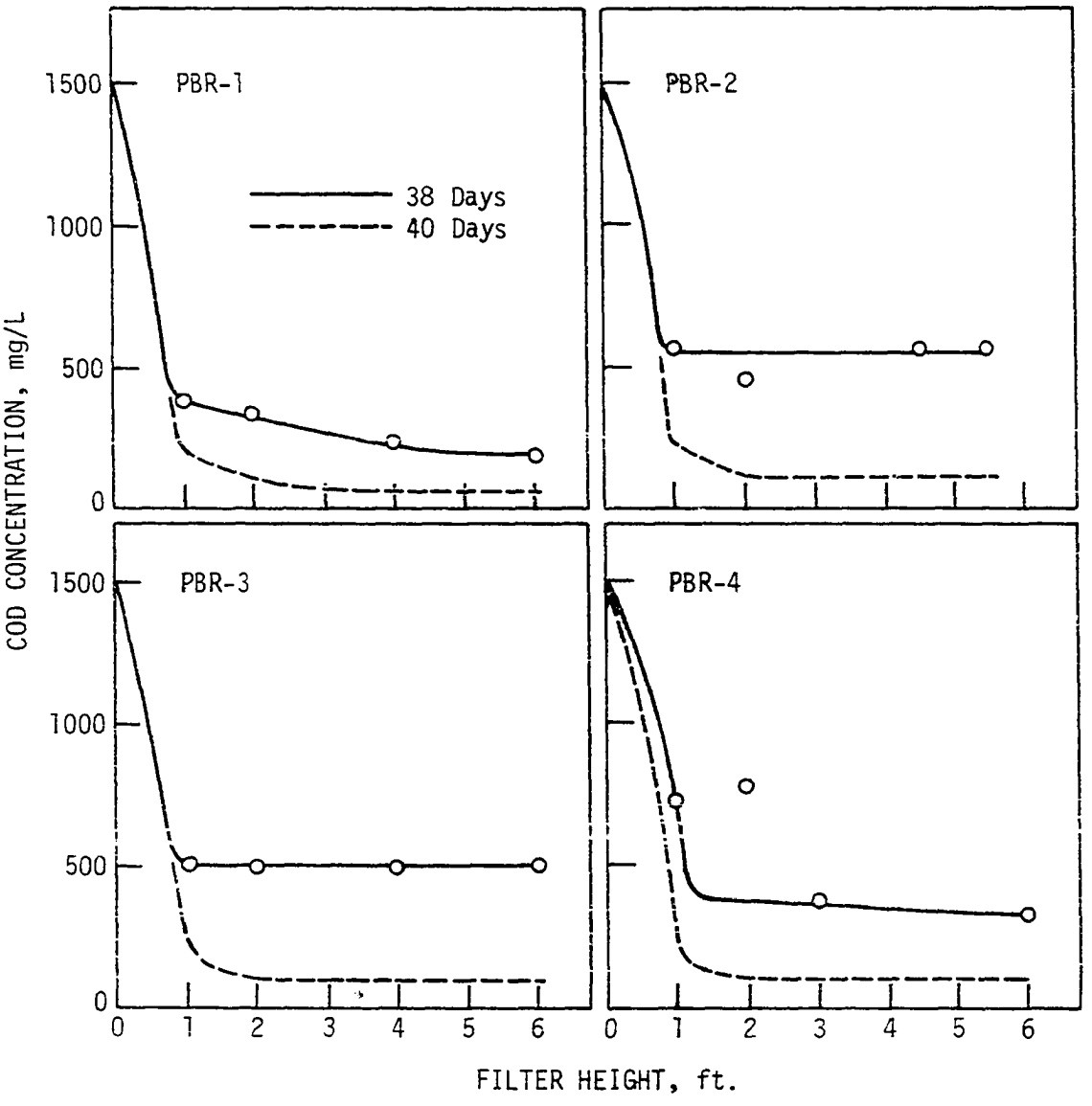

Figure 44. Measured and calculated (dashed line) COD concentrations in all reactors after about 40 days since loading rate change. L.R. = 1.0 gm COD/L-day and influent COD = 1500 mg/L

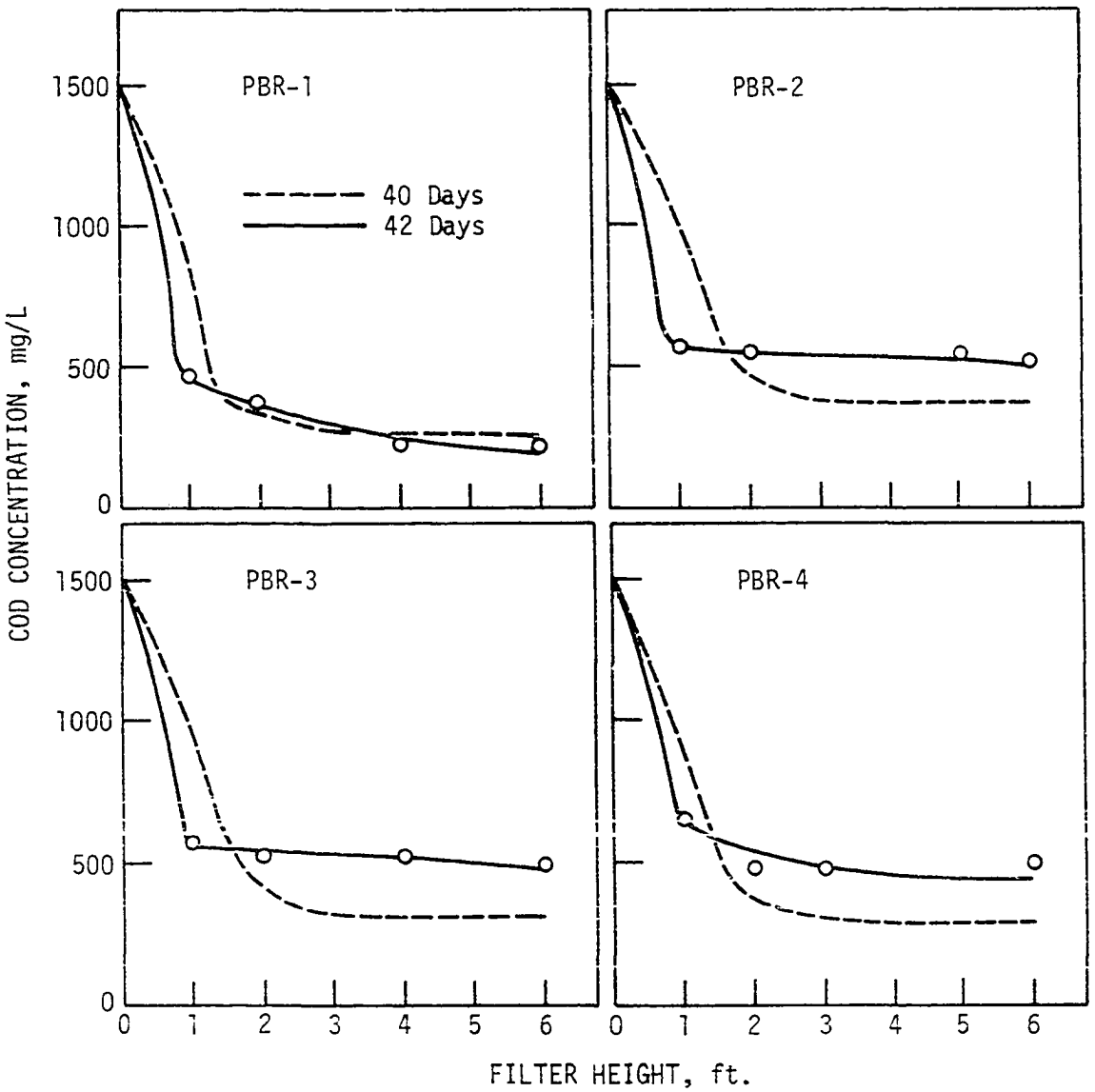

Figure 45. Measured and calculated (dashed line) COD concentrations in all reactors after about 40 days since loading rate change. L.R. = 2.0 gm COD/L-day and influent COD = 1500 mg/L

rate of 1.0 gm COD/L-day (62.4 lb COD/MCF-day).

When the influent COD concentration was doubled from 1500 to 3000 mg/L while maintaining the loading rate at 2.0 gm COD/L-day (125 lb COD/MCF-day) the model was successful in reproducing measured results with PBR-1 and PBR-4 (Figure 46). The model's ability to simulate conditions in PBR-2 and PBR-3 was not satisfactory under these loading conditions indicating that the physical and hydraulic factors were not fully accounted for. In particular, it should be pointed out that both the mass transport and channelling coefficients were assumed to be the same for all four reactors. This assumption appeared to be untrue in view of the results shown in Figure 46. Another possible contributing factor to the difference between measured and calculated results with PBR-2 and PBR-3 is the potential error in estimating their media equivalent pore diameters as shown in Table 24.

Figure 47 shows a comparison between measured and calculated COD profiles during operation at a loading rate of 4.0 gm COD/L-day (250 lb COD/MCF-day) and an influent COD concentration of 6000 mg/L. Although both simulated and measured profiles indicate that some agreement was evident with reactors PBR-1 and PBR-4 in terms of effluent quality, it is clear that simulated results are not in agreement with pilot-plant data for any of the four reactors when entire COD removal profiles are considered. In general, simulated results at this loading rate tended to show that the bulk of COD was removed in the middle section of the anaerobic filters whereas measured results indicate that the bulk of COD removal took place in the lower sections (i.e. the first one foot of filter height) despite the fact that the anaerobic filter model resulted in generally better overall

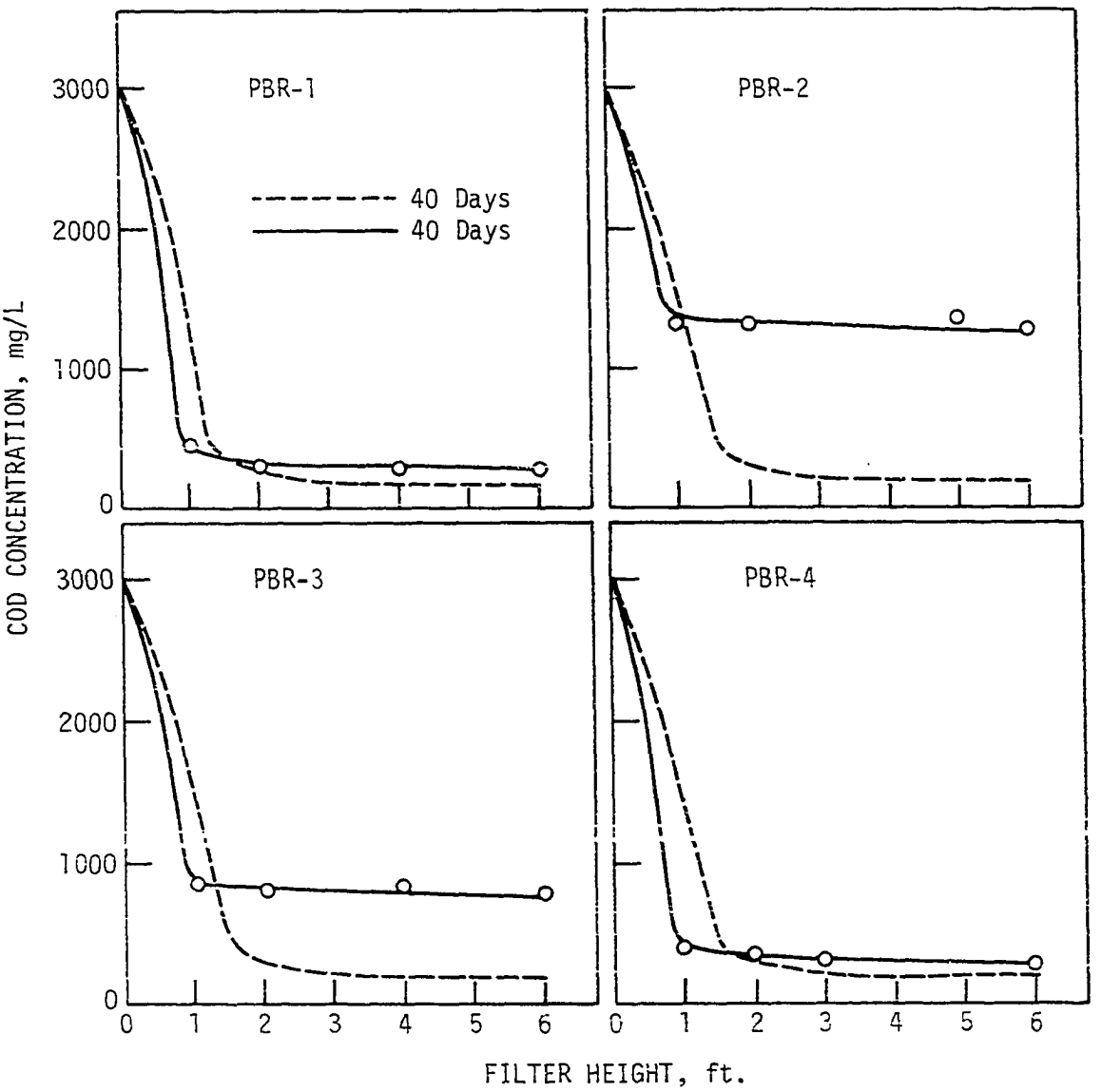

Figure 46. Measured and calculated (dashed line) COD concentrations in all reactors after 40 days since loading rate change. L.R. = 2.0 gm COD/L-day and influent COD = 3000 mg/L

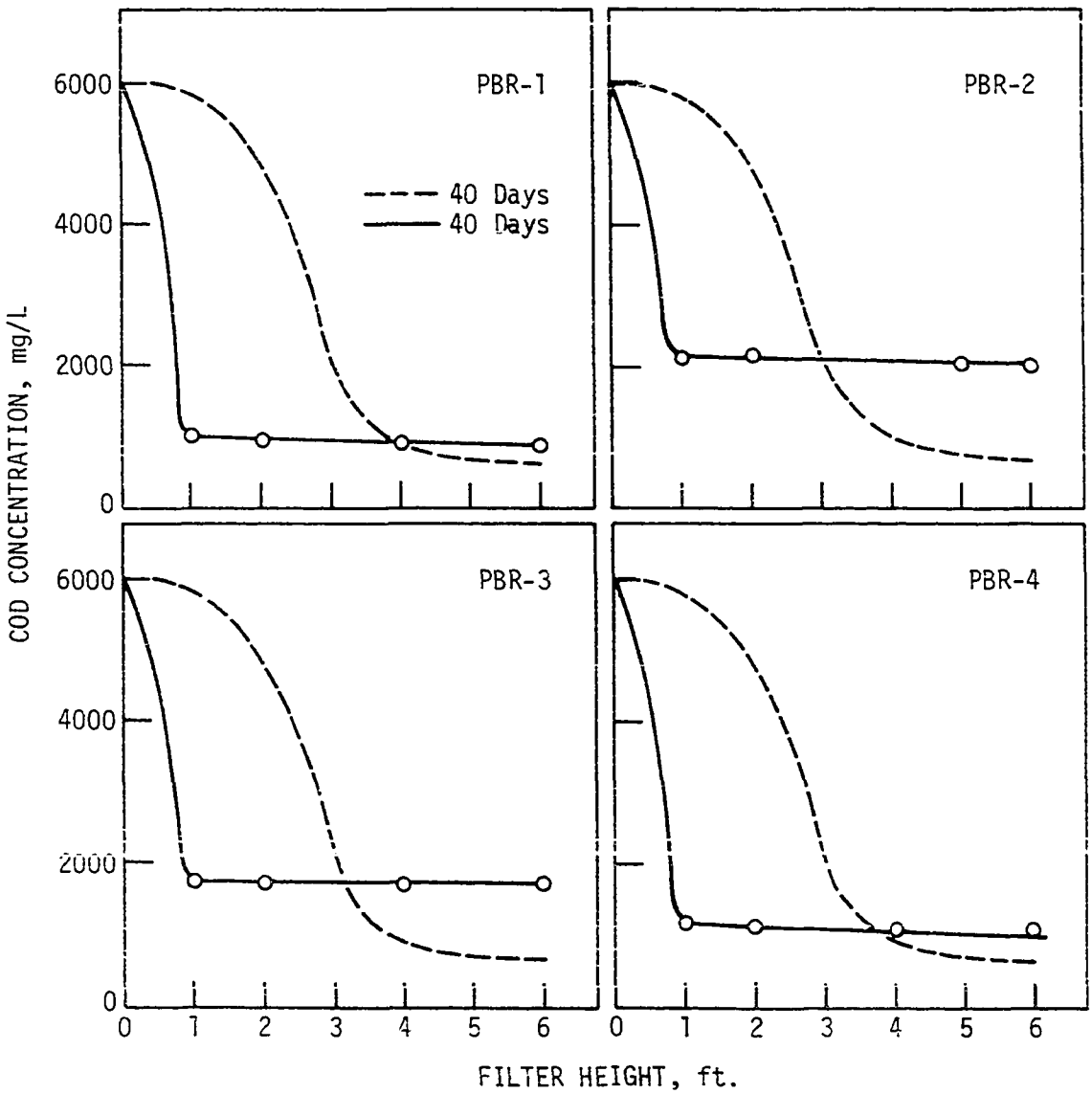

Figure 47. Measured and calculated (dashed line) COD concentrations in all reactors after 40 days since loading rate change. L.R. = 4.0 gm COD/L-day and influent COD = 6000 mg/L

COD removal. The disparity between measured and calculated results is undoubtedly a consequence of the inadequacy of model's physical and perhaps kinetic coefficients as well.

Anaerobic filter performance prediction using the anaerobic filter model

The anaerobic filter model can be used for prediction of anaerobic filter performance under a variety of loading and operating conditions. The ability of this model to make such prediction has already been demonstrated (65, 69). In order to further demonstrate the model's ability a number of runs were made and are shown below.

The first of these runs of the anaerobic filter model were made assuming an influent waste COD concentration of 1500 mg/L and an organic loading rate of 1.0 gm COD/L-day (62.4 lb COD/MCF-day). The loading rate was then doubled to 2.0 gm COD/L-day (125 lb COD/MCF-day); in the same manner as was done during the laboratory phase of this study. Figure 48 shows calculated COD profiles when simulating the conditions in all four reactors used during this investigation. These profiles indicate that all simulated filters achieved high COD removals and that almost all of the substrate removal took place in the first 1.0 foot (0.3 m) of filter height, similar to actual COD removal profiles observed earlier. Comparison of substrate removal between all four simulated reactors indicates that PBR-1 and PBR-4 resulted in slightly better removal efficiency than did PBR-2 and PBR-3. The difference in COD removal between the modular media and loose-fill media was small. However, the COD removal trend observed with actual reactors was evident nonetheless.

At the higher organic loading rate of 2.0 gm COD/L-day, the COD profiles observed in the simulated filters (Figure 48) were similar to

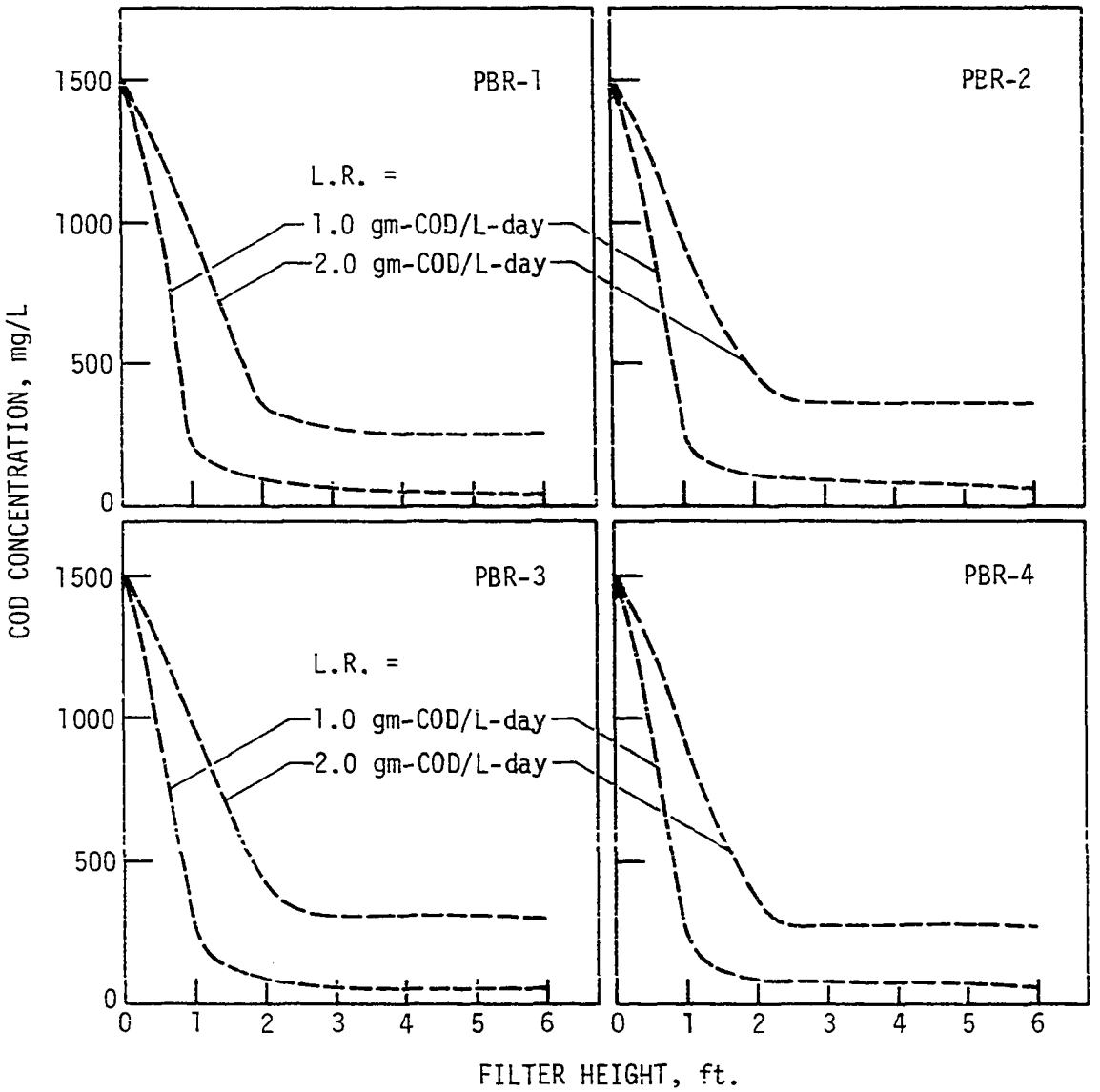

Figure 48. Calculated COD concentrations in all reactors after 40 days of operation at loading rates of 1.0 and 2.0 gm COD/L-day. Influent COD = 1500 mg/L

actual profiles observed earlier but in this case more of the filter height was utilized in the COD removal process. The profiles shown in Figure 48 indicate that most of the COD removal was achieved in the first 2 feet (0.61 m) of height. The differences in COD removal between the individual filters were again evident although these differences were not as pronounced as they were in the actual profiles obtained during this study.

When the influent COD concentration was doubled from 1500 to 3000 mg/L to all simulated filters while keeping the loading rate constant at 2.0 gm COD/L-day (125 lb COD/MCF-day), the subsequent increase in hydraulic detention time (HRT) had the same effect as observed with the actual anaerobic filters on improving COD removal in all reactors (Figure 49). The profiles shown in Figure 49 indicate that most of the COD removal took place in the first 2-feet (0.61 m) of filter height. Once again, the differences in COD removal were small compared to actual data obtained during the pilot-plant testing although the actual removal trend was evident.

The COD profiles obtained during simulated anaerobic filter operation at a loading rate of 4.0 gm COD/L-day (250 lb COD/MCF-day) and an influent COD concentration of 6000 mg/L are shown in Figure 50. As shown, the increased loading rate resulted in different COD profiles from those observed earlier from actual pilot plant data. The difference in COD removal profiles between actual and simulated anaerobic filters at this loading rate was probably due to a number of reasons such as the possibility that the change in loading rate may have required a change in the physical factors from values used at lower loading rates. Another reason may have been the possibility that some of the kinetic coefficients and biological growth factors may have needed some refinements.

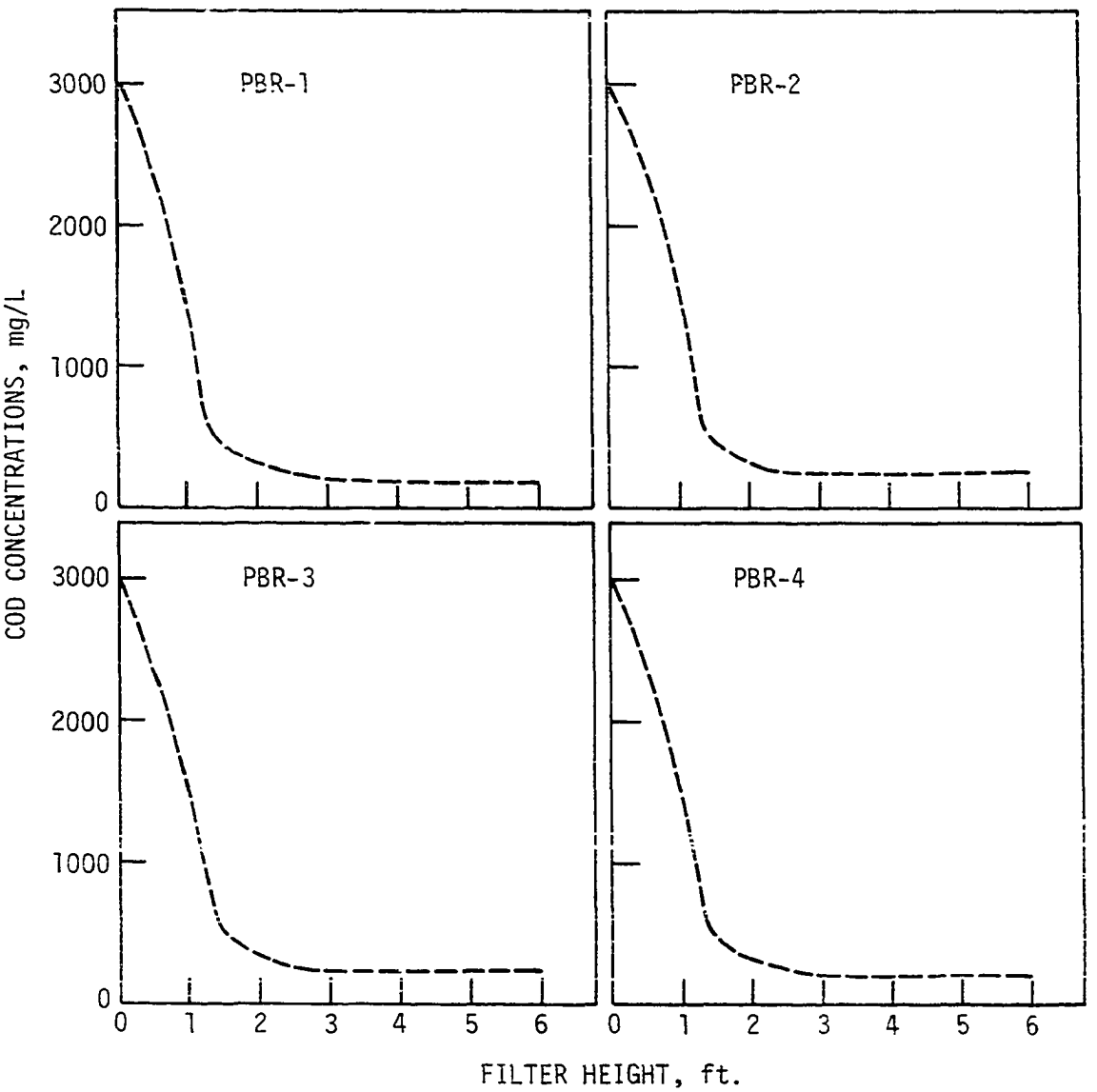

Figure 49. Calculated COD concentrations in all reactors after 40 days of operation at a loading rate of 2.0 gm COD/L-day. Influent COD = 3000 mg/L

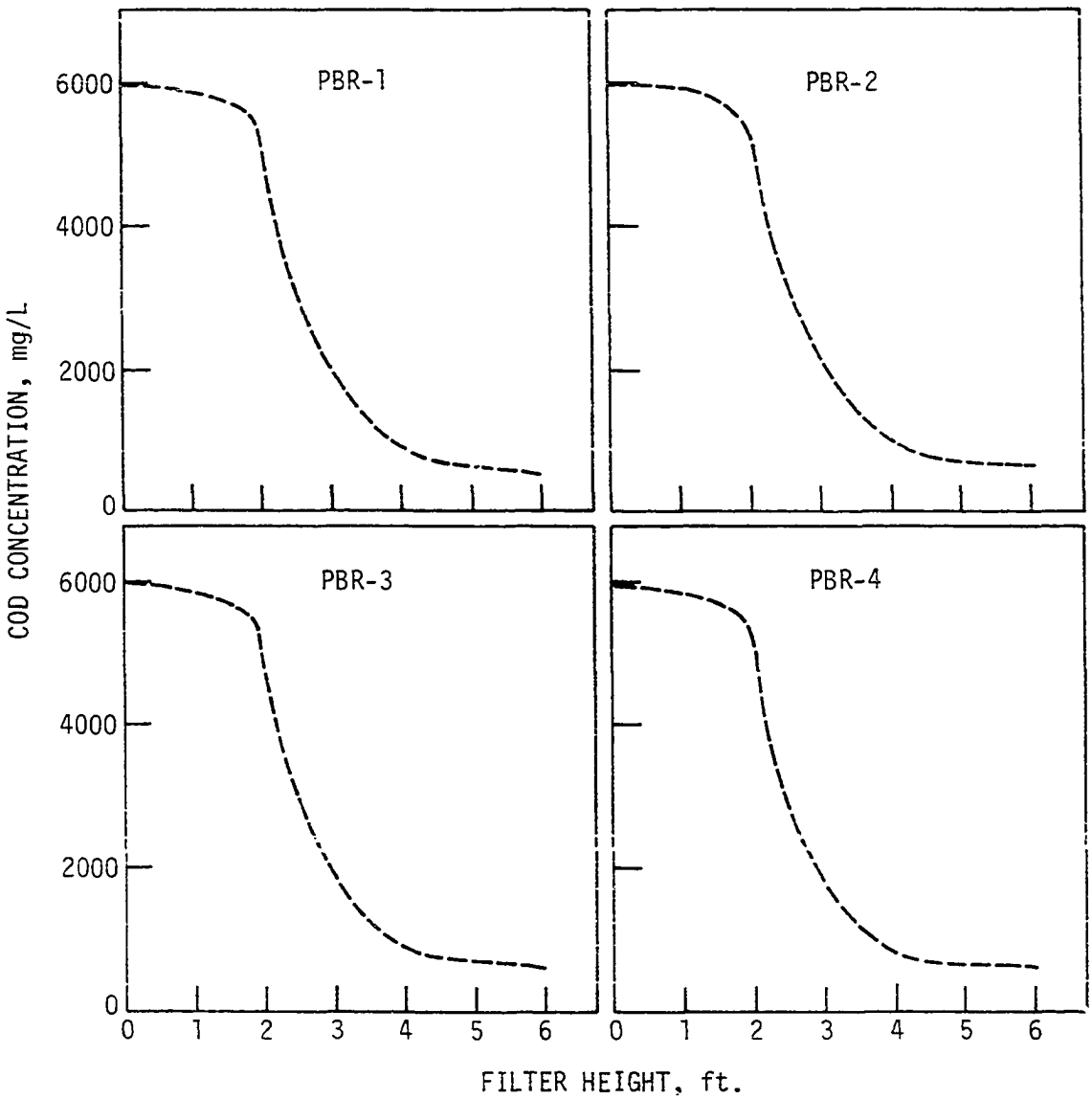

Figure 50. Calculated COD concentrations in all reactors after 40 days of operation at a loading rate of 4.0 gm COD/L-day. Influent COD = 6000 mg/L

Limitations of the anaerobic filter model

There are several factors that contribute to limiting the applicability of the anaerobic filter model. Such limitations arise due to the dependency of the simulation technique on a variety of physical and biological factors that are not all fully understood or entirely error-free. In addition, the model incorporates some assumptions that may not be uniformly applicable under a wide range of operating conditions.

One of the basic assumptions in the development of the anaerobic filter model was that, in the absence of gas flow and biomass accumulation and transport, ideal plug flow takes place within the filter. This assumption is not unreasonable as long as channelling within the filter matrix is kept at a minimum. The choice of the media configuration (or design) can lead to an effective reduction in the extent of channelling. Given that biomass accumulation does not reach limiting proportions, modular media, as shown in this study, can be instrumental in improving anaerobic filter performance indirectly through establishing uniform flow patterns that closely parallel ideal plug-flow. Although plug-flow can be achieved in anaerobic filters packed with loose-fill media (65), the susceptibility of this type of media to the occurrence of gas-induced channelling seems to be greater than modular media by virtue of the fact that flow through the former is not as uniformly distributed through the media matrix as it is with the latter.

The anaerobic filter model is also limited by the inherent variability of the biological growth coefficients. These factors were held constant at all loading rates at which simulation was attempted; up to 4.0 gm COD/L-day (250 lb COD/MCF-day). Attempts were also made to test the model at

8.0 and 16.0 gm COD/L-day (500 and 1000 lb COD/MCF-day). However, the results obtained at these loading rates were not satisfactory when compared to measured results. The inability of the model to simulate measured conditions at high loading rates is indicative of the fact that biological growth coefficients were not indeed constant over a wide range of loading conditions. This fact was evident through studies conducted by Young (65, 66) and Young and McCarty (69).

The variability of biological growth coefficients stems from the heterogeneity of microbial populations in anaerobic treatment systems. The kinetic responses of these populations are undoubtedly affected by variations in waste loading rates and concentrations as well as environmental factors such as pH and temperature.

The ability of the anaerobic filter model to simulate true anaerobic filter performance is also limited by physical factors such as biomass transport, channelling and, perhaps to a lesser extent, the substrate gradient concept. The expressions used in simulating these factors were developed empirically on the basis of laboratory results and as such need to be refined.

Biomass transport induced hydraulically or by the action of rising gas bubbles can have a significant impact on anaerobic filter performance. In the anaerobic filter model, the mass transport coefficient (Table 21) was held constant at all loading rates. Young (65) indicated that although a ± 25 percent change in the value of this parameter resulted in a small change in the COD profiles, the biological solids profiles were changed significantly. Therefore, it appears that further refinement of this coefficient is needed.

The occurrence of channelling has a net effect of reducing the effective filter volume available for waste treatment and, as pointed out earlier, is in direct proportion to total gas flow. The channelling, or short circuiting, coefficient used in the anaerobic filter model was kept constant at all loading rates. This was done based on results obtained by Young (65) where this coefficient did not appear to result in serious changes in anaerobic filter performance as a result of a $\pm$25 percent change in the value of this parameter. However, Young speculated that the value of the channelling coefficient should change with differing type and design of filter media. The results obtained in this study suggest that the channelling coefficient should differ with differing media types and designs. However, simulated anaerobic filter runs indicated that a $\pm$30 percent change did not affect calculated filter performance seriously at high organic loading rates.

A physical parameter more related to media type and design than other physical factors used in the anaerobic filter model is the media equivalent pore diameter as defined in Equation 35. For modular media this parameter is easily determined due to the regularity and uniformity of the media configuration. However, for randomly packed loose-fill media this parameter proved to be difficult to calculate due to the usual multiplicity of the openings in individual media particles. Estimates of the equivalent pore size diameters for media used in this study were shown in Table 23.

In the application of the equivalent pore diameter concept in the anaerobic filter model it was possible to simulate anaerobic filter performance with some degree of success particularly at low organic loading rates and with reactors PBR-1 and PBR-4. At high organic loading rates it

was evident that the inadequacy of other physical and biological factors, combined, contributed to distorting the results of the simulation and thus masked the effects of pore diameter on filter performance. Nonetheless, it was possible to establish the trend by which the effects of media pore diameter could be measured. This trend, as pointed out earlier, was observed consistently at all loading conditions. It is obvious that any refinement in the media equivalent pore diameter concept will depend on further refinements of other physical and biological coefficients that control the operation, and subsequently the performance, of the anaerobic filter model.

SUMMARY AND DISCUSSION

Experimental Design

This experimental study was conducted with the objective of attempting to identify some of the packing media characteristics that have tangible effects on the performance of anaerobic filters under a variety of loading conditions. Due to the different nature of the waste stream introduced to the anaerobic reactors (i.e. grain alcohol distilling wastewaters), the treatability of this waste material using the anaerobic filter process constituted an added secondary objective. With these objectives in mind, four pilot-scale anaerobic filter reactors were designed and operated for a period of about 13 months at organic loading rates ranging from 0.5 gm COD/L-day (31 lb COD/MCF-day) to 16 gm COD/L-day (1000 lb COD/L-day) and influent COD concentrations ranging from 1500 to 6000 mg/L.

The anaerobic reactors used in this study were 6 ft. (1.83 m) tall circular columns with an inner diameter of 20 in. (0.51 m) and a 2 in. (51 mm) shell around each reactor for constant temperature water recirculation. The basic design was aimed at a pilot-plant scale of operation in order to avoid the basic 5.5 in. (14 mm) diameter plexiglass columns often encountered in the literature. However, the reactor sizes had to be selected so that minimum scale-up distortion could be attained without having to resort to smaller sizes of packing materials than commercially available for full-scale applications. Although the selection of the 20 in. (0.51 m) reactor diameter was basically arbitrary, it did, however, maintain an adequate scale factor (i.e. the ratio of reactor diameter to the packing

media diameter) of about 6. A more desirable scale factor recommended for packed towers in chemical engineering practice is normally about 8 (37).

Media selection

Each reactor was packed with a different, commercially available, packing medium. Two of these media were of the modular block type (i.e. corrugated sheet design) and the other two were of the loose-fill (perforated balls and Pall rings) type. The specific surface area of these media were 30 and 42 ft^2/ft^3 (100 and 140 m^2/m^3) for the two sizes of the modular media and 25 and 31 ft^2/ft^3 (82 and 103 m^2/m^3) for the perforated balls and Pall rings, respectively. The modular blocks media were made of polyvinyl chloride (PVC), perforated spheres were made of polypropylene, and the Pall rings were made of a polyethylene resin. All of the media used in this study were therefore basically impermeable.

Influent waste selection

The waste material used in this study as the influent to the anaerobic filters was simulated grain alcohol distilling wastewater. The specific make-up of this wastewater was based on the results of a survey and a sampling program of farm-sized grain alcohol stills located throughout the state of Iowa. The synthetic waste material was basically composed of a volatile fatty acids fraction (6.7 percent), an alcohols (mostly ethyl alcohol) fraction (66.6 percent), and a carbohydrate (table sugar) fraction (26.7 percent). This waste was fortified with basic nutrients and buffers (sodium bicarbonate) needed for biological growth and prepared as a solution containing about 51 gm COD/L and was metered to the reactors, as required,

using tubing pumps. This waste was diluted to the desired strength using tap water immediately before feeding to the reactors.

Loading rates and influent concentrations

The reactors were operated at an influent COD concentration of 1500 mg/L at organic loading rates of 0.5, 1.0, and 2.0 gm COD/L-day (31, 62.4, and 125 lb COD/MCF-day), 3000 mg/L at an organic loading rate of 2.0 gm COD/L-day (125 lb COD/MCF-day), and 6000 mg/L at loading rates of 4.0, 8.0, and 16.0 gm COD/L-day (250, 500, and 1000 lb COD/MCF-day). All reactors were operated simultaneously and under the same loading conditions except at the high organic loading rate of 8.0 and 16.0 gm COD/L-day. At these two loading rates reactors PBR-2 and PBR-3 (loose-fill media) were taken out of service due to their inferior performance at lower loading rates and more importantly due to the high cost of operating all four reactors at such high loading conditions.

The basic operational mode was such that the reactors were run for few weeks after steady-state conditions had become apparent so that enough steady-state operational data were collected and then switched to the next higher loading rate. Steady-state operation was basically determined by constant gas production rates and effluent COD and was generally attained after two to three weeks of operation.

Sampling and analysis

Reactor profile as well as effluent samples were collected from all columns on a regular basis for soluble COD, volatile acids, and suspended and volatile suspended solids. There was no need for regular analysis of the influent stream since its make-up was known at all times. The effluent

gas stream was routinely analyzed.

All COD data used in the evaluation of the anaerobic filters used in this study were based on soluble (i.e. filtered) measurements. This was done in the belief that suspended solids (which are included in total COD measurements) were not true performance parameters that could be relied on. In addition, there were no apparent correlation between effluent COD and effluent suspended solids even during steady-state operation. Effluent suspended solids concentrations appeared to be controlled by inter-reactor hydraulics as well as the extent of solids build-up inside the anaerobic filter matrix.

Start-up

As indicated previously, all reactors were seeded using the supernatant from a primary tank of a municipal anaerobic digester system by adding 10 gallons (about 40 L) of this supernatant to each column. Due to the low solids content of the seed material, starting conditions were not as favorable as it was hoped although only one reactor had to be reseeded. The sluggish nature of the starting conditions, particularly in reactor PBR-1, were also due, in part, to a miscalculation in the amount of bicarbonate buffer needed. This miscalculation was discovered quickly before serious damage was done to all reactors.

The seed material added to most of the reactors resulted in an overall initial suspended solids concentration of about 1000 mg/L. The volatile fraction of these solids were estimated at about 80 percent and thus the actual "active" fraction could not exceed this estimate. As the start-up data shown previously had indicated, better starting conditions would have

resulted had more seed material been added or had the concentration of this seed material been higher as was the case with reactor PBR-4.

Anaerobic Filter Performance

In general, the anaerobic filter performance data obtained during this study have shown the basic utility of the anaerobic filter as a viable waste treatment process. It was shown that this process is capable of handling high strength waste streams at high loading rates while resulting in low solids production rates and high organics removals. The process' ability to recover a major fraction of the energy lost in the waste stream as methane gas adds an attractive advantage that could be instrumental in augmenting the continually dwindling fossil-fuel supplies.

During this study, the performance of all anaerobic filters, except reactor PBR-2, was such that COD removal efficiency was consistently better than 70 percent at organic loading rates as high as 8.0 gm COD/L-day (500 lb COD/MCF-day). For the reactors packed with modular media, removal efficiencies were higher than 85 percent at a loading rate of 4.0 gm COD/L-day (250 lb COD/MCF-day). This latter loading rate seemed to represent an optimum loading condition for all reactors particularly those packed with modular media.

Effects of anaerobic filter media

The choice of anaerobic filter packing material should be approached carefully since the packing media appeared to be more critical to the performance of anaerobic filters than recent literature seemed to suggest. The media not only should provide an adequate matrix to hold and retain biological growth but also must be conducive to minimizing the effects of

short-circuiting and excessive upward biomass transport. These remarks are supported by data presented previously where it was shown that loose-fill media, which appeared to have been subject to excessive channeling and short-circuiting, was consistently inferior to the modular media used in this study.

Comparison of data obtained from reactors PBR-1 and PBR-4 revealed that the medium's ability to retain biological solids within its matrix was more important than the unit surface area available for bacterial growth. It was apparent that the majority of COD removal was effected by suspended growth and therefore the role of attached growth, and subsequently that of unit surface area, was diminished.

Within the loose-fill media used in this study, the perforated spheres were less desirable than the Pall rings as was previously shown on Figure 35. In general, these media were not as uniformly packed within the reactor volume as were the modular media which were generally packed with regularity. Loose-fill media tended to leave near-vertical voids which undoubtedly served as channels for short-circuiting to take place whereas the modular blocks forced the liquid to follow its inclined tubes back and forth through the blocks thus increasing effective contact time and subsequently increased organics removal efficiency.

The modular block medium used in this study was also promoted by its manufacturer as behaving as tube settlers to enhance solids retention within the reactor itself. While it was difficult to measure, with certainty, the accuracy of this claim, suspended solids profiles during the operation of all reactors tended to lend some credibility to this claim. It is highly plausible to assume that the corrugated-sheet blocks enhanced

solids settling and retention in view of the better performance results obtained with this type of media. Furthermore, the inclined flutes that resulted from the corrugation of the sheets from which this media was made and the lamination of these sheets to form the modular blocks resulted in inclined channels much like the tube settler arrangements common in some sedimentation processes. The desirability of using channel rather than random packing media designs to reduce plugging and the effects of short-circuiting was confirmed by van den Berg and Lentz (59). These two investigators concluded that channel-type packing induced vigorous agitation within the media matrix due to the gas-lift pump action of the product gas. This gas-lift pump action serves to expose the anaerobic film and the solids in suspension to more of the organics available in the liquid stream and thus enhancing removal efficiency.

The perforated spherical media produced the worst performance characteristics of all the media used in this study at all loading rates. These results were rather disappointing since it was first thought that the shape of these media may lead to the compartmentalization of the reaction vessel and thus serve to trap the solids in the reactor for better removal rates. As it was, the spherical shape of the media evidently resulted in the creation of large semi-vertical voids through which the liquid flowed directly upwards thus escaping treatment while the inside volumes of these spheres being closed to liquid flow despite the relatively large perforations through the spheres themselves. The fact that the spherical shape represented a surface area minimum can be discounted as the reason for the poor performance of these media since surface area did not seem to be a critical media design factor.

In summary, media selection in anaerobic filter treatment system design should be based on individual process requirements, characteristics of the waste stream, and economic considerations. In general, discounting economic considerations, if any, the media should be selected to provide maximum opportunities for the waste stream to be contacted with the solids within the reactor matrix. Stated differently, the media should minimize short-circuiting and at the same time should have large enough pore spaces to minimize possible plugging problems after extended periods of operation. The media should also be conducive to solids settling since it appears that granulated suspended solids within the anaerobic reactor are primarily responsible for waste removal, more so than are attached growth solids. These desirable media characteristics are not likely to be obtained through the use of loose-fill, randomly placed media similar to those used in this study.

Other obvious desirable media characteristics that should influence their selection include high porosity to minimize the frequency of accumulated solids withdrawals, low density to minimize costly foundations and underdrain manifold systems, and ease of installation as well as removal. It should be pointed out that loose-fill media are not expected to meet the requirement of easy removal although it may be easier to install.

The materials from which anaerobic filter media are made could have some effect on the performance of anaerobic filters. Although some effects were not detectable in this study since the materials from which the pilot-plant anaerobic filters media were made (i.e. PVC and polypropylene) were essentially similar, van den Berg and Lentz (59) reported that the use of clay support media provided far better process stability than glass or

plastic materials. These investigators indicated that the improved performance when using clay media may have been related to the surface roughness, porosity, and the physical-chemical characteristics of the clay. It is quite possible that the use of clay or stone materials as media in anaerobic filters may result in providing some of the trace elements needed for biological growth that may otherwise be absent in the waste stream such as iron, phosphorous and cobalt.

In this study, it was found that the attached biological film on the plastic media could easily be sloughed off the relatively smooth surface of the media. Such sloughing should not occur unless the reactor vessel is subjected to severe hydraulic or physical shocks. Therefore, it may be possible to sustain better attachment of biological films when using rough media surfaces such as clay or stones. The use of clay or stone materials as packing media, however, would result in drastic reductions of the effective void volume of the filter thus leading to more frequent solids wasting and the fact that these materials are considerably heavier than plastic media could result in higher costs of underdrain manifolds and reactor foundations.

Effects of reactor height

Due to the low solids production characteristics of the anaerobic reaction, the effects of reactor height on the anaerobic filter process performance should become critical only after an extended period of operation. The length of such period would be determined by filter porosity, reactor height, and the nature of the waste being treated in addition to the rates at which such waste are being introduced to the reactor.

In this study, it was found that only the bottom 2 ft. (0.61 m) of height were effectively exhausted almost at the end of study (i.e. after more than 13 months of continuous operation of reactors PBR-1 and PBR-4). It was estimated that reactors PBR-1 and PBR-4 could have been operated for an additional one year period at a loading rate of 4.0 gm COD/L-day (250 lb COD/MCF-day) before the reactors height affected the effluent suspended solids concentration in a damaging manner. This estimate was based on the assumption that a practical limit to the extent of reactor height exhaustion should not exceed about 4 feet (1.22 m) of the total reactor height of 6 ft. (1.83 m) before solids should be withdrawn from the anaerobic filter. This estimate is supported by the typical suspended solids profiles shown on Figure 38.

The length of period of operation before solids withdrawal could be estimated with a good degree of accuracy if actual design of full-scale anaerobic filters is based on laboratory experiments and a concrete knowledge of media porosity, filter height, and anticipated organic loading rates of a particular waste stream. The characteristics of such waste stream are important to the prediction of filter volume exhaustion since the presence of suspended solids in the influent would contribute to the rapid exhaustion of the effective volume of the reaction vessel depending on the concentration of these solids in the influent and the degree of their volatility. In addition, the exact nature of the soluble waste should also be known. Young (65) suggested that different waste characteristics (e.g. volatile acids waste as opposed to protein-carbohydrate waste) could have differing volatile solids production rates. For such reasons pilot plant or laboratory testing is highly

expedient and extremely beneficial in the performance prediction as well as the design of anaerobic filters.

Biological solids

As shown previously in an earlier section, attached growth was fairly evenly distributed throughout the reactor height. However suspended biomass was concentrated in the bottom two feet (0.61 m) of filter height (See Figure 38). Attached solids were considerably less volatile than suspended solids indicating that a major fraction of organics removal was attributable to suspended solids. Suspended solids were found to be highly granulated and very settleable under quiescent conditions. The granulation of these solids was seen as a key factor in the ability of anaerobic filters to retain solids and perhaps a key to the success of this biological treatment process.

The suspended solids in the bottom of the anaerobic filters were typically putrescible with a distinct anaerobic odor. Since these solids are the first to be withdrawn for wasting, they probably would require treatment before final disposal. Since these solids are also the most active, solids wasting must be done carefully to avoid possible filter failures upon restarting.

The suspended solids in the upper levels of the anaerobic filter column appeared to be not as putrescible as those from the bottom of the reactor. These solids were not well-flocculated and did not settle as easily as solids from the bottom. Although these solids were fairly volatile, activity tests indicated that they were much less active than reactor bottom solids (Figure 41). The results of the activity test

suggest that these solids were probably made up mostly of inactive cells or cell fragments.

Performance comparison between anaerobic filters and expanded-bed reactors

As was pointed out earlier, the anaerobic attached-film expanded-bed process (AAFEB) represents a recent modification of the basic anaerobic filter process. Although it has been suggested (8, 56, 59) that this process is more amenable treatment of more wastewater streams than normally can be treated with anaerobic filters, the similarity of these two processes merits performance comparison particularly in view of the fact that anaerobic filters are also suitable for treating fairly low strength wastewaters as was demonstrated in this study (i.e. influent COD concentrations of 1500 mg/L is generally considered fairly low in the realm of anaerobic waste treatment).

Switzenbaum and Jewell (56) reported the results of extensive AAFEB studies using glucose-based substrate at influent concentrations of 200, 400, and 600 mg/L. These influent concentrations were undoubtedly low in comparison to waste concentrations encountered in conventional anaerobic treatment. However, these investigators reported COD removal efficiencies ranging from about 50 to about 75 percent at a loading rate of 8.0 gm COD/L-day and influent COD concentrations ranging from 200 to 600 mg/L. At the higher organic loading rate of 16.0 gm COD/L-day treatment efficiency was in the range of about 25 percent (C_i = 200 mg/L) to about 65 percent (C_i = 600 mg/L) (56).

The results reported by Switzenbaum and Jewell (56) not only show that treatment efficiency improved with increased influent waste concentrations but also showed that at low influent concentrations (i.e. 200 mg/L

COD) and high organic loading rates (i.e. 16 gm COD/L-day) treatment efficiency was too low to warrant the expense of maintaining a fluidized or near-fluidized bed. At such low influent concentrations, other conventional treatment methods (i.e. aerobic treatment) may be more suitable and more reliable than the anaerobic expanded-bed process. At high influent concentrations the anaerobic filter process is probably more advantageous since it requires much lower operating costs (i.e. energy) than the expanded-bed process particularly since removal efficiencies are comparable in both processes.

Anaerobic Filter Simulation

A mathematical model developed by Young (65) was used to simulate anaerobic filter performance for the purposes of comparison with pilot-plant results obtained in this study. The model was modified to account for differing media characteristics through the use of a packing shape factor which incorporates a measured media equivalent pore diameter.

The results obtained with the anaerobic filter model were in substantial agreement with measured performance results at low organic loading rates particularly with reactors containing the modular corrugated media. At high loading rates (i.e. exceeding 4.0 gm COD/L-day) it appeared that many of the physical and biological factors incorporated into the model needed extensive modification and refinement before simulation results could agree with measured ones.

Attempts to simulate the performance of pilot plant anaerobic filters packed with perforated spheres and Pall rings were less successful than when using modular media. The apparent reason behind this lack of success

was that physical factors such as the biomass transport, and the channeling and short-circuiting coefficients were not changed to reflect differing media characteristics. It was evident that loose-fill media were greatly affected by these factors; much more so than were modular media as indicated by actual performance data. It was necessary to keep all physical and biological coefficients constant with differing media in order to test the effect of the media equivalent pore diameter on anaerobic filter performance.

Without question, media design has a considerable effect on the performance of anaerobic filters as the results of this study consistently indicated. Barring any chemical effects media may have on the chemistry of the anaerobic reaction (i.e. assuming that media are made of chemically inert materials), the net effect of media, therefore, is purely physical. Stated differently, differing media designs influence anaerobic filter performance by providing different hydraulic regimes that could either be conducive to improving organics removal or otherwise be detrimental to it. Such hydraulic effects are related to flow velocities through the media and subsequently to the effective pore diameter of the packing material. Obviously, the validity of the pore diameter concept can only be measured mathematically when all other physical and biological factors are held constant.

As shown earlier, the simulation results indicated that the anaerobic filter model, including the equivalent pore diameter concept, reproduced measured performance data with a good degree of accuracy when operating at low organic loading rates and using reactors packed with modular media. However, when using loose-fill media, other physical factors such as

channelling and short-circuiting seemed to have played a major role in the creation of some deviation between measured and calculated results. Regardless of the operating conditions, using different media with different pore diameters resulted in establishing a calculated performance trend which corresponded to measured performance trends obtained during pilot plant testing. This trend basically indicated that, for the range of equivalent pore diameters used, COD removal efficiency was inversely proportional to media equivalent pore diameters. This relationship should not, however, be extended beyond the range of media sizes used in this study since that would result in the erroneous conclusion that reactors containing extremely large media should result in the best attainable performance characteristics. Such maximum performance can only be reached, for a given loading rate, when using media having pore diameters such that hydraulic conditions are conducive to suspended biomass retention and where the effects of short-circuiting due to channelling are kept at a minimum.

CONCLUSIONS

The results of the investigation described in this report support the following conclusions concerning the effects of media design on anaerobic filter performance:

1. A strong correlation between COD removal efficiencies and media type, size, and shape was observed throughout this study and when operating at a wide range of organic loading rates. In general, all COD removal took place within the first 2.0 feet (0.61 m) of reactor height regardless of the type of media used. In addition, the majority of COD removal was attributable to the biological solids held in suspension in the media void spaces.

2. Among the media used in this study, modular corrugated media consistently provided better performance results than were possible when using loose-fill media. This relatively better performance was, in all likelihood, due to two main reasons. The first was the fact that the well-structured and uniformly-packed modular media had larger effective pore spaces than randomly-packed loose-fill media having equivalent specific surface areas. The second was that the poorer performance of the loose-fill media suggests that considerable short-circuiting was taking place, possibly due to the channelling in the smaller pore spaces of these media. The results suggested that channelling is more likely to take place within loose-fill media than modular media.

3. Comparison between the two sizes of modular media used in this study shows that the larger size having a lower specific surface area but larger pore size diameter was associated with better performance than the

smaller media size having the higher specific surface area. Such results were observed when operating at all loading rates and all influent COD concentrations. These results suggest that the media equivalent pore diameter is a more important factor in the selection of such media than specific surface area since larger pore diameters should result in the entrapment of more suspended biomass solids and possibly better prevention of the washout of these solids.

4. The anaerobic filter process can be successfully simulated mathematically with considerable predictability. Simulation results confirmed that the media equivalent pore diameter was a factor that should be considered in anaerobic filter design. Simulation results also suggested that the loose-fill media reactors were possibly subject to considerable channelling and short-circuiting.

5. Regardless of the type of medium used in this study, all anaerobic filters demonstrated remarkable abilities to adapt to differing organic loading rates including rates as high as 8.0 and 16.0 gm COD/L-day (500 and 1000 lb COD/MCF-day) and influent COD concentrations as high as 6000 mg/L.

6. The performance results clearly showed that alcohol stillage wastewater was highly amenable to anaerobic filter treatment. It is possible to recover a considerable fraction of the energy lost in the waste stream as methane gas; energy that is currently, and most likely always will be, in high demand.

RECOMMENDED FUTURE WORK

The following topics are recommended for future work:

1. There are several anaerobic filter media designs that are available on the market other than those used in this study. The effects of these media on anaerobic filter performance need to be investigated.
2. Many of the biological growth and physical coefficients used in the anaerobic filter model need to be refined and their applicability, particularly at high organic loading rates, should be investigated further.
3. The concept of the media equivalent pore diameter introduced in this study is undoubtedly in need of further refinement. A simple methodology of accurately estimating this parameter should be developed so that this concept could easily be utilized in the design of full-scale packed-bed reactors.

ACKNOWLEDGMENTS

The author expresses his sincere appreciation to his major professor, Dr. James C. Young, for his continued assistance, guidance, and encouragement during the course of this investigation and the author's entire course of graduate study.

Assistance and support provided by Dr. Tom Al Austin during the author's graduate work are also acknowledged and appreciated.

Harley Young provided valuable assistance in assembling the entire anaerobic filter system and portions of the data obtained during this study were collected by him, Walter Allen, and Jeff McLanathen.

Analytical assistance was provided by Lyle D. Johnson and Elizabeth Harrold. Their assistance is also acknowledged.

Mrs. Pat Soliday typed the manuscripts. Her skill and patience are also appreciated.

The author also thanks his wife, Debbie, for her patience, encouragement, and support during the entire course of graduate study.

This study was supported, in part, by the Engineering Research Institute of Iowa State University and by the U.S. Department of Energy and Ames Laboratory, Iowa State University, Ames, Iowa.

BIBLIOGRAPHY

1. Andrews, J. F., and Graef, S. P. "Dynamic modeling and simulation of the anaerobic digestion process." In Anaerobic Biological Treatment Processes. American Chemical Society, Advances in Chemistry Series 105, 1971.

2. Arora, H. C., Chattopadhya, S. N., and Routh, R. "Treatment of vegetable tanning effluent by the anaerobic contact filter process." Water Pollution Control, 74, (1975), 504-596.

3. Barney, W. K., and Chang, H. "Environmental considerations for fuel ethanol production from biomass." Proceedings of the Second U. S. Department of Energy Environmental Control Symposium, Reston, VA, March 17-19, 1980.

4. Brooks, R. E., Ballamy, W. D., and Su, T. H. "Conversion of plant biomass to ethanol." Proceedings of the Second Annual Symposium on Fuels From Biomass, Renesselaer Polytechnic Institute, June 20-22, 1978.

5. Brown, G. T., Lin, K. C., Landine, R. C., and Cocci, A. A. "Lime use in anaerobic filters." Journal of the Environmental Engineering Division, American Society of Civil Engineers, 106, (1980), 837-840.

6. Chian, E. S. K., and DeWalle, F. B. "Treatment of high strength acidic wastewater with a completely mixed anaerobic filter." Water Research, 11, (1977), 295-304.

7. Clark, R. H., and Speece, R. E. "The pH tolerance of anaerobic digestion." Proceedings of the Fifth International Water Pollution Research Conference, Pergamon Press, Spring 1971.

8. Culp-Wesner-Culp Consulting Engineers. "The submerged media anaerobic reactor in municipal waste treatment." Prepared for the U. S. Department of Energy, Argonne National Laboratory, Oct. 1980.

9. Dague, R. R. "State of the art in anaerobic waste treatment." Presented at the 19th Water Resources Design Conference, Iowa State University, Ames, IA, Feb. 4-5, 1981.

10. Dague, R. R. "Anaerobic biological treatment of liquid wastes from pyrolysis processes." Proceedings of the 54th Annual Conference of the Water Pollution Control Federation, Detroit, MI, Oct. 4-9, 1981.

11. Dague, R. R., Brindley, D. R., and Liang, P.S. "Anaerobic filter treatment of recycle from thermal sludge conditioning and dewatering." Proceedings of the 53rd Annual Conference of the Water Pollution Control Federation, Las Vegas, NV, Sept. 28-Oct. 3, 1980.

12. Dahab, M. F., and Young, J.C. "Energy recovery from alcohol stillage using anaerobic filters." Biotechnology and Bioengineering Symposium No. 11, (1981), 381-397.

13. DeWalle, F. B., and Chian, E. S. K. "Kinetics of substrate removal in a completely mixed anaerobic filter." Biotechnology and Bioengineering, 18, (1976), 1275-1295.

14. DeWalle, F. B., Kennedy, J. C., Zeisig, T., and Seabloom, R. "Treatment of domestic sewage with the anaerobic filter." Proceedings of the Seminar/Workshop on Anaerobic Filters: An Energy Plus for Wastewater Treatment, Orlando, FL, Jan. 1980.

15. de Zeeuw, W., and Lettinga, G. "Acclimation of digested sewage sludge during start-up of an upflow anaerobic sludge blanket (UASB) reactor." Proceedings of the 35th Purdue Industrial Waste Conference, West Lafayette, IN, May 13-15, 1980.

16. Donovan, E. J., Jr. "Treatment of high strength wastes by anaerobic filters." Proceedings of the Seminar/Workshop on Anaerobic Filters: An Energy Plus for Wastewater Treatment, Orlando, FL, Jan. 1980.

17. El-Shafie, A. T., and Bloodgood, D. E. "Anaerobic treatment in a multiple up-flow filter system." Journal Water Pollution Control Federation, 45, (1973), 2345-2357.

18. Energy and Environmental Analysis, Inc. "Solar Program Assessment, Final Report: Fuels from Biomass." Submitted to the U. S. Energy Research and Development Administration, Jan. 1977.

19. Friedman, A. A., Young, K. S., Baily, D. G., and Tait, S. J. "New observations with anaerobic fixed-film reactors." Proceedings of the Seminar/Workshop on Anaerobic Filters: An Energy Plus for Wastewater Treatment, Orlando, FL., Jan. 1980.

20. Genung, R. K., Pitt, W. W., Jr., Davis, G. M., and Koon, J. H. "Development of a wastewater treatment system based on a fixed-film anaerobic bioreactor." Proceedings of the Seminar/Workshop on Anaerobic Filters: An Energy Plus for Wastewater Treatment, Orlando, FL, Jan. 1980.

21. Haug, R. T., and McCarty, P. L. "Nitrification with the subjerged filter." Stanford University, Department of Civil Engineering, Technical Report No. 149, 1971.

22. Haug, R. T., Reksit, S. K., and Wong, G. G. "Anaerobic filter treats waste activated sludge." Water and Sewage Works, 124, (1977), 40-43.

23. Holladay, D. W., Hancher, C. W., Scott, C. D., and Chilcote, D. D. "Biodegradation of phenotic waste liquors in stirred-tank, packed-

bed, and fluidized-bed bioreactors." Journal Water Pollution Control Federation, 50, (1978), 2573-2589.

24. Hovious, J. C., Fisher, J. A., and Conway, R. A. "Anaerobic treatment of synthetic organic wastes." U. S. Environmental Protection Agency Report, Project No. 12020 DIS, Jan. 1972.

25. Hudson, J. W., Pohland, F. G., and Pendergrass, R. P. "Anaerobic packed-column treatment of shellfish process wastewater." Proceedings of the 33rd Purdue Industrial Waste Conference, West Lafayette, IN, May 1978.

26. Jennet, J. C., and Dennis, N. D., Jr. "Anaerobic filter treatment of pharmaceutical waste." Journal Water Pollution Control Federation, 47, (1975), 104-121.

27. Jennet, J. C., and Rand, M. C. "A comparison of anaerobic versus aerobic treatment of pharmaceutical waste." Proceedings of the Seminar/Workshop on Anaerobic Filters: An Energy Plus for Wastewater Treatment, Orlando, FL, Jan. 1980.

28. Jennings, P. A., Snoeyink, V. L., and Chian, E. S. K. "Theoretical model for a submerged biological filter." Biotechnology and Bioengineering, 18, (1976), 1249-1273.

29. Johansen, O. J., and Carlson, D. A. "Treatment of sanitary landfill leachate by anaerobic filters." Proceedings of the National Conference on Environmental Engineering, American Society of Civil Engineers, Seattle, WA, July, 1976.

30. Johnson, L. D., and Young, J. C. "Inhibition of anaerobic digestion by organic priority pollutants." Proceedings of the 54th Annual Conference of the Water Pollution Control Federation, Detroit, MI, Oct. 1981.

31. Kotze, J. P., Thiel, P. G., and Hattingh, W. H. J. "Anaerobic digestion II: The characteristics and control of anaerobic digestion." Water Research, 3, (1969), 459-493.

32. Lawrence, A. W., and McCarty, P. L. "Kinetics of methane fermentation in anaerobic treatment." Journal Water Pollution Control Federation, 41, Part 2, (1969), R1-R17.

33. Lawrence, A. W., and McCarty, P. L. "Unified basis for biological treatment design and operation." Journal of the Sanitary Engineering Division, American Society of Civil Engineers, 96, (1970), 757-778.

34. Lettinga, G., van Velsen, A. F. M., de Zeeuw, W., and Hobma, S. W. "Feasibility of the upflow anaerobic sludge blanket process." Proceedings of The National Conference on Environmental

Engineering, American Society of Civil Engineers, San Francisco, July, 1979.

35. Lettinga, G., de Zeeuw, W., and Ouborg, E. "Anaerobic treatment of waste containing methanol and higher alcohols." Water Research, 15, (1981), 171-182.

36. Lovan, C. R., and Foree, E. G. "The anaerobic filter for treatment of brewery press liquor waste." Proceedings of the 26th Purdue Industrial Waste Conference, West Lafayette, IN, May, 1975.

37. McCabe, W. L., and Smith, J. C. Unit Operations of Chemical Engineering. Third Edition, McGraw-Hill Book Company, New York, NY, 1976.

38. McCarty, P. L. "Anaerobic waste treatment fundamentals, part one: chemistry and microbiology." Public Works, 95, 9, (1964), 107-112.

39. McCarty, P. L. "Anaerobic waste treatment fundamentals, part two: environmental requirements and control." Public Works, 95, 10, (1964), 123-126.

40. McCarty, P. L. "Anaerobic waste treatment fundamentals, part three: toxic materials and their control." Public Works, 95, 11, (1964), 91-94.

41. McCarty, P. L. "Anaerobic waste treatment fundamentals, part four: process design." Public Works, 95, 12, (1964), 95-99.

42. McCarty, P. L. "Thermodynamics of biological synthesis and growth." International Journal of Air and Water Pollution, 9, (1965), 621-639.

43. McCarty, P. L. "Energetics and kinetics of anaerobic treatment." Anaerobic Biological Treatment Processes, American Chemical Society Advances in Chemistry Series, 105, 1971.

44. Mueller, J. A., and Mancini, J. L. "Anaerobic filter-kinetics and application." Proceedings of the 30th Purdue Industrial Waste Conference, West Lafayette, IN, May, 1975.

45. Park. W. R. "The near-term potential of biomass-based alcohol-gasoline transportation fuels." Proceedings of the Second Annual Symposium on Fuels from Biomass, Renesselaer Polytechnic Institute, June 20-22, 1978.

46. Pirt, S. J. "A quantitative theory of the action of microbes attached to a packed column: relevant to trickling filter effluent purification and to microbial action in soil." Journal of Applied Chemistry and Biotechnology, 23, (1973), 389-400.

47. Plummer, A. H., Malina, J. F., and Eckenfelder, W. W. "Stabilization of low solids carbohydrate waste by an anaerobic submerged filter." Proceedings of the 23rd Purdue Industrial Waste Conference, West Lafayette, IN, May, 1968.

48. Ragan, J. L. "Celanese experience with anaerobic filters." Proceedings of the Seminar/Workshop on Anaerobic Filters: An Energy Plus for Wastewater Treatment, Orlando, FL, Jan. 1980.

49. Rittman, B. E., and McCarty, P. L. "Variable-order model of bacterial-film kinetics." Journal of the Environmental Engineering Division, American Society of Civil Engineers, 104, (1978), 889-900.

50. Rittman, B. E., and McCarty, P. L. "Model of steady-state biofilm kinetics," Biotechnology and Bioengineering, 22, (1980), 2343-2357.

51. Saunders, P. T., and Bazin, M. J. "Attachment of microorganisms in a packed column: metabolite diffusion through the microbial film as a limiting factor." Journal of Applied Chemistry and Biotechnology, 23, (1973), 847-853.

52. Sitton, O. C., Foutch, G. L., Book, N. L., and Gaddy, J. L. "Ethanol from agricultural residues." Chemical Engineering Progress, 75, 12, (1979), 52-57.

53. Smith, R. E., Reed, M. J., and Kiker, J. T. "Two-phase anaerobic digestion of swine waste." Transactions of the American Society of Agricultural Engineers, 20, (1977), 1123-1128.

54. Speece, R. E., and McCarty, P. L. "Nutrients requirements and biological solids accumulation in anaerobic digestion." Proceedings of the First International Conference on Water Pollution Research, London, Sept. 1962.

55. Standard Methods for the Examination of Water and Wastewater, Fifteenth Edition. American Public Health Association, Washington, D. C., 1981.

56. Switzenbaum, M. S., and Jewell, W. J. "Anaerobic attached-film expanded-bed reactor treatment." Journal Water Pollution Control Federation, 52, (1980), 1953-1965.

57. Taylor, D. W., and Brum, R. J. "Full-scale anaerobic filter treatment of wheat starch plant wastes." American Institute of Chemical Engineers Symposium Series, 69, (1972), 129.

58. van den Berg, L., and Lentz, C. P. "Comparison between up and down-flow anaerobic fixed film reactors of varying surface-to-volume ratios for the treatment of bean blanching wastes." Proceedings

of the 34th Purdue Industrial Waste Conference, West Lafayette, IN, May, 1979.

59. van den Berg, L., and Lentz, C. P. "Effects of film area-to volume ratio, film support, height, and direction of flow on performance of methanogenic fixed film reactors." Proceedings of the Seminar/ Workshop on Anaerobic Filters: An Energy Plus for Wastewater Treatment, Orlando, FL, Jan., 1980.

60. Van der Meer, R. R., Van Brakel, J., and Heertjes, P. M. "Anaerobic treatment of dilute waste waters." Delft Progress Report, Series A: Chemistry and Physics, Chemical and Physical Engineering, 1, (1976), 143-149.

61. Watson, D. A., and Young, J. C. "Environmental control technology requirements for production of ethyl alcohol from biomass." Iowa State University, Engineering Research Institute, 1981.

62. Williamson, K., and McCarty, P. L. "A model for substrate utilization by bacterial films." Journal Water Pollution Control Federation, 48, (1976), 9-24.

63. Williamson, K., and McCarty, P. L. "Vertification studies of the biofilm model for bacterial substrate utilization." Journal Water Pollution Control Federation, 48, (1976), 281-296.

64. Witt, E. R., Humphrey, W. J., and Roberts, T. E. "Full-scale anaerobic filter treats high strength wastes." Proceedings of the 34th Purdue Industrial Waste Conference, West Lafayette, IN, May, 1979.

65. Young, J. C. "The anaerobic filter for waste treatment." Ph.D. Dissertation. Stanford University, Stanford, CA, 1968.

66. Young, J. C. "Factors affecting waste treatment in fixed-film anaerobic processes." Proceedings of the 162nd Annual Meeting of the American Chemical Society, Washington, D. C., Sept. 1971.

67. Young, J. C. "Performance of anaerobic filters under transient loading and operating conditions." Proceedings of the Seminar/ Workshop on Anaerobic Filters: An Energy Plus for Wastewater Treatment, Orlando, FL, Jan., 1980.

68. Young, J. C., and McCarty, P. L. "The anaerobic filter for waste treatment." Journal Water Pollution Control Federation, 41, (1969), R160-R173.

69. Young, J. C., and McCarty, P. L. "The anaerobic filter for waste treatment." Technical Report Number 87, Department of Civil Engineering, Stanford University, 1968.

70. Young, J. C., and Stewart, M. C. "PBR-a new addition to the AWT family." Water and Waste Engineering, 16, 8, (1979), 20-25.

APPENDIX:

ANAEROBIC FILTER SIMULATION MODEL

Listed below is the computer program for the anaerobic filter model. The program is written in FORTRAN and was executed using a WATFIV compiler at the Iowa State University Computation Center. An identification of program variables, statements, and sample output follow the program listing.

COMPUTER PROGRAM LISTING

```
                DAHAB,TIME=20,PAGES=20
          ANAEROBIC FILTER SIMULATION MODEL

 1          INTEGER  T,H,L,L2,N,RUN
 2          REAL K,KS,A,B,S0,M0,Q,MAX,E,M(26),SA(51,25),
           CSP(51,25),S(25),MAA(51,25),MAP(51,25),MA(25),
           CMAPM,MAPV,MAAM,MAPT,MAAT,KP,KSP,MP0,MAXP,
           CSC(25),MC(25),HH(25),ML,MC0,MAAV,MAXC,SGFA,SGFP,KSF,DP

          READ KINETIC CONSTANTS AND COEFFICIENTS

 3          READ(5,101)K,KS,A,B,S0,M0,MAX,SGFA,
           CKP,KSP,AP,BP,SP0,MP0,MAXP,SGFP,
           CSC0,MC0,AC,BC,RC,RA,RP
 4      101 FORMAT(8F10.2/8F10.2/7F10.2,10X)

          READ OPERATING PARAMETERS

 5          READ(5,102)L,L2,L3,NT,ND,N,NO,RUN,Q,AREA,FSG,PER,C,E
 6      102 FORMAT(8I10/6F10.5,20X)

          READ MEDIA-RELATED PARAMETERS

 7          READ(5,104)RS0,RM0,V0,ALPH,ZKV,KSF,DP,R
 8      104 FORMAT(8F10.5)

         READ IF NO = 2

 9          GO TO (3,2),NO
10        1 FORMAT(8F10.2/8F10.2/8F10.2)
11        2 READ(5,1)(MAA(1,H),H=2,25)
12          READ(5,1)(MAP(1,H),H=2,25)
13          READ(5,1)(M(H),H=2,25)
14          READ(5,1) (SA(1,H),H=2,25)
15          READ(5,1) (SP(1,H),H=2,25)
16          READ(5,103)Q1,S01,SP01,SC01,N
17      103 FORMAT(4F10.2,I10)
18          Q  =  Q1
19          S0 =  S01
20          SP0=  SP01
21          SC0=  SC01
22          GO TO 5

         INITIALIZE  VARIABLES

23        3 DO 4 H=1,24
24          SA(1,H+1)=S0
25          SP(1,H+1)=SP0
26          S(H+1)=S0+SP0+SC0
27          MAA(1,H+1)=M0
28          MAP(1,H+1)=MP0
29          MA(H+1)=M0+MP0
30          MC(H+1)=MC0
31        4 M(H+1) =M0+MP0+MC0
32        5 HH(1)    =0.0
33          ML       =0.0
34          SL       =0.0
35          M(1)     =0.0
36          HRT      =0.0
37          M(26)    =0.0
```

```
38          MC(1)    =0.0
39          MA(1)    =0.0
40          MAA(1,1)=0.0
41          MAP(1,1)=0.0
42          SA(1,1) = S0
43          SP(1,1) = SP0
44          SC(1)    =SC0
45          S(1)     =S0+SP0+SC0
46        6 DO 10 H=1,24
47          MC(H+1) = MC0
48          MA(H+1) = MAA(1,H+1)+MAP(1,H+1)+MC(H+1)
49          HH(H+1)=HH(H)+0.25
50          SC(H+1)=0.0
51       10 S(H+1)    = SA(1,H+1)+SP(1,H+1)+SC(H+1)
52          I = 1
53          GO TO (9,99),NO
54        9 NO = 1
55          T=1
56          J=NT*ND
57          I=J+1
58          ZNT=NT
59          K = K/E
60          KP= KP/E
61          STORM = 0.0

            TIME LOOP THRU 40

62       20 DO 40 T=1,J
63          X = 1
64          HRT=0.0
65          SP(T,1)=SP0
66          SA(T,1)=S0
67          MAA(T+1,1)=0.0
68          MAP(T+1,1)=0.0
69          GASHI    =0.0

            HEIGHT LOOP THRU 30

70          DO 30 H=1,24

            SHORTCIRCUITING FACTORS

71          V = V0*ALPH
72          RS =  RS0
73          RM =  RM0
74          VFAC= 1.0-ZKV*M(H+1)/1000.0
75          QFS = (1.0-RS*GASHI)*VFAC
76          PSF = (1-(KSF*Q*2.943E-4)/(DP**R))
77          VE = V*QFS*PSF
78          HRT=HRT+VE*24.0/Q

            COMPLEX WASTE DECOMPOSITION,MASS PRODUCTION,
            AND VOLATILE ACID FORMATION

79          SC(H+1) = SC(H)- (RC*1000.0*V/Q)
80          IF(SC(H+1).LT.0.0)SC(H+1)=0.0
81          YLDMC=  AC*(Q*(SC(H)-SC(H+1)))/V
82          DCAYC=  BC*MC(H+1)
83          PARMC=(E*YLDMC-DCAYC)/ZNT
84          DCAYM=(1.4*DCAYC*V/Q)/(RP+RA)
```

```
 85          FRMSA=RA*((SC(H)-SC(H+1))+DCAYM)
 86          FRMSP=RP*((SC(H)-SC(H+1))+DCAYM)

             PROPIONATE COD REMOVAL AND MASS PRODUCTION

 87          SP(T+1,1)=SP0
 88          SPV=(SP(T+1,H)+SP(T,H+1))/2.0
 89          SFAC = 1.00+(SGFP-1)*EXP(-1.5*SPV/1000.0)
 90          SPV = SPV/SFAC
 91          MAPM=MAP(T,H+1)
 92          MAPT=MAP(T,H+1)
 93       11 IF(MAPM.GT.MAXP)MAPM=MAXP
 94          YLDP=(((QFS*AP*0.43*KP*SPV)/
            C(KSP+SPV))*MAPM)
 95          DCAYP=BP*MAPT
 96          PARMP=(E*YLDP-DCAYP)/ZNT
 97       12 MAPV=(MAP(T,H+1)+PARMP)
 98          IF(MAPV.GT.MAXP)MAPV=MAXP
 99       13 PARSP=((KP*SPV*VE/Q)*MAPV/(KSP+SPV))
100          PARSP = PARSP-(SP(T,H)-SP(T+1,H))*ZNT*V/Q
101          IF(PARSP.GT.SP(T+1,H))PARSP=SP(T+1,H)

             ACETATE COD REMOVAL AND MASS PRODUCTION

102          SA(T+1,1)=S0
103          SAV=(SA(T+1,H)+SA(T,H+1))/2.0
104          SFAC = 1.00+(SGFA-1)*EXP(-1.5*SAV/1000.0)
105          SAV = SAV/SFAC
106          MAAM=MAA(T,H+1)
107          MAAT=MAA(T,H+1)
108       21 IF(MAAM.GT.MAX)MAAM=MAX
109          YLDA=(((QFS*A*K*SAV)/(KS+SAV))*MAAM)
110          DCAYA=B*MAAT
111          PARMA=(E*YLDA-DCAYA)/ZNT
112       22 MAAV=(MAA(T,H+1)+PARMA)
113          IF(MAAV.GT.MAX)MAAV=MAX
114       23 PARSA= ((K*SAV*VE/Q)*MAAV/(KS+SAV))
115          PARSA = PARSA-(SA(T,H)-SA(T+1,H))*ZNT*V/Q

             SUBSTRATE AND MASS ADJUSTMENTS

116       24 SP(T+1,H+1)=SP(T+1,H)-PARSP+FRMSP
117          SA(T+1,H+1)=SA(T+1,H)-PARSA+FRMSA+0.57*PARSP
118          S(H+1)=SP(T+1,H+1)+SA(T+1,H+1)+SC(H+1)
119          GASLO=(C*FSG/PER)*Q*(S(X)-S(H))/1000.0
120          GASHI=(C*FSG/PER)*Q*(S(X)-S(H+1))/1000.0
121          MAP(T+1,H+1)=((MAP(T,H+1)+PARMP)*
            C(1.-RM*GASHI))
            C+MAP(T+1,H)*RM*GASLO
122          MAA(T+1,H+1)=((MAA(T,H+1)+PARMA)*
            C(1.-RM*GASHI))
            C+MAA(T+1,H)*RM*GASLO
123          MC(H+1)=((MC(H+1)+PARMC)*
            C(1.-RM*GASHI))
            C+MC(H)*RM*GASLO
124          MA(H+1)=MAA(T+1,H+1)+MAP(T+1,H+1)+MC(H+1)
125          M(H+1)=(M(H+1)+PARMA+PARMP+PARMC+STORM+
            C(1.-E)*(YLDA+YLDP+YLDMC)/ZNT)
126          IF(M(H+1).LE.50000.0) STORM = 0.0
127          IF(M(H+1).GT.50000.0) STORM = M(H+1)-50000.0
```

```
128           M(H+1) = M(H+1)-STORM
129           M(H+1) = M(H+1)*
             C(1.-RM*GASHI)
             C+M(H)*RM*GASLO

130          30 CONTINUE
131             SL = SL+Q*(S(1)-S(25))/ZNT
132             M(26)=M(25)*RM*ZNT*GASHI*V/Q
133             ML = ML+M(26)*Q/ZNT
134          40 CONTINUE
135             N=N+ND
136          99 WRITE(6,100)
137         100 FORMAT(1H1,4X,1HN,3X,1HH,8X,1HS,9X,2HMA,11X,2HSA,8X,
             C3HMAA,11X,2HSP,8X,3HMAP,12X,2HSC,8X,2HMC,11X,1HM)
138             WRITE(6,200)(N,HH(H),S(H),MA(H),SA(I,H),
             CMAA(I,H),SP(I,H),MAP(I,H),SC(H),MC(H),M(H),H=1,25)
139         200 FORMAT(1H-,I5,F6.2,2F10.1,3(F14.1,F10.1),F13.1
             C/(I6,F6.2,2F10.1,3(F14.1,F10.1),F13.1))
140             SUMMA=0.0
141             SUMMP=0.0
142             SUMMC=0.0
143             SUMM =0.0
144             SUM  =0.0
145             DO 50 H=1,25
146             V = V0*ALPH
147             SA(1,H) =SA(I,H)
148             SP(1,H) =SP(I,H)
149             MAA(1,H)=MAA(I,H)
150             MAP(1,H)=MAP(I,H)
151             SUMMA   =SUMMA+MAA(I,H)*V
152             SUMMP   =SUMMP+MAP(I,H)*V
153             SUMMC   =SUMMC+MC(H)*V
154             SUMM    =SUMM+MA(H)*V
155          50 SUM     =SUM+M(H)*V
156             GAS=      (C*FSG/PER)*Q*(S(1)-S(25))/1000.0
157             TM = SUM+ ML
158             WRITE(6,300)SUMM,SUMMA,SUMMP,SUMMC,SUM,M(26),GAS,
             CML,HRT,SL,TM
159         300 FORMAT(1H-,4X,10HTOTAL MASS,F17.1,3(F24.1),
             CF13.1/1H0,4X,27HEFFLUENT SUSPENDED SOLIDS =,
             CF13.1,2X,4HMG/L,10X,5HGAS =,F10.1,2X,5HL/DAY,
             C10X,13HSOLIDS LOST =,F11.1/1H0,4X,5HHRT =,F7.3,
             C4X,5HHOURS,15X,19HTOTAL COD REMOVED =,F11.1,
             C10X,19HTOTAL MASS FORMED =,F17.1)
160             WRITE(6,400) K,KS,A,B,M0,MAX,KP,KSP,AP,BP,MP0,
             CMAXP,MC0,RC,RP,RA,AC,BC,
             CQ,E,PER,RS0,RM0,NT,FSG,C,ZKV,SGFA,SGFP,RUN,DP,PSF
161         400 FORMAT(1H-,4X,20HOPERATING PARAMETERS,4X,
             C3HK= ,F6.3,2X,4HKS= ,F7.1,2X,3HA= ,F6.3,2X,3HB= ,
             CF5.2,2X,4HM0= ,F6.1,2X,5HMAX= ,F7.1/
             C1H0,28X,3HKP=,F6.3,2X,4HKSP=,F7.1,2X,3HAP=,
             CF6.3,2X,3HBP=,F5.2,2X,4HMP0=,F6.1,2X,5HMAXP=,F7.1/
             C1H0,28X,4HMC0=,F6.1,2X,3HRC=,F6.1,2X,3HRP=,F6.3,
             C2X,3HRA=,F6.3,2X,3HAC=,F6.3,2X,3HBC=,F6.3/
             C1H0,28X,2HQ=,F6.1,2X,2HE=,F6.3,2X,4HPER=,F5.2,2X,
             C4HRS0=,F7.4,2X,4HRM0=,F7.4,2X,3HNT=,I4/
             C1H0,28X,4HFSG=,F6.3,2X,2HC=,F6.3,2X,3HKV=,F6.3,2X,
             C2X,5HSGFP=,F4.2,2X,12H*** RUN NO.=,I3,1X,3H***/
             C1H0,28X,28HMEDIA EQUIV. PORE DIAMETER =,F5.3,2X,
             C22HPACKING SHAPE FACTOR =,F5.3)
```

```
      GO TO(59,9),NO
   59 IF(N.EQ.L3) GO TO 90
   61 IF(N.LT.L) GO TO 20
      IF(N.GE.L2) GO TO 90
      L=L2
      MP0 = 100.0
   60 DO 70 H=1,24
      MAP(1,H+1)=MP0
      MA(H+1)= MA(H+1)+MP0
      M(H+1) = M(H+1) +MP0
   70 CONTINUE
      GO TO 20
   90 WRITE(6,600)
  600 FORMAT(1H1,10HEND OF RUN)
      RETURN
      END
```

IDENTIFICATION OF PROGRAM STATEMENTS AND VARIABLES

Line

3

K = Maximum rate of utilization of acetic acid, uncorrected for fraction of inactive mass production, mg COD/day - mg VSS

KS = "Half-velocity" coefficient for acetic acid, mg COD/liter

A = Growth yield of microorganism mass from acetic acid utilization, mg VSS/mg COD

B = Decay coefficient for biological solids synthesized from acetic acid, day^{-1}

SO = Initial acetic acid concentration, mg COD/liter

MO = Initial concentration of active acetic acid utilizing microorganisms, mg VSS/liter

MAX = A limiting concentration for MA used only for investigative purposes

SGFA = Maximum value of the substrate gradient factor for acetic acid, unitless

KP = Maximum rate of utilization of propionic acid uncorrected for fraction of inactive mass production, mg COD/day - mg VSS

KSP = "Half-velocity" coefficient for propionic acid, mg COD/liter

AP = Growth yield of microorganisms from propionic acid utilization, mg VSS/mg COD converted to methane and cell solids

BP = Decay coefficient for biological solids synthesized from propionic acid, day^{-1}

SPO = Initial propionic acid concentration, mg COD/liter

MPO = Initial concentration of active propionic utilizing microorganisms, mg VSS/liter

MAXP = A limiting concentration for MP used only for investigative purposes

Line

3 SGFP = Maximum value of the substrate gradient factor for propionic acid, unitless

SCO = Initial concentration of complex waste, mg COD/liter

MCO = Initial concentration of microorganisms active in first stage complex waste conversion, mg VSS/liter

AC = Growth yield from first stage complex waste conversion, mg VSS/mg COD converted

BC = Decay coefficient for active biological solids synthesized from first stage waste conversion, day^{-1}

RC = Rate of first stage complex waste conversion, gm COD/day/liter of filter volume

RA = Fraction of complex waste converted to acetic acid, mg COD/mg COD

RP = Fraction of complex waste converted to propionic acid, mg COD/mg COD

5 L = Time of operation to first change in operating conditions, days

L2 = Total time of simulated operation, days

L3 = Time of operation to first output, days, cannot equal L or L2

NT = Number of time periods per day of operation

ND = Number of days of simulated operation between print out of data - Note: the product, NT x ND, cannot exceed 50

N = Initial starting time, days

NO = Control card - If NO = 2, read MAA, MAP, M, SA, SP at T = 1 and all filter levels from cards. If NO = 1 initialize variables at T = 1

RUN = Run number

Q = Hydraulic flow rate, L/day

Line			
5	AREA	=	Cross-sectional area of anaerobic filter, ft^2
	FSG	=	Fraction of soluble substrate converted to methane, mg methane COD/mg soluble COD removed
	PER	=	Liters of methane produced per gram of COD converted to methane, liters/ gram COD
	E	=	Fraction of active mass production per unit of cell mass synthesized
7	RSO	=	Channeling coefficient, $(\text{liters of gas/day} - ft^2)^{-1}$
	RMO	=	Mass transport coefficient, $(\text{liter}/ft^3)^{-1}$
	VO	=	Initial void volume, liters per height increment
	ALPH	=	Initial porosity of filter
	ZKV	=	Fractional decrease in void volume, $(\text{gm VSS})^{-1}$
	KSF	=	Media packing shape factor, min/ft^2
	DP	=	Media equivalent pore diameter, inches
	R	=	Dimensionless exponent, (symbol n in Equation 35)
9-22		=	Read input data if N=2
23-44		=	If NO = 1, sets initial concentration of SA, SP, S, MAA, MAP, MA, MC, and M throughout filter height at T = 1 equal to initial concentrations specified
46-51		=	Initializes MC, MA, HH, SC, and S at T = 1. These variables cannot be read from punched cards.
49	HH	=	Filter height, feet
53		=	Print initialized variables if NO = 2
56	J	=	Number of time periods between printout of data
57	I	=	Time storage position for data to be printed
59-60		=	Converts K and KP to terms of gm COD/day/gm active VSS
61	STORM	=	Location for storing mass in excess of 50 gm/L - only used for complex waste

Line

62-130		=	Time loop during which calculation for J time periods are made
64	HRT	=	Initialize hydraulic retention time
65-68		=	Initialize SP, SA, MAA, MAP, at H = 1 and T + 1
69	GASHI	=	Set gas flow at H = 1 equal to zero
70-134		=	Height loop through line 143, during which calculations are made throughout the filter height for a specified time interval, T + 1
71	V	=	Total void volume in section H + 1, liters
72	RS	=	Channeling coefficient, $(\text{liters/day} - \text{ft}^2)^{-1}$ (see line 7)
73	RM	=	Mass transport coefficient, $(\text{liters/ft}^3)^{-1}$ (see line 7)
74	VFAC	=	Fractional reduction in void volume, H + 1, due to both solids accumulation and channeling (see Equation 33)
75	QFS	=	Fractional reduction in void volume due to both solids accumulation and channeling
76	PSF	=	Packing shape factor (see Equation 34).
77	VE	=	Effective void volume in Section H + 1, liters
78	HRT	=	Hydraulic retention time in section H + 1, hours
79-80		=	Calculates concentration of complex waste COD at H + 1 if SC (H+1) is greater than zero
81	YLDMC	=	Yield of biological solids from first stage conversion in section H + 1, mg/day/liter of filter volume
82	DCAYC	=	Decay of biological solids produced from first stage conversion and remaining in section H + 1, day^{-1}
83	PARMC	=	Change in concentration of biological solids in section H + 1 formed from first stage complex waste conversion, uncorrected for transport, mg VSS/liter

Line			
84	DCAYM	=	Increase in volatile acids concentration as a result of decay of MC, mg COD/liter
85	FRMSA	=	Total increase in acetic acid from H to H +1 as a result of first stage complex waste conversion, mg COD/liter
86	FRMSP	=	Total increase in propionic acid from H to H + 1 as a result of first stage complex waste conversion, mg COD/liter
88	SPV	=	Average propionic acid concentration in section H + 1, mg COD/liter
89	SFAC	=	Substrate gradient factor in section H + 1
90	SPV	=	Effective concentration of propionic acid in filter section H + 1, mg COD/liter
94	YLDP	=	Gross yield of biological solids from propionic acid decomposition in section H + 1, mg/day - liter of filter volume
95	DCAYP	=	Decay of MAP in section H + 1, mg VSS/day
96	PARMP	=	Net synthesis of MAP in section H + 1 during time period T + 1, mg/liter of filter volume
97	MAPV	=	Concentration of propionic acid decomposing mass in section H + 1 and time period T + 1 uncorrected for solids transport, mg VSS/liter
98	PARSP	=	Change in SP due to removal of propionic acid from section H to H + 1 at the end of time period T + 1
100		=	Corrects PARSP for the rate of accumulation of SP
101		=	Control card, not needed with normal operation
103	SAV	=	Average concentration of acetic acid in section H + 1, mg COD/liter
104	SFAC	=	Substrate gradient factor for acetic acid in section H + 1
105	SAV	=	Effective concentration of acetic acid in section H + 1, mg COD/liter

Line			
109	YLDA	=	Gross yield of biological solids from acetic acid removal in section H + 1, mg VSS/day - liter of filter volume
110	DCAYA	=	Decay of active acetic acid decomposing mass in section H + 1, mg VSS/day
111	PARMA	=	Net synthesis of acetic acid decomposing mass in section H + 1 during time period T + 1, mg/liter of filter volume
112	MAAV	=	Concentration of acetic acid decomposing mass in section H + 1 and time period T + 1 uncorrected for mass transport, mg/liter
114	PARSA	=	Change in SA due to removal of acetic acid from section H to H + 1 at the end of time period T + 1, mg COD/liter
115		=	Corrects PARSA for rate of change in storage of acetic acid
116-118		=	Calculates concentration of SA, SP, and S at the top of section H + 1 and at the end of time period T + 1, mg-COD/liter
119	GASLO	=	Gas flowing into section H + 1 at the end of time period T + 1, (liters/day - ft^2)
120	GASHI	=	Gas flowing out of section H + 1 at the end of time period T + 1, (liters/day - ft^2)
121-129		=	Adjusts for MAP, MAA, MC, MA, and M in section H + 1 for mass transport during time period T + 1
131	SL	=	Accumulated removal of COD in filter, mg-COD
132	M(26)	=	Effluent suspended solids concentration, mg VSS/liter
133	ML	=	Accumulated loss of biological solids from filter, mg VSS
135	N	=	Time of operation at end of Time loop, days
136		=	Writes headings on printed output
138		=	Writes substrate and biological solids concentrations for all filter sections

Line			
140-144		=	Clears storage locations for total biological solids determination
145-150		=	Shifts calculated results for time period I = J + 1 to time period T = 1 to conserve storage locations
151-155		=	Calculates total accumulation of biological solids synthesized from each waste component and remaining in the filter, mg VSS
156		=	Effluent gas production rate, liters/day
157	TM	=	Total biological solids formed up to N days of operation, equals accumulation plus loss with effluent, mg VSS
158		=	Writes results calculated from lines 151-157
160		=	Writes operating parameters and coefficients
162		=	Control card if input is read from cards
163-165		=	Control cards for printing output and stopping program operation
166-171		=	Routine for adding propionic acid decomposing seed mass at L days of operation

SAMPLE OUTPUT

N	H	S	MA	SA	MAA	SP	MAP	SC	MC	M
40	0.00	1500.0	0.0	80.0	0.0	20.0	0.0	1400.0	0.0	0.0
40	0.25	1445.8	32673.3	396.1	162.2	393.5	1035.5	656.2	31475.6	49714.9
40	0.50	1268.1	20820.5	762.1	1359.0	506.0	3266.2	0.0	24195.3	49064.6
40	0.75	991.1	11196.2	791.5	3376.2	199.6	3184.8	0.0	4635.2	34154.3
40	1.00	724.0	8139.4	628.7	4303.4	95.3	2067.2	0.0	1688.8	21611.8
40	1.25	540.8	6628.8	481.2	4345.1	59.7	1435.8	0.0	847.8	16116.3
40	1.50	424.4	5422.9	380.7	3883.4	43.6	1051.7	0.0	487.8	12576.2
40	1.75	350.0	4347.8	314.9	3274.4	35.1	778.2	0.0	295.2	9879.4
40	2.00	301.6	3385.2	271.5	2639.7	30.1	565.4	0.0	180.1	7690.7
40	2.25	269.8	2547.3	242.6	2042.3	27.2	396.7	0.0	108.3	5880.8
40	2.50	248.8	1848.7	223.4	1518.6	25.4	265.3	0.0	63.7	4392.1
40	2.75	235.0	1294.5	210.7	1087.5	24.3	170.3	0.0	36.7	3194.2
40	3.00	226.0	877.7	202.4	752.8	23.7	103.8	0.0	21.1	2261.1
40	3.25	220.3	580.4	197.0	507.4	23.3	60.6	0.0	12.4	1561.7
40	3.50	216.6	378.5	193.5	336.6	23.1	34.1	0.0	7.8	1057.7
40	3.75	214.2	247.4	191.2	223.0	23.0	18.8	0.0	5.5	707.4
40	4.00	212.7	165.2	189.7	150.4	22.9	10.4	0.0	4.4	471.1
40	4.25	211.6	115.1	188.7	105.2	22.9	6.0	0.0	3.9	315.1
40	4.50	210.8	84.9	187.9	77.4	22.9	3.8	0.0	3.7	212.9
40	4.75	210.2	66.5	187.4	60.3	22.9	2.6	0.0	3.6	145.5
40	5.00	209.8	55.2	186.9	49.5	22.9	2.1	0.0	3.6	100.2
40	5.25	209.4	47.9	186.5	42.5	22.8	1.8	0.0	3.6	68.8
40	5.50	209.0	42.9	186.2	37.8	22.8	1.6	0.0	3.5	46.0
40	5.75	208.7	39.4	185.9	34.3	22.8	1.5	0.0	3.5	28.9
40	6.00	208.4	36.7	185.6	31.8	22.8	1.4	0.0	3.5	15.5

TOTAL MASS 1599420.0 447095.1 212196.1 940140.9 3248540.0

EFFLUENT SUSPENDED SOLIDS = 0.1 MG/L GAS = 331.1 L/DAY SOLIDS LOST = 1575.2

HRT = 6.083 HOURS TOTAL COD REMOVED = 24233530.0 TOTAL MASS FORMED = 3247115.0

OPERATING PARAMETERS K= 7.625 KS= 355.0 A= 0.050 B= 0.04 M0= 600.0 MAX= 9000.0

KP=22.875 KSP= 205.0 AP= 0.050 BP= 0.04 MP0= 100.0 MAXP= 9000.0

MC0= 100.0 RC= 25.0 RP= 0.450 RA= 0.350 AC= 0.140 BC= 0.080

Q= 493.0 E= 0.800 PER= 0.75 RS0= 0.0017 RM0= 0.0004 NT= 1

FSG= 1.000 E= 0.390 KV= 0.015 SGFA=4.00 SGFP=4.00 *** RUN NO.= 12 ***

MEDIA EQUIV. PORE DIAMETER =1.800 PACKING SHAPE FACTOR =0.839